

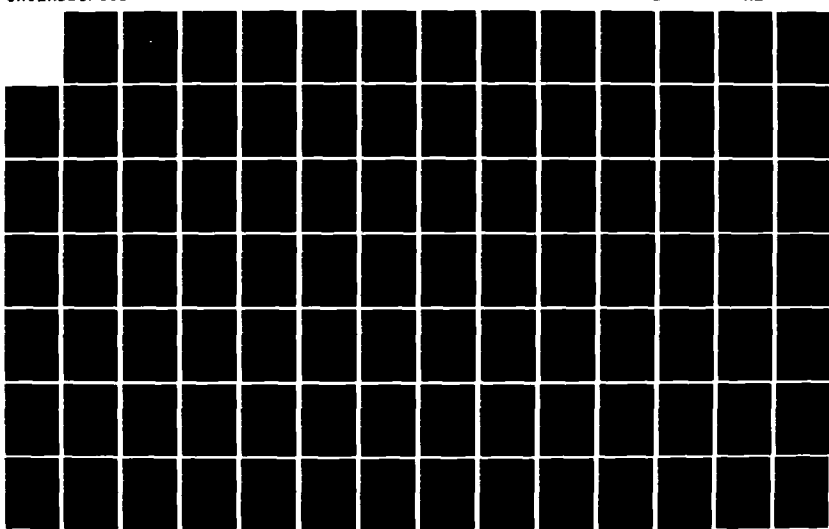
AD-A155 739 BROADSIDE SCATTERING OF A TUBULAR CYLINDER FOR  
EVALUATION OF TARGET IDENTIFICATION(U) NAVAL  
POSTGRADUATE SCHOOL MONTEREY CA B HAKLAY MAR 85

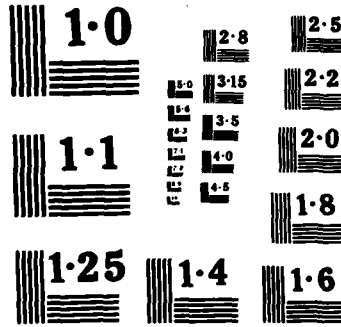
172

UNCLASSIFIED

F/G 17/9

NL





NATIONAL BUREAU OF STANDARDS  
MICROCOPY RESOLUTION TEST CHART

(2)

AD-A155 739

# NAVAL POSTGRADUATE SCHOOL

## Monterey, California



DTIC  
ELECTED  
JUL 1 1985  
S D  
B

## THESIS

BROADSIDE SCATTERING OF A TUBULAR  
CYLINDER FOR EVALUATION OF  
TARGET IDENTIFICATION

by

Boaz Haklay

March 1985

Thesis Advisor:

H. M. Lee

Approved for public release; distribution is unlimited

DTIC FILE COPY

85 06 17 075

REPRODUCED AT GOVERNMENT EXPENSE

## SECURITY CLASSIFICATION OF THIS PAGE (When Data Entered)

REPORT DOCUMENTATION PAGE		READ INSTRUCTIONS BEFORE COMPLETING FORM
1. REPORT NUMBER	2. GOVT ACCESSION NO.	3. RECIPIENT'S CATALOG NUMBER
		A-A-155139
4. TITLE (and Subtitle) Broadside Scattering of a Tubular Cylinder for Evaluation of Target Identification		5. TYPE OF REPORT & PERIOD COVERED Master's Thesis; March 1985
7. AUTHOR(s) Boaz Haklay		6. PERFORMING ORG. REPORT NUMBER
9. PERFORMING ORGANIZATION NAME AND ADDRESS Naval Postgraduate School Monterey, California 93943		10. PROGRAM ELEMENT, PROJECT, TASK AREA & WORK UNIT NUMBERS
11. CONTROLLING OFFICE NAME AND ADDRESS Naval Postgraduate School Monterey, California 93943		12. REPORT DATE March 1985
14. MONITORING AGENCY NAME & ADDRESS (if different from Controlling Office)		13. NUMBER OF PAGES 151
		15. SECURITY CLASS. (of this report) UNCLASSIFIED
		15a. DECLASSIFICATION/DOWNGRADING SCHEDULE
16. DISTRIBUTION STATEMENT (of this Report) Approved for public release; distribution is unlimited		
17. DISTRIBUTION STATEMENT (of the abstract entered in Block 20, if different from Report)		
18. SUPPLEMENTARY NOTES		
19. KEY WORDS (Continue on reverse side if necessary and identify by block number) Electromagnetic Scattering; Target Identification; Back-Scattering Cross-Section; Finite Tubular Cylinder		
20. ABSTRACT (Continue on reverse side if necessary and identify by block number) The concept of target identification through its back scattering cross section, in the resonance region was investigated. Measurements from the broadside aspect angle of several scaled tubular cylinders have been used for this purpose. The experimental results and theoretical approximation for some of the cylinders are presented. That data will serve as the baseline for further investigation in this project.		

Approved for public release; distribution is unlimited.

Broadside Scattering of a Tubular Cylinder  
for  
Evaluation of Target Identification

by

Boaz Haklay  
Lieutenant, Israeli Navy  
B.S., Jerusalem College of Technology, 1980

Submitted in partial fulfillment of the  
requirements for the degree of

MASTER OF SCIENCE IN ELECTRICAL ENGINEERING

from the

NAVAL POSTGRADUATE SCHOOL  
March 1985

Author: \_\_\_\_\_  
Boaz Haklay

Approved by: \_\_\_\_\_  
Hung-Mou Lee, Thesis Advisor

Jin-Fu Chang, Second Reader

\_\_\_\_\_  
Harriett B. Rigas, Chairman,  
Department of Electrical and Computer Engineering

\_\_\_\_\_  
John N. Dyer,  
Dean of Science and Engineering

## ABSTRACT

The concept of target identification through its back scattering cross section, in the resonance region was investigated. Measurements from the broadside aspect angle of several scaled tubular cylinders have been used for this purpose. The experimental results and theoretical approximation for some of the cylinders are presented. That data will serve as the baseline for further investigation in this project.

DTIC	
COPY	
INSPECTED	
Accession For	
NTIS GRA&I	<input checked="" type="checkbox"/>
DTIC TAB	<input type="checkbox"/>
Unannounced	<input type="checkbox"/>
Justification	
By	
Distribution/	
Availability Codes	
Avail and/or	
DIST	Special
A-1	

## TABLE OF CONTENTS

I.	INTRODUCTION . . . . .	9
II.	ANALYTICAL SOLUTION FOR SCATTERING PROBLEM . . . . .	12
	A. GENERAL APPROACH TO SCATTERING PROBLEM . . . . .	12
	B. SCATTERING BY A TUBULAR CYLINDER . . . . .	15
III.	MEASUREMENTS . . . . .	27
	A. SET-UP . . . . .	27
	B. TARGETS . . . . .	32
	C. MEASUREMENT PROCEDURE . . . . .	37
	D. MEASURED DATA . . . . .	38
IV.	DATA ANALYSIS . . . . .	102
	A. ANALYSIS OF EXPERIMENTAL DATA . . . . .	102
	B. COMPARISON BETWEEN MEASUREMENTS AND THEORY .	103
	C. RESULTS FOR CYLINDERS WITH FINS . . . . .	107
V.	SUMMARY . . . . .	123
	A. KNOWN PROBLEM AREAS . . . . .	123
	B. WHERE FUTURE WORK IS NEEDED . . . . .	124
	APPENDIX A: ANTENNAS CHARACTERISTICS . . . . .	125
	APPENDIX B: ANECHOIC CHAMBER . . . . .	126
	APPENDIX C: SPHERE PROGRAM . . . . .	129
	APPENDIX D: CALIB PROGRAM . . . . .	132
	APPENDIX E: TARGET PROGRAM . . . . .	138
	LIST OF REFERENCES . . . . .	149
	INITIAL DISTRIBUTION LIST . . . . .	151

## LIST OF TABLES

1.	Equipment . . . . .	28
2.	Targets Description . . . . .	36
3.	TARGET1 Measured Data . . . . .	41
4.	TARGET2 Measured Data . . . . .	44
5.	TARGET3 Measured Data . . . . .	47
6.	TARGET4 Measured Data . . . . .	50
7.	TARGET5 Measured Data . . . . .	53
8.	TARGET6 Measured Data . . . . .	56
9.	TARGET7 Measured Data . . . . .	59
10.	TARGET8 Measured Data . . . . .	62
11.	TARGET9 Measured Data . . . . .	65
12.	TARGET10 Measured Data . . . . .	68
13.	TARGET11 Measured Data . . . . .	71
14.	TARGET12 Measured Data . . . . .	74
15.	TARGET13 Measured Data . . . . .	77
16.	TARGET14 Measured Data . . . . .	80
17.	TARGET15 Measured Data . . . . .	83
18.	TARGET16 Measured Data . . . . .	86
19.	TARGET17 Measured Data . . . . .	89
20.	TARGET18 Measured Data . . . . .	92
21.	TARGET19 Measured Data . . . . .	95
22.	TARGET20 Measured Data . . . . .	98
23.	TARGET21 Measured Data . . . . .	101
24.	Targets with Constant 2a . . . . .	103
25.	2hf for Discontinuity Points . . . . .	104
26.	Cylinders with the Same h/a . . . . .	105
27.	ka Range Covered by Each Target . . . . .	105

## LIST OF FIGURES

2.1	Configuration of a Scattering Problem . . . . .	13
2.2	Cylinder in Cartesian Coordinates . . . . .	17
2.3	Cylinder in Cylindrical Coordinates . . . . .	18
3.1	Signal Flowing Diagram . . . . .	29
3.2	Orientation of Targets in Anechoic Chamber . . . . .	33
3.3	Cylinders Dimensions . . . . .	34
3.4	The Fins Orientation . . . . .	35
3.5	TARGET1 Cross-Section vs. Frequency . . . . .	39
3.6	TARGET1 Phase Shift vs. Frequency . . . . .	40
3.7	TARGET2 Cross-Section vs. Frequency . . . . .	42
3.8	TARGET2 Phase Shift vs. Frequency . . . . .	43
3.9	TARGET3 Cross-Section vs. Frequency . . . . .	45
3.10	TARGET3 Phase Shift vs. Frequency . . . . .	46
3.11	TARGET4 Cross-Section vs. Frequency . . . . .	48
3.12	TARGET4 Phase Shift vs. Frequency . . . . .	49
3.13	TARGET5 Cross-Section vs. Frequency . . . . .	51
3.14	TARGET5 Phase Shift vs. Frequency . . . . .	52
3.15	TARGET6 Cross-Section vs. Frequency . . . . .	54
3.16	TARGET6 Phase Shift vs. Frequency . . . . .	55
3.17	TARGET7 Cross-Section vs. Frequency . . . . .	57
3.18	TARGET7 Phase Shift vs. Frequency . . . . .	58
3.19	TARGET8 Cross-Section vs. Frequency . . . . .	60
3.20	TARGET8 Phase Shift vs. Frequency . . . . .	61
3.21	TARGET9 Cross-Section vs. Frequency . . . . .	63
3.22	TARGET9 Phase Shift vs. Frequency . . . . .	64
3.23	TARGET10 Cross-Section vs. Frequency . . . . .	66
3.24	TARGET10 Phase Shift vs. Frequency . . . . .	67
3.25	TARGET11 Cross-Section vs. Frequency . . . . .	69

3.26	TARGET11 Phase Shift vs. Frequency . . . . .	70
3.27	TARGET12 Cross-Section vs. Frequency . . . . .	72
3.28	TARGET12 Phase Shift vs. Frequency . . . . .	73
3.29	TARGET13 Cross-Section vs. Frequency . . . . .	75
3.30	TARGET13 Phase Shift vs. Frequency . . . . .	76
3.31	TARGET14 Cross-Section vs. Frequency . . . . .	78
3.32	TARGET14 Phase Shift vs. Frequency . . . . .	79
3.33	TARGET15 Cross-Section vs. Frequency . . . . .	81
3.34	TARGET15 Phase Shift vs. Frequency . . . . .	82
3.35	TARGET16 Cross-Section vs. Frequency . . . . .	84
3.36	TARGET16 Phase Shift vs. Frequency . . . . .	85
3.37	TARGET17 Cross-Section vs. Frequency . . . . .	87
3.38	TARGET17 Phase Shift vs. Frequency . . . . .	88
3.39	TARGET18 Cross-Section vs. Frequency . . . . .	90
3.40	TARGET18 Phase Shift vs. Frequency . . . . .	91
3.41	TARGET19 Cross-Section vs. Frequency . . . . .	93
3.42	TARGET19 Phase Shift vs. Frequency . . . . .	94
3.43	TARGET20 Cross-Section vs. Frequency . . . . .	96
3.44	TARGET20 Phase Shift vs. Frequency . . . . .	97
3.45	TARGET21 Cross-Section vs. Frequency . . . . .	99
3.46	TARGET21 Phase Shift vs. Frequency . . . . .	100
4.1	Length Dependence of Cross Section for $2a=0.375$ .	108
4.2	Length Dependence of Cross Section for $2a=0.5$ .	109
4.3	Length Dependence of Cross Section for $2a=0.75$ .	110
4.4	Measured Cross Section/ $4ah$ vs. $ka$ for $h/a=4$ .	111
4.5	Measured Cross Section/ $4ah$ vs. $ka$ for $h/a=6$ .	112
4.6	Theoretical Cross Section for $h/a=4$ . . . . .	113
4.7	Theoretical Cross Section for $h/a=6$ . . . . .	114
4.8	Comparison of Cross Section Between Theoretical & Experimental Data for $h/a=4$ . . . . .	115
4.9	Comparison of Cross Section Between Theoretical & Experimental Data for $h/a=6$ . . . . .	116
4.10	Measured Phase Shift vs. $ka$ for $h/a=4$ . . . . .	117

4.11	Measured Phase Shift vs. $ka$ for $h/a=6$ . . . . .	118
4.12	Theoretical Phase Shift for $h/a=4$ . . . . .	119
4.13	Theoretical Phase Shift for $h/a=6$ . . . . .	120
4.14	Comparison of Phase Shift Between Theoretical & Experimental Data for $h/a=4$ . . . . .	121
4.15	Comparison of Phase Shift Between Theoretical & Experimental Data for $h/a=6$ . . . . .	122
B.1	Specifications of the Absorber Material of the Front Wall . . . . .	127
B.2	Specifications of the Absorber Material of the Back Wall . . . . .	128

## I. INTRODUCTION

Target identification is desirable if different actions are to be taken toward different targets. Today when missiles can be sent long before a target comes within visual range, there is a need of identify target by some means other then visual.

The use of radar provides a greater range for target detection. Radars have the ability to detect the presence of a target, and to obtain information about target position, speed and acceleration. A trained operator can identify the kind of target infront of him by the size of the spot on the screen and from the direction such a target is approaching, but he may not always be correct.

→ Detection by a radar is done by detecting the back scattered electromagnetic signal returned from a target. The back scattered signal originates from the surface currents excited on the object when it is irradiated by an incident electromagnetic wave. Different targets have different outer surface that cause different surface currents to flow on the target when identical incident waves are irradiating the targets.

Assume the presence of a continuous incident electromagnetic wave. The incident wave keeps impinging on the target and excites new surface current which add vectorally to the existing ones. The total surface current, and therefore the back scattered signal are functions of the target shape and the wavelength of the incident wave.

Assuming a uniform plane incident wave, the back scattering cross section of a target is a quantitative measure of the ratio of power density in the vector signal scattered in the direction of the receiver to the power density of the

electromagnetic wave incident upon the target [Ref. 1], The back scattering cross section of a target as a function of the wavelength or the frequency of the incident wave can be used as a working tool for target identification

One approach to this problem, is by looking into the Rayleigh region [Ref. 2], where the frequency ranges from zero up to a wavelength about half the linear dimension of the target. A different approach is to study the scattering of a target in the resonance region where its cross section varies rapidly with frequency, and is a critical function of the shape of the target [Ref. 3]. Even though some resonances may not be observable at some particular target aspect angles. The advantages of using the resonance region are that the scattered fields of interests are stronger and thus are easier to be detected. Because the resonance frequencies depend critically on target shapes, and because there are only a finite number of targets of interest only a few resonances will be needed before a target can be identified.

This thesis is part of an ongoing project at the Naval Postgraduate School on target identification. It studies the broadside scattering of a tubular cylinder of finite length, made of very thin brass walls. The targets used in this research were a set of tubular circular cylinders with different lengths and diameters. This shape has been chosen because of its resemblance to a missile body and because its theoretical solution is available. This work should serve as the basis for further efforts in developing a target identification scheme employing the frequency dependence of the back scattered field from a target in the resonance region. The effects of adding fins to the cylinders will be investigated next and will lead to the last step where models of real targets will be identify through this scheme.

Chapter II describes the general approach to the solution of the back scattering cross section problem. The exact solution for the scattering by a perfectly conducting tubular cylinder having very thin walls from the broadside aspect angle is presented. Chapter III contains the experimental setup at the Naval Postgraduate School, the measurement procedure and the experimental data. Chapter IV presents data analysis of the results as well as comparison between theoretical data obtained from the solution shown in Chapter II. Because this was the first time frequency dependence of the cross section of tubular cylinder was ever tested at the resonance region, the results are very surprising and can be used to direct further efforts in this project. Chapter V contains a summary of the result, the problems encountered and areas of future work.

## II. ANALYTICAL SOLUTION FOR SCATTERING PROBLEM

### A. GENERAL APPROACH TO SCATTERING PROBLEM

A parameter that defines the scattering efficiency of a target was sought in the earliest days of radar. This parameter when refers to the equivalent isotropic reflector is called cross section and denoted by the symbol  $\sigma$ . The theoretical definition of back scattering cross section is given by 2.1 .

$$\sigma = 4\pi r^2 \lim_{r \rightarrow \infty} |E_s/E_i|^2 \quad (2.1)$$

Where  $E_i$ -Magnitude of electric-field component of incident electromagnetic (EM) field at the target.

$E_s$ -Magnitude of electric-field component of scattered EM field as measured by a hypothetical observer

$r$ -Distance from target to the hypothetical observer

In this definition the incident and scattered fields are introduced. The incident field means the field maintained by the oscillating charges and currents in the driving or primary antenna constitutes the source. When the target is irradiated with an incident EM wave, surface current is excited on the target. This surface current will radiate and generate the scattered field. The configuration of a scattering problem is shown in Figure 2.1 .

The limiting process is introduced to assure that the distance at which the hypothetical observation is made is

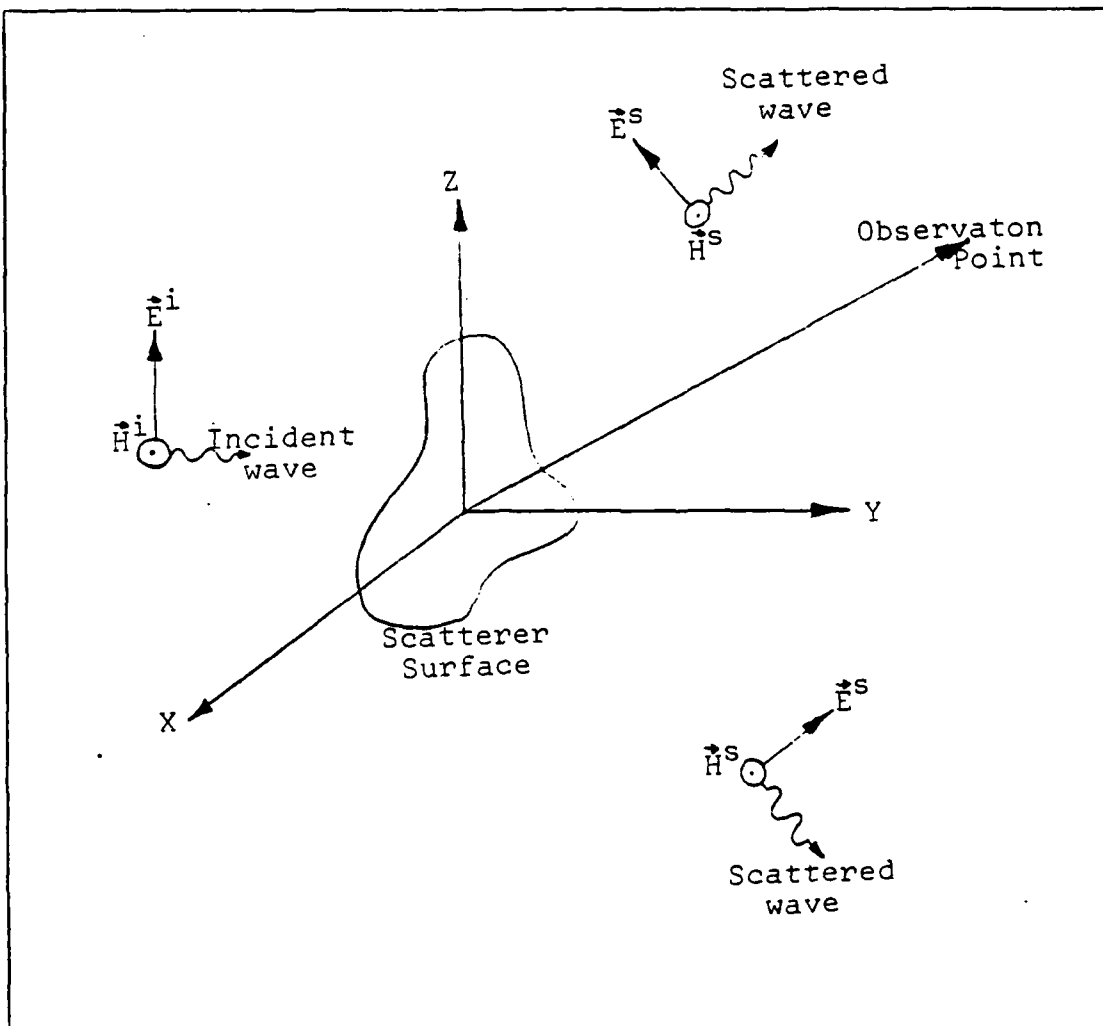


Figure 2.1 Configuration of a Scattering Problem

far enough from the target so that only the  $R^{-1}$  dependent term of the scattered field is retained. Under the free-space conditions assumed here, the ratio  $|E_s/E_i|^2$  is the same as the ratio of the power flux density of the scattered waves at the observer to that of the incident wave at the target.

The incident field is not independent of the presence of the target because of the coupling between the currents and

charges in the source and the currents and charges on the target. To simplify the problem, it is usually assumed that the source is separated from the target by a large distance and thus the incident field is independent of the presence of the target.

Ideally, one would compute the radar cross section of a target through the formal solution of Maxwell equations under the boundary conditions appropriate to the body. The integral equation formulation shows that electromagnetic scattering of an incident wave by an arbitrary body can be described in terms of an integral of various vector products involving the surface electric and magnetic fields on the target. The Chu-Stratton integral [Ref. 4 p. 464] is convenient for this purpose. This integral is an exact representation of the scattered electromagnetic field in terms of an integration over a complete surface enclosing the body in question. In particular, if there is available knowledge of the total distribution of electric and magnetic fields about the body (or what is equivalent, surface currents), insertion of these values in the Chu-Stratton integral would permit the immediate evaluation of the scattered fields. Approximate numerical solutions of such integral equations require the use of high speed digital computers to estimate surface currents flowing on the body. Because of the limitation of computation time and storage capacity, this method is applicable only when the dimensions of the target do not exceed a very few wavelengths.

Exact solutions for the scattering problem are rare. For many practical problems, only approximate solutions are obtainable. Aside from different numerical schemes, asymptotic techniques are also used when the target dimensions are much larger than the wavelength. It is called geometrical diffraction theory and it combines the simplicity inherent in the ray optics with the necessary consideration

of wavelengths and phases. This method uses the concept of scattering centers and localizes them at the points of surface discontinuity in the belief that specular diffractions occur only at these discontinuities with contributions from surface regions a few wavelength within these points. Each center is assigned a magnitude and a phase based upon asymptotic expansion of the exact solution of a two dimensional case of a plane geometry. By concentrating on scattering centers, it is possible to predict the polarization of the signal reradiated from each center and so to preserve polarization dependence in computed result. It is also possible to predict the dependence of radar scattering upon bistatic angle, but this approach cannot include resonances of the target.

#### B. SCATTERING BY A TUBULAR CYLINDER

Electromagnetic scattering from an infinite cylinder is a two dimensional problem. Its solution has been established for decades. For finite cylinders, Storer [Ref. 5] deals with the case of long thin cylinder (a wire) and Kennedy [Ref. 6] with a short thick cylinder (a disc). In practical applications the finite structures are the cases of interest.

The geometric diffraction theory has been used by Ross [Ref. 7] to calculate the EM scattering from a finite cylinder where the cylinder was  $25\lambda$  long and  $5\lambda$  in diameter. This approach can only deal with problems near the optical region. When dealing with problems in the resonance region the complete Maxwell equations have to be used. One approach to setup the boundary value problem is by using the Chu-Stratton integral to formulate an integrodifferential equation.

The solution that will be shown in this chapter is for circular tubular cylinder having very thin walls. Cylinder with those specifications were tested in the Scattering Laboratory at the Naval Postgraduate School and the measurement data as shown in Chapter III was used to compare with this theory.

The finite cylinder is assumed to be an infinitesimally thin walled, perfectly conducting circular tube of radius "a" and length "2h". Its center is located at the origin of the cartesian coordinates  $(x, y, z)$ ; its axis coincides with the  $z$  axis of the coordinates, so that the length extends from  $z=-h$  to  $z=+h$ ; Figure 2.2. To simplify the equations, the scaled cylindrical coordinates  $(\rho, \phi, z)$  have been used (Figure 2.3) in which the cylinder length extends from  $z=-1$  to  $z=+1$  and its radius is 1.

The surface current can flow only on the perfectly conducting surfaces when the free space case is assumed; and because of the thin walls the total surface current can be assumed to exist only for  $-1 \leq z \leq +1$  and  $\rho = 1$ . There are only two current components: the circumferential current circles around the cylinder in the  $\phi$  direction while the axial current travels along the cylinder in the  $z$  direction. Both currents are functions of the position on the cylinder. In terms of their Fourier coefficients the axial current density  $K_z(\phi, z)$  and the circumferential current density  $K_\phi(\phi, z)$  can be represented as equations 2.2 and 2.3.

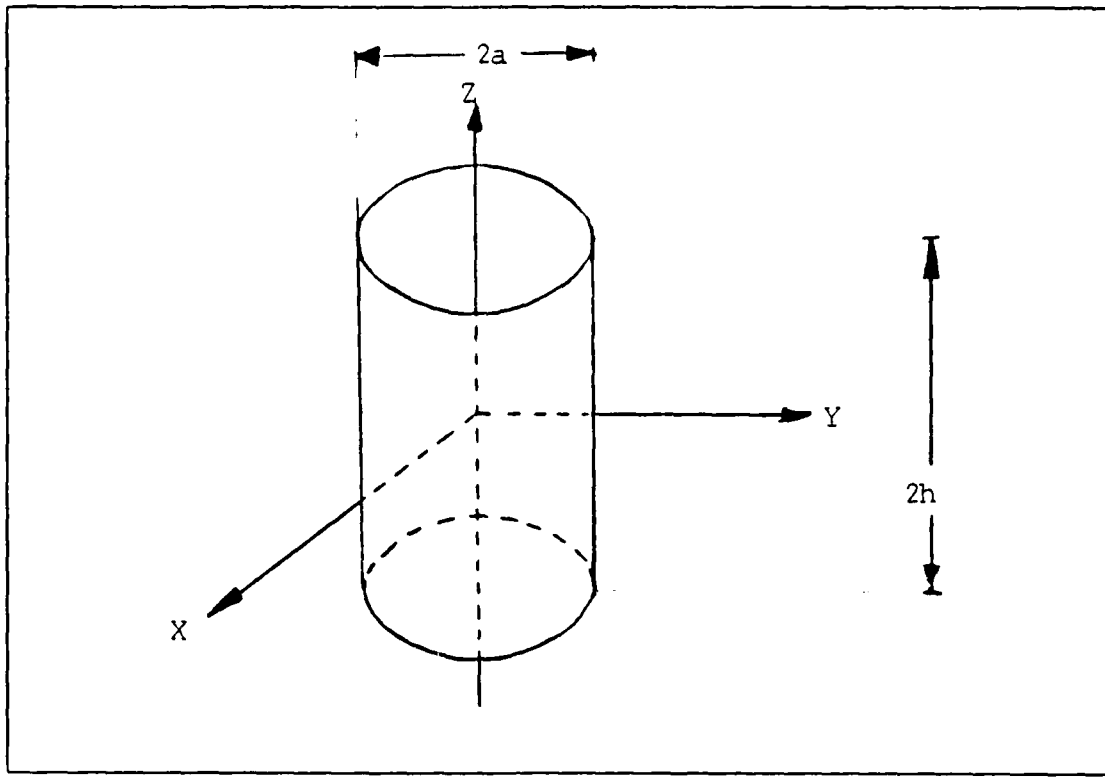


Figure 2.2 Cylinder in Cartesian Coordinates

$$K_z(\phi, z) = \sum_{n=-\infty}^{\infty} K_{zn}(z) \exp(in\phi) = \quad (2.2)$$

$$= \sum_{n=0}^{\infty} K_{zn}^{(+)}(z) \cos(n\phi) + i K_{zn}^{(-)}(z) \sin(n\phi)$$

Where-  $K_{z0}^{(+)}(z) = K_{z0}(z)$   $K_{z0}^{(-)}(z) = 0$   $(2.2 \text{ a})$

$$K_{zn}^{(\pm)}(z) = K_{zn}(z) \pm K_{z(-n)}(z) \quad n \neq 0 \quad (2.2 \text{ b})$$

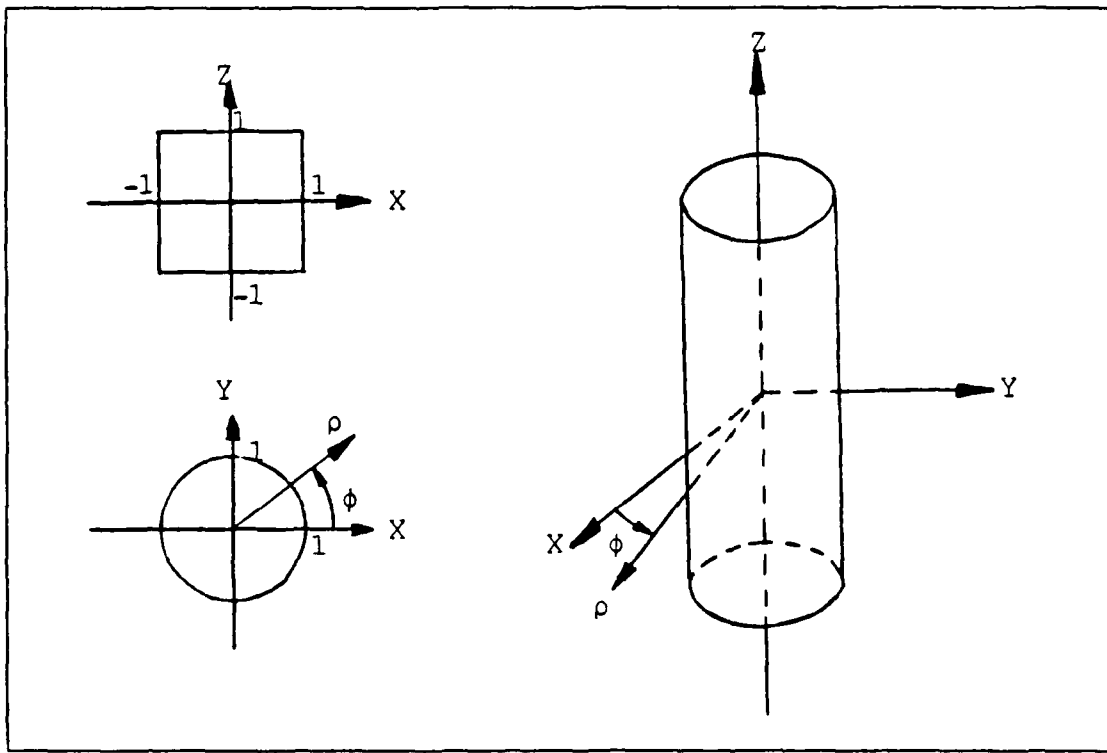


Figure 2.3 Cylinder in Cylindrical Coordinates

$$K_{\phi}(\phi, z) = \sum_{n=-\infty}^{\infty} K_{\phi n}(z) \exp(in\phi) = \quad (2.3)$$

$$= \sum_{n=0}^{\infty} K_{\phi n}^{(+)}(z) \cos(n\phi) + i K_{\phi n}^{(-)}(z) \sin(n\phi)$$

Where-  $K_{\phi 0}^{(+)}(z) = K_{\phi 0}(z)$   $K_{\phi 0}^{(-)}(z) = 0$   $(2.3 \text{ a})$

$$K_{\phi n}^{(\pm)}(z) = K_{\phi n}(z) \pm K_{\phi(-n)}(z) \quad n \neq 0 \quad (2.3 \text{ b})$$

On the surface of the cylinder  $z$  takes on values in the range of  $-1 \leq z \leq +1$  and thus we can represent  $z$  by  $z = \cos(\nu)$  where  $0 \leq \nu \leq \pi$ . Near the edges  $z = \pm 1$ , the current density in  $\phi$  direction approaches  $(1 - z^2)^{-1/2}$  and in  $z$  direction approaches  $(1 - z^2)^{+1/2}$  because of the edge conditions. This leads to the definitions of  $K_{zn}^p$  and  $K_{\phi n}^p$  in equations 2.4 and 2.5.  $K_{zn}^{(\pm)p}$  can be defined by 2.2 a , 2.2 b ; and  $K_{\phi n}^{(\pm)p}$  by 2.3 a , 2.3 b.

$$K_{zn}(z) = (1/\pi) \sum_{p=0}^{\infty} K_{zn}^p \sin[(p+1)\nu] \quad (2.4)$$

$$K_{\phi n}(z) = (1/\pi \sin \nu) \sum_{p=0}^{\infty} K_{\phi n}^p \cos(p\nu) \quad (2.5)$$

The surface current that described here in terms of  $K_{zn}^p$  2.4 and  $K_{\phi n}^p$  in 2.5 is the sum of the inside and outside surface currents. The inside surface current is on  $\rho = 1^-$  while the outside surface current is on  $\rho = 1^+$ . The radiations due to these currents together with the incident electric field  $E_i$  should satisfy the boundary conditions of Maxwell's theory. For a tubular cylinder in a medium with homogeneous, isotropic permittivity  $\epsilon$  and permeability  $\mu$  the relations among the tangential components of the electric fields and the surface current can be written as 2.6 , 2.7 , 2.8 and 2.9 [Ref. 8].

$$(1 + \frac{1}{l_1^2} \frac{\partial^2}{\partial z^2}) \int_{-1}^1 dz_0 K_{zn}(z_0) G_n(l_1 |z - z_0|, l_2) \quad (2.6)$$

$$+ \frac{i n}{l_1 l_2} \frac{\partial}{\partial z} \int_{-1}^1 dz_0 K_{\phi n}(z_0) G_n(l_1 |z - z_0|, l_2) =$$

$$= -(2i/l_1 l_2 \zeta_0) E_{zn}^s(z)$$

$$-\int_{-1}^1 dz_0 K_{\phi n}(z_0) \{ 1/2 [G_{n-1}(l_1|z-z_0|, l_2)$$

$$+ G_{n+1}(l_1|z-z_0|, l_2)] - \frac{n^2}{l_2^2} G_n(l_1|z-z_0|, l_2)\}$$

$$+ (in/l_1 l_2) \frac{\partial}{\partial z} \int_{-1}^1 dz_0 K_{zn}(z_0) G_n(l_1|z-z_0|, l_2)$$

$$= -(2i/l_1 l_2 \xi_0) E_{\phi n}^s(z)$$

$$E_{zn}^s(z) + E_{zn}^i(z) = 0 \quad -1 < z < +1 \quad (2.8)$$

$$E_{\phi n}^s(z) + E_{\phi n}^i(z) = 0 \quad -1 < z < +1 \quad (2.9)$$

Where:  $l_1 = kh = 2\pi h/\lambda$

$$l_2 = ka = 2\pi a/\lambda$$

$$\xi_0 = (\mu/\epsilon)^{1/2}$$

$$G_n(l_1|z-z_0|, l_2) =$$

$$\frac{1}{2\pi} \int_{-\pi}^{\pi} (d\phi/2\pi) \exp[-in(\phi-\phi_0)] G[l_1|z-z_0|, 2l_2|\sin(\phi-\phi_0)/2|]$$

$$G(x_1, x_2) = \{\exp[i(x_1^2+x_2^2)^{1/2}]\} / (x_1^2+x_2^2)^{1/2}$$

Equations 2.6 and 2.7 can be obtained from the Stratton-Chu equations [Refs. 9,4 pp. 99-107,464], together with the edge condition that  $K_z(\phi, z) = 0(1-z^2)^{1/2}$  as  $|z| \rightarrow 1$ . Equations 2.8 and 2.9 are boundary conditions for the tangential electric field components on a perfectly conducting surface.

Equation 2.6 , 2.7 , 2.8 and 2.9 give the connection between the current density on the cylinder surface and the electric fields on the surface. For the back scattering cross section, the far field should be obtained. Denote an arbitrary point in the far field  $(\rho, \phi, z)$  by the vector  $\mathbf{r}$  and a point on the cylinder surface by the vector  $\mathbf{r}_0$ , then in the far field:

$$k|\vec{r}| = (l_2^2 \rho^2 + l_1^2 z^2)^{1/2} \gg 1 \quad (2.10)$$

$$k|\vec{r}| \gg (l_1^2 + l_2^2)^{1/2} \geq k|\vec{r}_0|$$

The scattered far field at point  $\mathbf{r}$  will be 2.11 , 2.12 and 2.13 where  $\theta$  is the angle between the  $z$  axis and the vector  $\mathbf{r}$ .

$$-(2i/l_1 l_2 \zeta_0) E_z(\rho, \phi, z) = \quad (2.11)$$

$$= \sin^2 \theta \int_{-1}^1 dz_0 \int_{-\pi}^{\pi} (d\phi_0 / 2\pi) G(\vec{r} - \vec{r}_0) K_z(\phi_0, z_0)$$

$$- \sin \theta \cos \theta \int_{-1}^1 dz_0 \int_{-\pi}^{\pi} (d\phi_0 / 2\pi) G(\vec{r} - \vec{r}_0) \sin(\phi - \phi_0) K_\phi(\phi_0, z_0)$$

$$-(2i/l_1 l_2 \zeta_0) E_\rho(\rho, \phi, z) = \quad (2.12)$$

$$\begin{aligned} &= -\sin\theta \cos\theta \int_{-1}^1 dz_0 \int_{-\pi}^{\pi} (d\phi_0/2\pi) G(\vec{r}-\vec{r}_0) K_z(\phi_0, z_0) \\ &\quad + \cos^2\theta \int_{-1}^1 dz_0 \int_{-\pi}^{\pi} (d\phi_0/2\pi) G(\vec{r}-\vec{r}_0) \sin(\phi-\phi_0) K_\phi(\phi_0, z_0) \end{aligned}$$

$$-(2i/l_1 l_2 \zeta_0) E_\phi(\rho, \phi, z) = \quad (2.13)$$

$$= \int_{-1}^1 dz_0 \int_{-\pi}^{\pi} (d\phi_0/2\pi) G(\vec{r}-\vec{r}_0) \cos(\phi-\phi_0) K_\phi(\phi_0, z_0)$$

To simplify the equations, spherical coordinate would be used; with the electric field components  $E_r(r, \theta, \phi)$ ,  $E_\theta(r, \theta, \phi)$  and  $E_\phi(r, \theta, \phi)$ .

Since:

$$E_r(r, \theta, \phi) = E_\rho(\rho, \phi, z) \sin\theta + E_z(\rho, \phi, z) \cos\theta \quad (2.14)$$

$$E_\theta(r, \theta, \phi) = E_\rho(\rho, \phi, z) \cos\theta - E_z(\rho, \phi, z) \sin\theta \quad (2.15)$$

The field components in the spherical coordinate are:

$$(-2i/l_1 l_2 \zeta_0) E_r(r, \theta, \phi) = 0 \quad (2.16)$$

$$(-2i/l_1 l_2 \zeta_0) E_\theta(r, \theta, \phi) = \quad (2.17)$$

$$\begin{aligned} &= -\sin\theta \int_{-1}^1 dz_0 \int_{-\pi}^{\pi} (d\phi_0/2\pi) G(\vec{r}-\vec{r}_0) K_z(\phi_0, z_0) \\ &\quad + \cos\theta \int_{-1}^1 dz_0 \int_{-\pi}^{\pi} (d\phi_0/2\pi) G(\vec{r}-\vec{r}_0) \sin(\phi-\phi_0) K_\phi(\phi_0, z_0) \end{aligned}$$

$$(-2i/l_1 l_2 \zeta_0) E_\phi(r, \theta, \phi) = \quad (2.18)$$

$$= \int_{-1}^1 dz_0 \int_{-\pi}^{\pi} (d\phi_0 / 2\pi) G(\vec{r} - \vec{r}_0) \cos(\phi - \phi_0) K_\phi(\phi_0, z_0)$$

Where  $G(\vec{r} - \vec{r}_0)$  are approximated by 2.19 in the far field.

$$G(\vec{r} - \vec{r}_0) = \quad (2.19)$$

$$= G(\vec{r}) \exp[-il_2 \sin \theta \cos(\phi - \phi_0)] \exp[-il_1 \cos \theta z_0]$$

$$G(\vec{r}) = \exp[ikr]/kr$$

Since:

$$\int_{-\pi}^{\pi} (d\phi / 2\pi) \cos(n\phi) \exp[-il_2 \sin \theta \cos(\phi - \phi_0)] = i^{-n} J_n(l_2 \sin \theta)$$

and

$$\int_{-1}^1 (dz / \pi \sqrt{1-z^2}) \cos(pv) \exp[-il_1 \cos(\theta) z_0] =$$

$$= \int_0^\pi (dv / \pi) \cos(pv) \exp[il_1 \cos(\theta) \cos v] = i^{-p} J_p(l_1 \cos \theta)$$

and by using  $K_{zn}^p$  and  $K_{\phi n}^p$  from equations 2.4 and 2.5 , the fields in the far field region can be written as equations 2.20 2.21 and 2.22 .

$$E_r(r, \theta, \phi) = 0 \quad (2.20)$$

$$[-2i/l_1 l_2 \zeta_0 G(\vec{r})] E_\theta(r, \theta, \phi) = \quad (2.21)$$

$$= - \sum_{n=0}^{\infty} \sum_{p=0}^{\infty} i^{-(n+p)} [(p+1)\sin\theta/l_1 \cos\theta] J_{p+1}(l_1 \cos\theta) J_n(l_2 \sin\theta)$$

$$[K_{zn}^{(+)} e^{in\phi} + i K_{zn}^{(-)} p \sin(n\phi)]$$

$$+ \sum_{n=1}^{\infty} \sum_{p=0}^{\infty} i^{-(n+p)} [n \cos\theta/l_2 \sin\theta] J_p(l_1 \cos\theta) J_n(l_2 \sin\theta)$$

$$[K_{pn}^{(-)} e^{in\phi} + i K_{pn}^{(+)} p \sin(n\phi)]$$

$$[-2i/l_1 l_2 \zeta_0 G(\vec{r})] E_\phi(r, \theta, \phi) = \quad (2.22)$$

$$= \sum_{n=0}^{\infty} \sum_{p=0}^{\infty} i^{-(n+p)} J_p(l_1 \cos\theta) J_n'(l_2 \sin\theta) [-K_{pn}^{(-)} p \sin(n\phi) + i K_{pn}^{(+)} p \cos(n\phi)]$$

At this point the scattered field in the far field region is written in terms of the Fourier series expansion of the surface current flowing on the cylinder. To calculate the back scattering cross section of a cylinder the incident wave should be inspected as in equation 2.1 . With a linearly polarized plane incident wave on the target having unit strength and zero phase at the center of the target, the cross section is given by equation 2.23 and the phase shift is given by equation 2.24 .

$$\sigma = \lim_{r \rightarrow \infty} 4\pi r^2 |E_s|^2 \quad (2.23)$$

$$\delta = \arg\{E_s \exp[-ikr]\} \quad (2.24)$$

In the special case of broadside incidence with polarization along the cylinder axis, which contained the z axis, the propagation vector  $\mathbf{k}$  is given by equation 2.25 and the incident field on the surface of the cylinder by equation 2.26 .

$$\hat{\mathbf{k}} = \hat{\mathbf{k}}_x \quad (2.25)$$

$$\vec{E}_i = \hat{\mathbf{z}} \cdot \exp[i\mathbf{k}\mathbf{x}] = \hat{\mathbf{z}} \cdot \exp[ik \cos(\phi)] \quad (2.26)$$

Since  $E_z^i$  is an even function in  $\phi$ ,  $K_{zn}^{(-)}(z) = 0$  and from 2.6 and 2.7 , only  $K_{\phi n}^{(-)}(z)$  is coupled to  $K_{zn}^{(+)}(z)$ . Thus  $K_{\phi n}^{(+)} = 0$ .

In the far field the back scattered field has the components  $E_\theta$  and  $E_\phi$  as shown on 2.27 and 2.28 and a total back scattered field as in 2.29 .

$$[-2i/l_1 l_2 \zeta_0 G(\vec{r})] E_\theta^s(r, \theta, \phi) = \quad (2.27)$$

$$= \sum_{n=0}^{\infty} \sum_{p=0}^{\infty} i^{-n} (-1)^{p+1} [(2p+1) \sin \theta / l_1 \cos \theta]$$

$$J_{2p+1}(l_1 \cos \theta) J_n(l_2 \sin \theta) K_{zn}^{(+)} e^{2p \cos(n\phi)} + \sum_{n=1}^{\infty} \sum_{p=0}^{\infty} i^{-n+1} (-1)^{p+1}$$

$$[n \cos \theta / l_2 \sin \theta] J_{2p+1}(l_1 \cos \theta) J_n(l_2 \sin \theta) K_{\phi n}^{(-)} e^{2p+1 \cos(n\phi)}$$

$$[-2i/l_1 l_2 \zeta_0 G(\vec{r})] E_\phi^s(r, \theta, \phi) = \quad (2.28)$$

$$= \sum_{n=1}^{\infty} \sum_{p=0}^{\infty} i^{-n+1} (-1)^p J_{2p+1}(l_1 \cos \theta) J_n'(l_2 \sin \theta) K_{\phi n}^{(-)} e^{2p+1 \sin(n\phi)}$$

$$[-2i/l_1 l_2 \zeta_0 G(\vec{r})] \hat{z} \vec{E}_{sc}(r, \pi/2, \pi) = \\ +1/2 \sum_{n=0}^{\infty} i^n J_n(l_2) K_{zn}^{(+),0}$$

Using equations 2.23 and 2.24 with 2.29 ,the back scattered cross section and the phase shift of a tubular cylinder is given by 2.30 and 2.31 .

$$\sigma/ah = \\ = \lim_{r \rightarrow \infty} (4\pi r^2/ah) \left| [l_1 l_2 \zeta_0 G(\vec{r})/-2i] 1/2 \sum_{n=0}^{\infty} i^n J_n(l_2) K_{zn}^{(+),0} \right|^2 \\ = (4\pi r^2/ah k^2 r^2) \left| (l_1 l_2 \zeta_0 /4) \sum_{n=0}^{\infty} i^n J_n(l_2) K_{zn}^{(+),0} \right|^2 \\ = \left| (4\pi^2 \zeta_0 / l_1 l_2) \sum_{n=0}^{\infty} i^n J_n(l_2) K_{zn}^{(+),0} \right|^2$$

$$\delta = \\ = \arg \{ [\exp(-ikr) G(\vec{r}) l_1 l_2 \zeta_0 / -2i] 1/2 \sum_{n=0}^{\infty} i^n J_n(l_2) K_{zn}^{(+),0} \} \\ = \arg \{ [\exp(-ikr) G(\vec{r}) / i] \sum_{n=0}^{\infty} i^n J_n(l_2) K_{zn}^{(+),0} \} \\ = \arg \{ \sum_{n=0}^{\infty} i^{n-1} J_n(l_2) K_{zn}^{(+),0} \}$$

From equation 2.30 one can see that the back scattered cross section of a tubular cylinder at the broadside aspect angle is depended only on the Fourier components of the axial surface current along the z direction. That assumption was tested against the experimental results and shown in Chapter IV.

### III. MEASUREMENTS

The exact solutions to the back scattering cross sections of targets are known only for few bodies. For almost all cases approximate solutions have to be sought. Experimental verification is the only justification for a good approximation.

The back scattering measurement facility in the Scattering Laboratory of the Naval Postgraduate School is an indoor range designed for model measurements above 2GHz. The distance from the antennas to the target, the target itself and the radar output wavelength are scaled down from life size. One advantage of using the indoor range is the practicability of testing models that are smaller and cheaper than full scale targets, even though tighter specifications on target details have to be met. This chapter deals with the experimental setup, the targets and the measurement procedures.

#### A. SET-UP

Figure 3.1 is a block diagram showing the signal flow of the setup. Table 1 is a list of the equipment in the setup.

The frequency and output power level of the signal generator HP-8672A is controled by an HP-85 Microcomputer. The output RF signal from the signal generator enters an GaAs wide band amplifier which is operated at saturation to provide an output of about 23dBm. The amplified RF signal is then passed through the directional coupler to feed the transmitting horn antenna. The returned signal from the scattered field of the target is collector by the receiving horn antenna to feed the test port of the harmonic frequency

TABLE 1  
Equipment

Microcomputer	HP-85
Flexible Disk Drive	HP-82901M
Plotter	HP-7225B
Synthesized Signal Generator	HP-8672A
RF Amplifier	Ananter SA83-2953
Dual DC Power Supply	HP-6227B
Digital Multimeter	HP-3466A
Directional Coupler	Narda 5292
Transmitting Antenna	
Receiving Antenna	
Harmonic Frequency Converter	HP-8411A
Network Analyzer	HP-8410C
Phase Magnitude Display	HP-8412B
Digital Voltmeter	HP-3455A
Digital Voltmeter	HP-3456A
HP Interface Bus	
Coaxial Cables	

converter, HP-8411A. The portion of the transmitting signal coupled out through the directional coupler, is attenuated to get 43dB attenuation before it is fed to the reference port of the harmonic frequency converter. The harmonic frequency converter and the network analyzer HP-8410C, with the phase-magnitude display HP-8412B function as a phase difference and magnitude ratio meter between the transmitting and receiving signals. The phase difference and the magnitude ratio are converted to volts that are measured by the digital voltmeters HP-3456A and HP-3455A. The digital word from the voltmeters is then transferred to the microcomputer for processing and then displayed on the plotter HP-82901M.

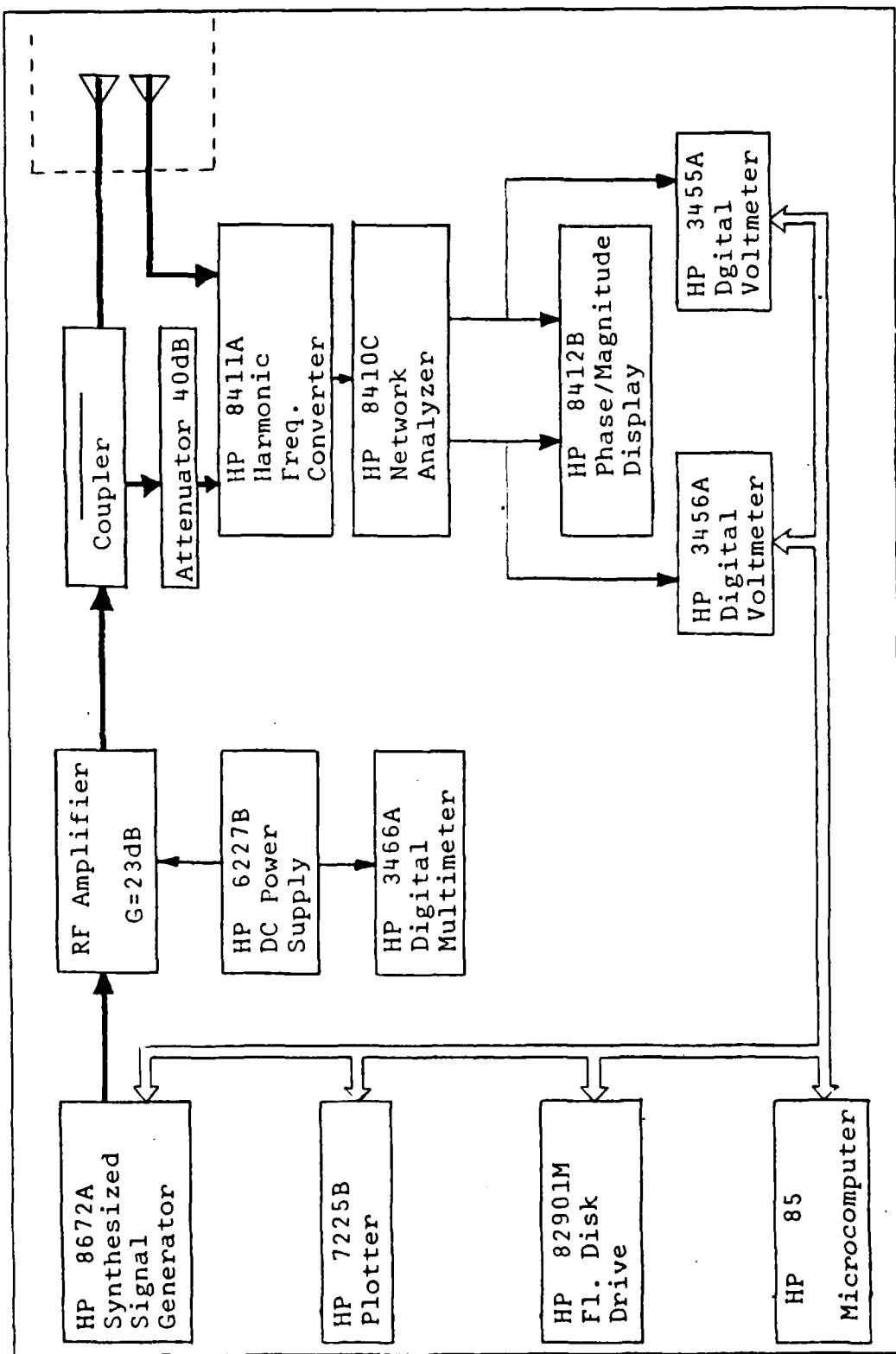


Figure 3.1 Signal Flowing Diagram

The antennas used in this system are identical linearly polarized horn antennas. The scattered electric field from a target has three components. An antenna will pick a linear combination of the components and couple it to the receiver through a transmission line.

The polarization of the transmitting and receiving antennas can be represent by the matrixes shown in equations 3.1 and 3.2

$$\hat{q} = \begin{bmatrix} \cos \gamma_t \\ \sin(\gamma_t) \exp(i\delta_t) \end{bmatrix} \quad (3.1)$$

$$\hat{p} = [\cos \gamma_r, \sin \gamma_r \exp(i\delta_r)] \quad (3.2)$$

Where       $\hat{q}$ -Unit column matrix defining the polarization  
of transmitting antenna

$\hat{p}$ -Unit row matrix defining the polarization of  
receiving antenna

$\gamma$ -An angle which donates the orientation of  
the linear polarization refered to the  
horizontal plane

$\delta$ -Phase angle

t-Denotes transmitting antenna

r-Denotes receiving antenna

For linear horizontal polarization the matrices are given by equation 3.3 and 3.4

$$\hat{q} = \begin{bmatrix} 1 \\ 0 \end{bmatrix} \quad (3.3)$$

$$\hat{p} = [1, 0]$$

(3.4)

The target has a complex scattering matrix which is a function of the geometry of the target and the frequency of the incident wave. Assuming a uniform plane incident wave at the target, the scattering matrix is a linear relation between the incident electric field and the scattered far field from the target. The Maxwell equations are linear as long as  $\epsilon$  and  $\mu$  are linear. This is true even if  $\epsilon$  and  $\mu$  are unisotropic and inhomogeneous. The scattering matrix can be written as 3.5

$$S = \begin{bmatrix} \sqrt{\sigma_{HH}} \exp(i\phi_{HH}) & \sqrt{\sigma_{HV}} \exp(i\phi_{HV}) \\ \sqrt{\sigma_{VH}} \exp(i\phi_{VH}) & \sqrt{\sigma_{VV}} \exp(i\phi_{VV}) \end{bmatrix} \quad (3.5)$$

Where  $\sqrt{\sigma}$ -Magnitude of the scattering matrix element  
 $\phi$ -Phase of the scattering matrix element  
H-Denotes horizontal polarization  
v-Denotes vertical polarization

The radar cross section of a target with scattering matrix S and obtained by a pair of transmitting and receiving antennas with polarization  $\hat{q}$  and  $\hat{p}$  respectively will be 3.6

$$\sigma = |\hat{p}S\hat{q}|^2 \quad (3.6)$$

In our system, the antennas are horizontally polarized so that:

$$\sigma = \sigma_{HH} \quad (3.7)$$

The characteristics of these antennas are given in Appendix A. These antennas are mounted on the wall of an anechoic chamber in the Scattering Laboratory at the Naval Postgraduate School. All measurements were taken inside the chamber. The characteristics of the anechoic chamber is given in Appendix B and it was discussed in great detail by Mariategui [Ref. 10].

## B. TARGETS

Figure 3.2 shows the orientation of the cylinder in the anechoic chamber. The antennas-to-target distance was two meters. The targets were a set of tubular circular cylinders made of thin walled brass of various lengths and diameters. Figure 3.3 shows the dimensions of the cylinders.

The back scattering cross section of a tubular cylinder depends on the following parameters:

- (1)The cylinder length ( $2h$ ).
- (2)The cylinder diameter ( $2a$ ).
- (3)The cylinder wall thickness.
- (4)Azimuth aspect angle.
- (5)Cylinder tilt angle.
- (6)Transmitting antenna polarization.
- (7)Receiving antenna polarization.
- (8)Transmitter frequency ( $f$ ).

In the measurements the effects of varying wall thickness was neglected because it was small compared to the wavelengths and other dimensions of the cylinders. The polarization was always parallel to the axis of the cylinder. The remaining three parameters were varied and their effects on the back-scattering cross section of the cylinder were studied. Table 2 gives the characteristics of the targets used in this experiment.

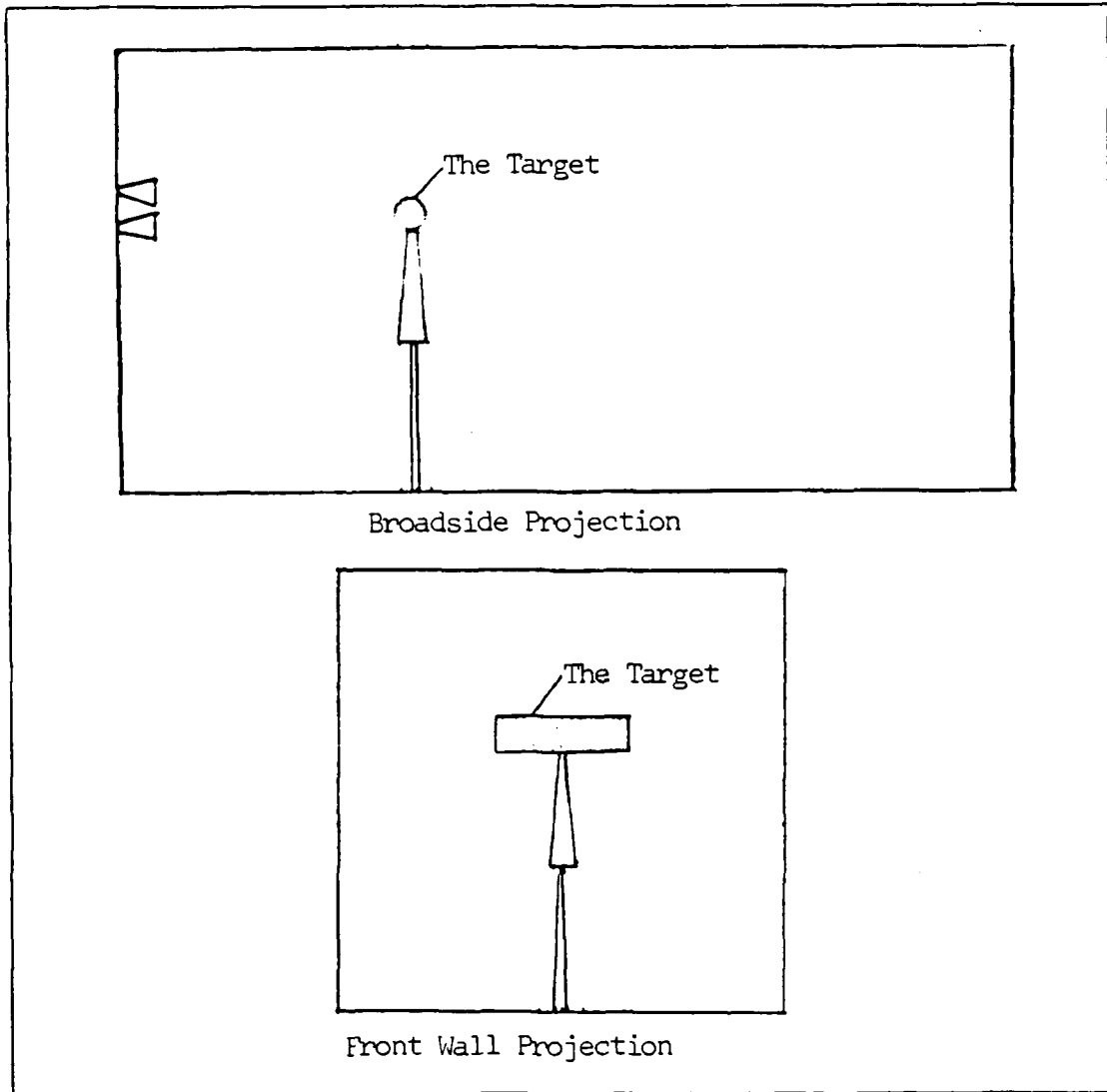


Figure 3.2 Orientation of Targets in Anechoic Chamber

Dimensions of TARGET20 and TARGET21 are shown in Figure 3.4 . These targets are cylinders with four rectangular fins having the dimensions: 0.75x0.375x0.01 inches. The axis of the cylinder coincides with the z axis in both targets while the fins are on the x-y axis in TARGET20 and 45 degrees of the axis in TARGET21.

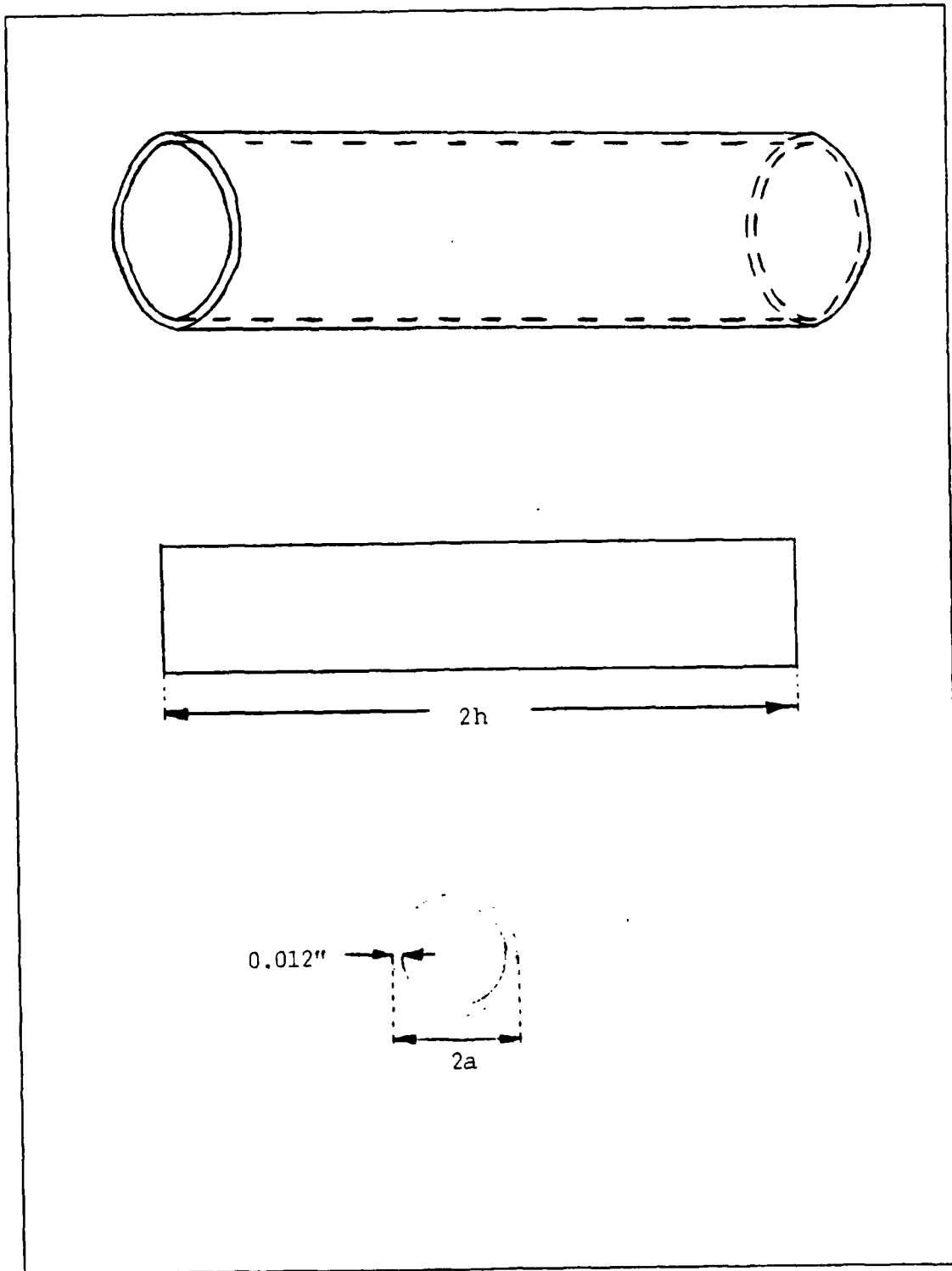


Figure 3.3    Cylinders Dimensions

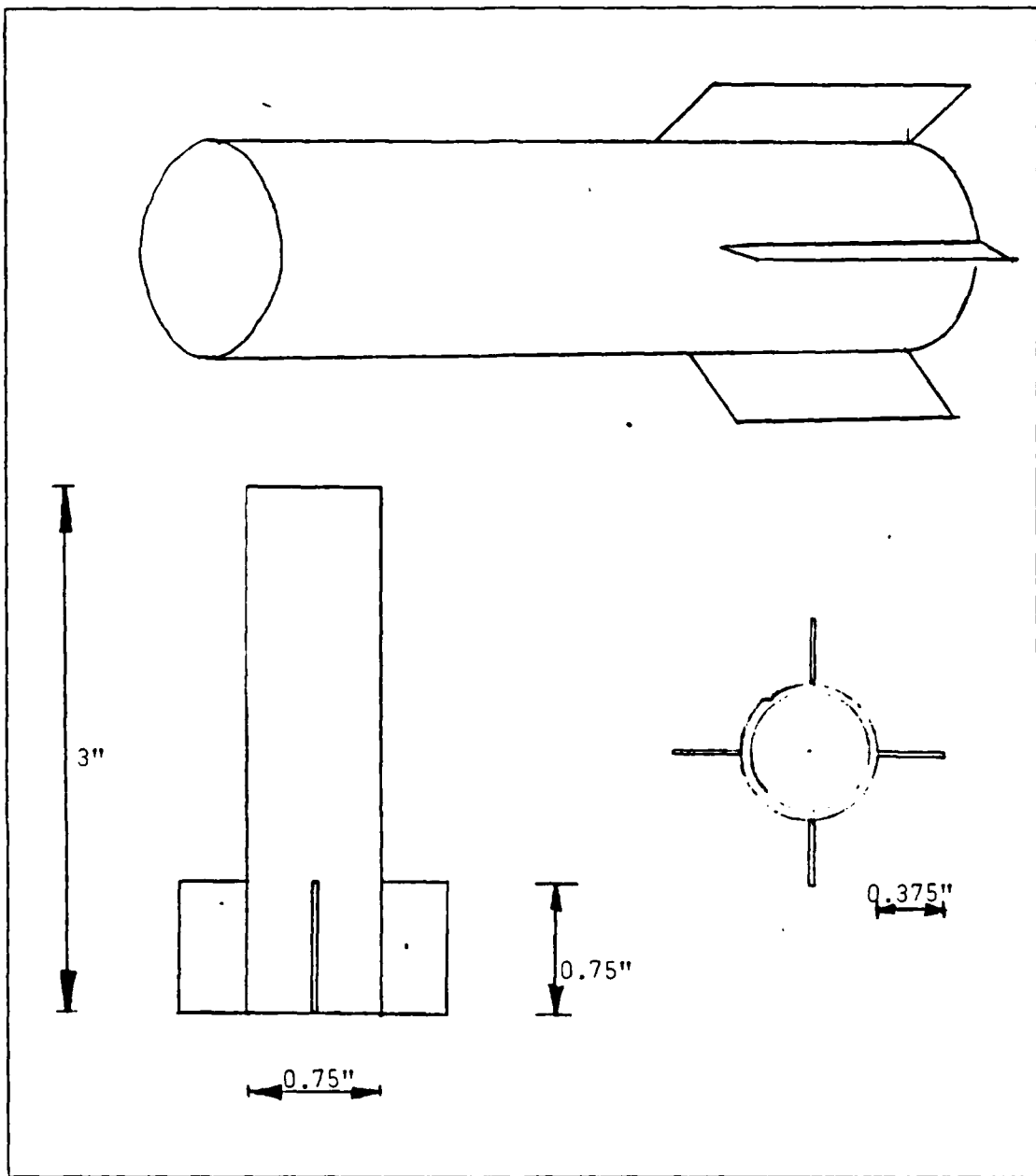


Figure 3.4 The Fins Orientation

TABLE 2  
Targets Description

Name	Description	Length (2h) in inches	Diameter (2a) in inches
TARGET1	Plane cylinder	2.0	0.375
TARGET2	Plane cylinder	2.0	0.5
TARGET3	Plane cylinder	2.0	0.75
TARGET4	Plane cylinder	2.25	0.375
TARGET5	Plane cylinder	2.25	0.5
TARGET6	Plane cylinder	2.25	0.75
TARGET7	Plane cylinder	2.5	0.375
TARGET8	Plane cylinder	2.5	0.5
TARGET9	Plane cylinder	2.5	0.75
TARGET10	Plane cylinder	2.75	0.375
TARGET11	Plane cylinder	2.75	0.5
TARGET12	Plane cylinder	2.75	0.75
TARGET13	Plane cylinder	3.0	0.375
TARGET14	Plane cylinder	3.0	0.5
TARGET15	Plane cylinder	3.0	0.75
TARGET16	Plane cylinder	1.5	0.375
TARGET17	Plane cylinder	4.5	0.75
TARGET18	Plane cylinder	2.5	0.625
TARGET19	Plane cylinder	3.75	0.625
TARGET20	Cylinder with fins	3.0	0.75
TARGET21	Cylinder with fins	3.0	0.75

### C. MEASUREMENT PROCEDURE

The cross section is defined in terms of a uniform plane incident wave. The radiation of the antenna approximates that of a dipole and is not a plane wave. To get a good plane wave approximation, a distance that satisfied 3.8 , 3.9 and 3.10 was chosen. The relationship shown in 3.10 assumed difference of no more then 20 degrees between the phase at the center and the edges of the target [Ref. 11].

$$r \geq 10\lambda \quad (3.8)$$

$$r \geq 10D \quad (3.9)$$

$$r \geq 2D^2/\lambda \quad (3.10)$$

Where r-Antenna to target distance.

D-Maximum dimension of the target.

$\lambda$ -Wavelength of the transmitted wave.

The signal picked up by the receiving antenna is the vectoral sum of the target echo and the background radiation. To cancel the coupling between the antennas and the direct back scattering from the support and the walls, background measurement was carried out by measuring the echo returned when the target was not present. The difference between signals when the target was present and when the target was absent gave the echo signal of the target.

Calibration of the system to take into account the characteristics of the system which are dependent on frequencies and to relate the echo signal power to the target back scattering cross section and phase shift was achieved by

measuring the echo signal from a sphere and comparing the experimental results to theoretical values. The theoretical data was calculated by Mie series computed with the Sphere program [Appendix C]. The calibration was done with the Calib program [Appendix D]. Measurements of back scattering of the target were done with the Target program [Appendix E]. Description and explanations of the computer programs were given by Lolic [Ref. 12].

The instruments add noise to the measurement data. This noise is white noise and to minimize its effects, each target was measured five times and averaged. Before each measurement new calibration was done to minimize the noise effects in the calibration. For phase shift near  $\pm 180$  degrees the average procedure did not take care of the discontinuity properly and the averaged result depended on the number of times the measured values took on +180 or -180 degrees.

Measurement errors that could not be controlled are the coupling between the target and the support and the bistatic coupling which is the strong target scattered lobs in the forward hemisphere (away from the antennas) and then back to the receiving antenna from the walls. The latter effect is believed to have been taken care of through the use of the microwave absorbers.

#### D. MEASURED DATA

The measured results of the 21 targets were plotted and given at the end of this chapter (Figure 3.5 to 3.46). Those plots contained cross section and phase shift versus frequency data, for each target. The theoretical data are given in Tables 3 to 23. The data was used for comparison with theoretical values and it shown in Chapter IV.

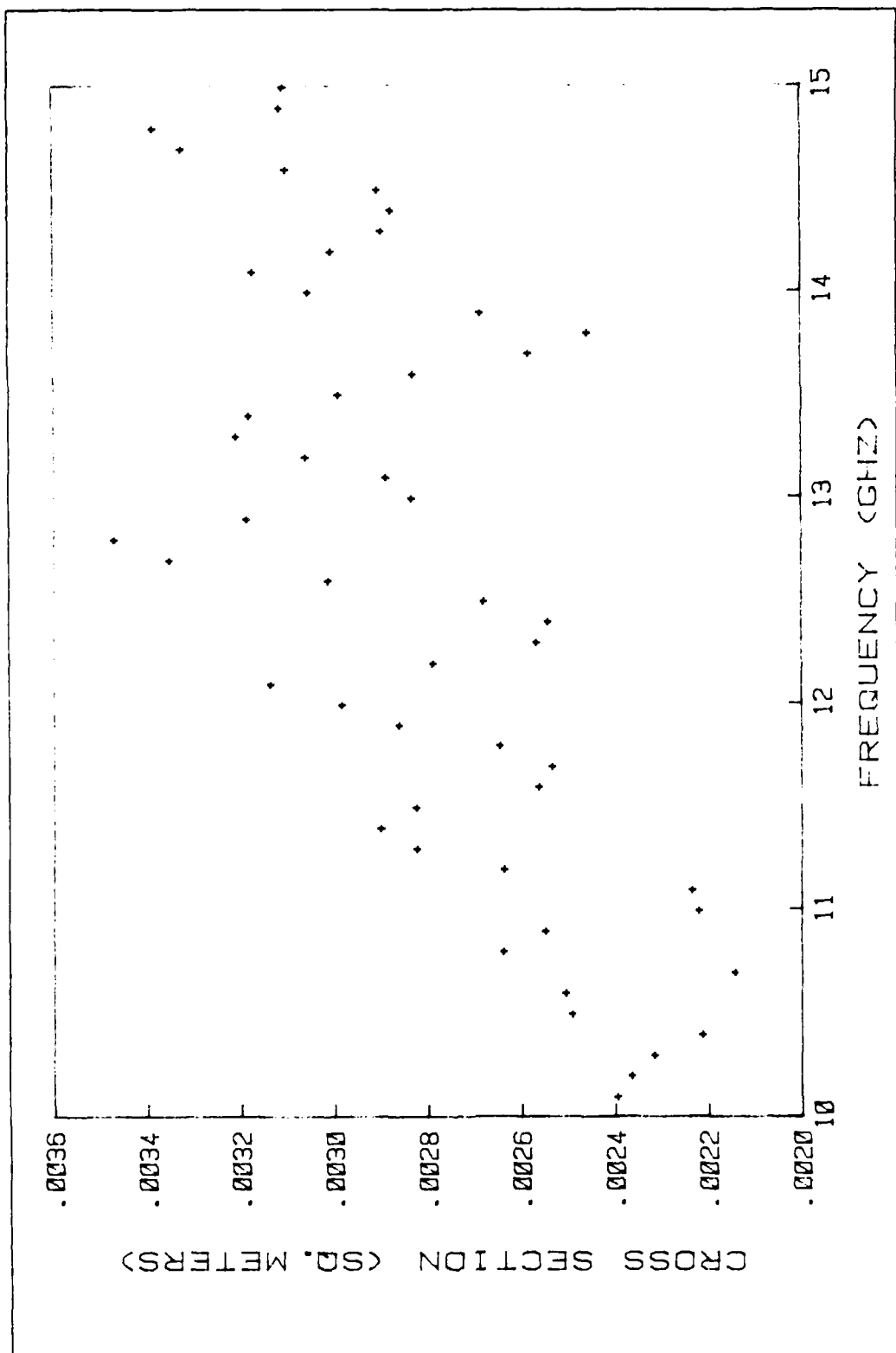


Figure 3.5 TARGET1 Cross-Section vs. Frequency

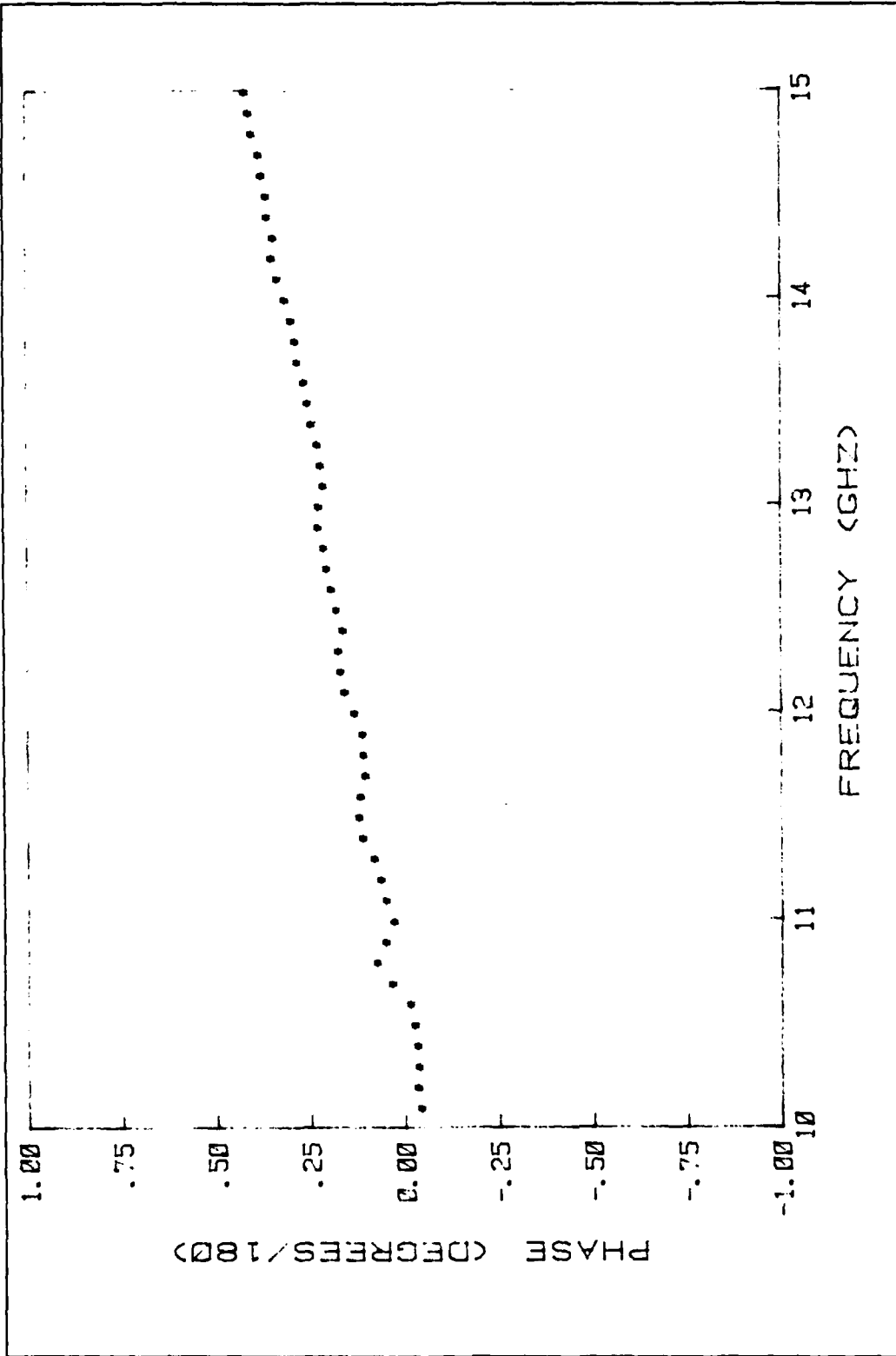


Figure 3.6 TARGET1 Phase Shift vs. Frequency

TABLE 3  
TARGET1 Measured Data

Frequency GHz	Cross-Section sq. meters	Phase Degrees/180
10.10	.00238	- .05747
10.20	.00235	- .04705
10.30	.00238	- .05245
10.40	.00220	- .04795
10.50	.00248	- .04077
10.60	.00249	- .02920
10.70	.00213	.01917
10.80	.00263	.05879
10.90	.00254	.03643
11.00	.00221	.01517
11.10	.00222	.03640
11.20	.00262	.04978
11.30	.00281	.06599
11.40	.00289	.09669
11.50	.00281	.10508
11.60	.00255	.10195
11.70	.00252	.08954
11.80	.00263	.09357
11.90	.00285	.09612
12.00	.00297	.11657
12.10	.00312	.14314
12.20	.00278	.15434
12.30	.00255	.15929
12.40	.00253	.14789
12.50	.00267	.16398
12.60	.00300	.17882
12.70	.00334	.18917
12.80	.00346	.19790
12.90	.00317	.21208
13.00	.00282	.20998
13.10	.00288	.19925
13.20	.00305	.20384
13.30	.00320	.21406
13.40	.00317	.22914
13.50	.00298	.24056
13.60	.00282	.25054
13.70	.00257	.26677
13.80	.00244	.27079
13.90	.00267	.28132
14.00	.00304	.29834
14.10	.00316	.31943
14.20	.00299	.33389
14.30	.00288	.33000
14.40	.00286	.34395
14.50	.00289	.34727
14.60	.00309	.35859
14.70	.00331	.36647
14.80	.00337	.38651
14.90	.00310	.39357
15.00	.00309	.40518

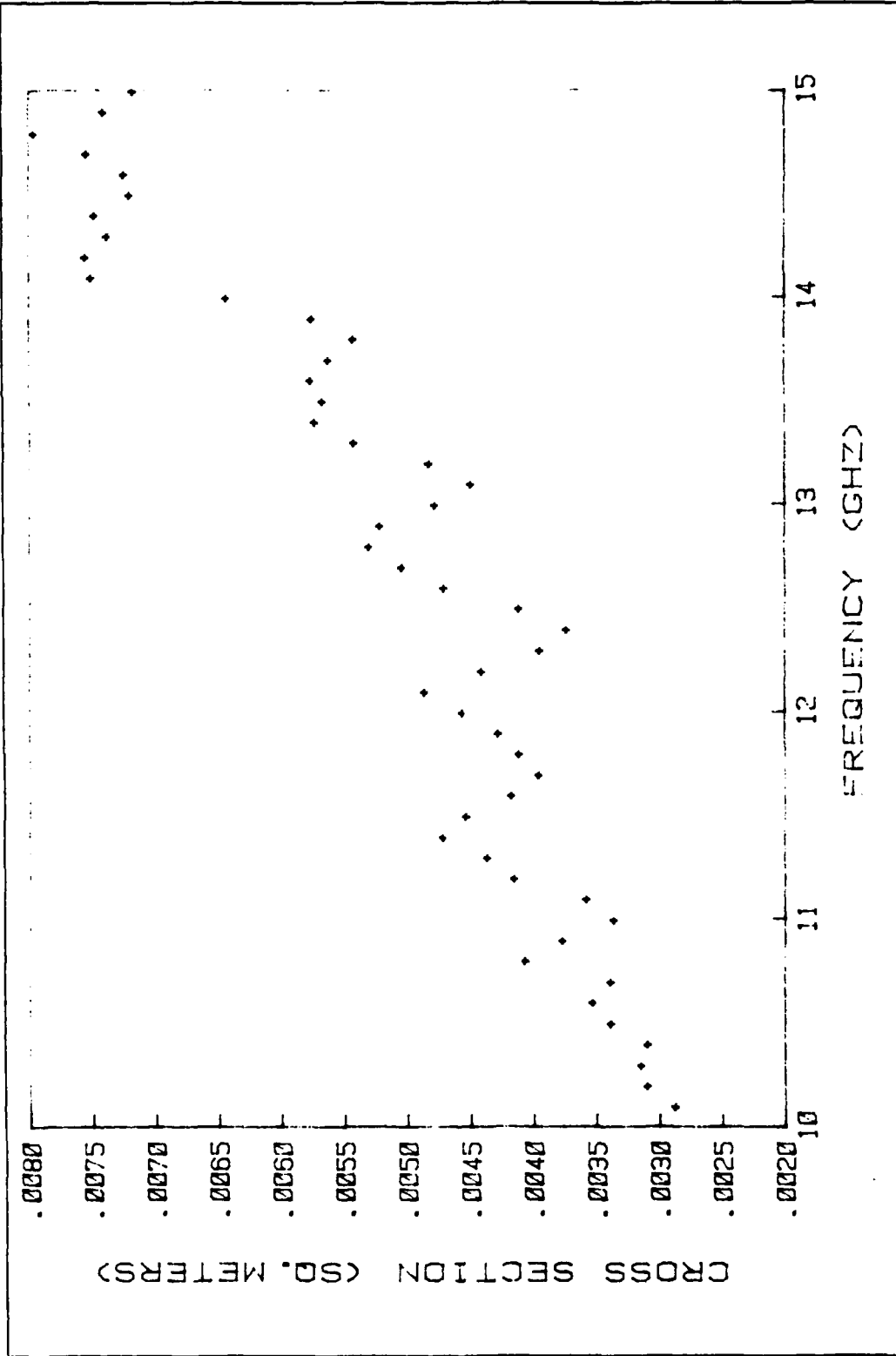


Figure 3.7 TARGET2 Cross-Section vs. Frequency

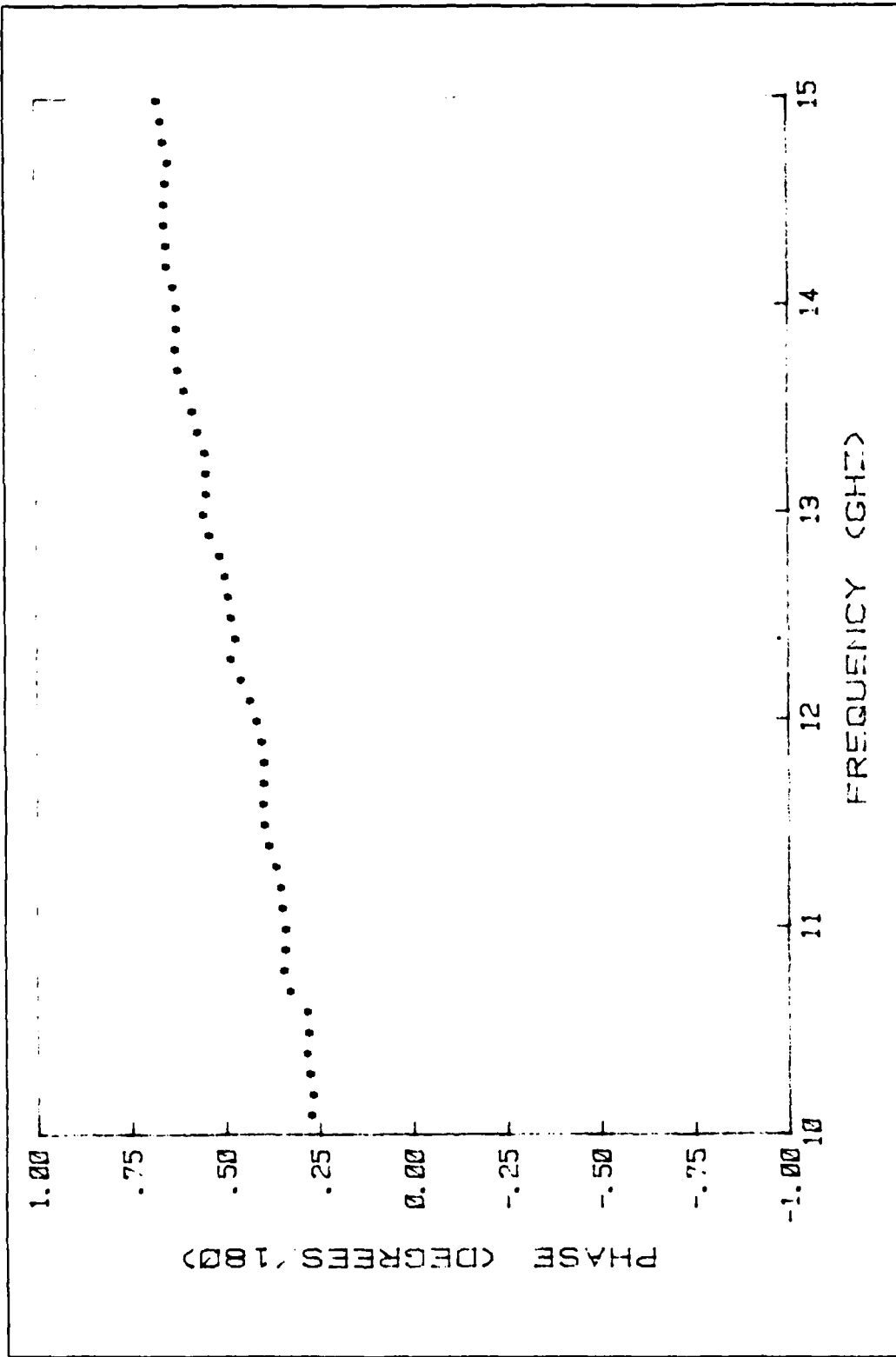


Figure 3.8 TARGET2 Phase Shift vs. Frequency

TABLE 4  
TARGET2 Measured Data

Frequency GHz	Cross-Section sq. meters	Phase Degrees/180
10.10	.00263	25839
10.20	.00305	25361
10.30	.00310	26044
10.40	.00305	26821
10.50	.00334	26394
10.60	.00349	26770
10.70	.00334	31194
10.80	.00402	32953
10.90	.00373	32441
11.00	.00332	32280
11.10	.00354	33313
11.20	.00411	33700
11.30	.00433	34961
11.40	.00467	36858
11.50	.00449	38109
11.60	.00413	38369
11.70	.00392	38388
11.80	.00407	38117
11.90	.00423	38694
12.00	.00452	39964
12.10	.00482	41753
12.20	.00437	44183
12.30	.00391	46831
12.40	.00369	45789
12.50	.00407	46705
12.60	.00467	47535
12.70	.00500	48302
12.80	.00526	49739
12.90	.00518	52512
13.00	.00474	54161
13.10	.00445	53261
13.20	.00478	53143
13.30	.00538	53374
13.40	.00569	55438
13.50	.00563	56610
13.60	.00572	58949
13.70	.00558	60685
13.80	.00538	61336
13.90	.00571	61026
14.00	.00639	61033
14.10	.00747	61938
14.20	.00751	63536
14.30	.00734	63648
14.40	.00744	64144
14.50	.00716	64136
14.60	.00720	63669
14.70	.00750	63151
14.80	.00792	64395
14.90	.00736	64818
15.00	.00713	65966

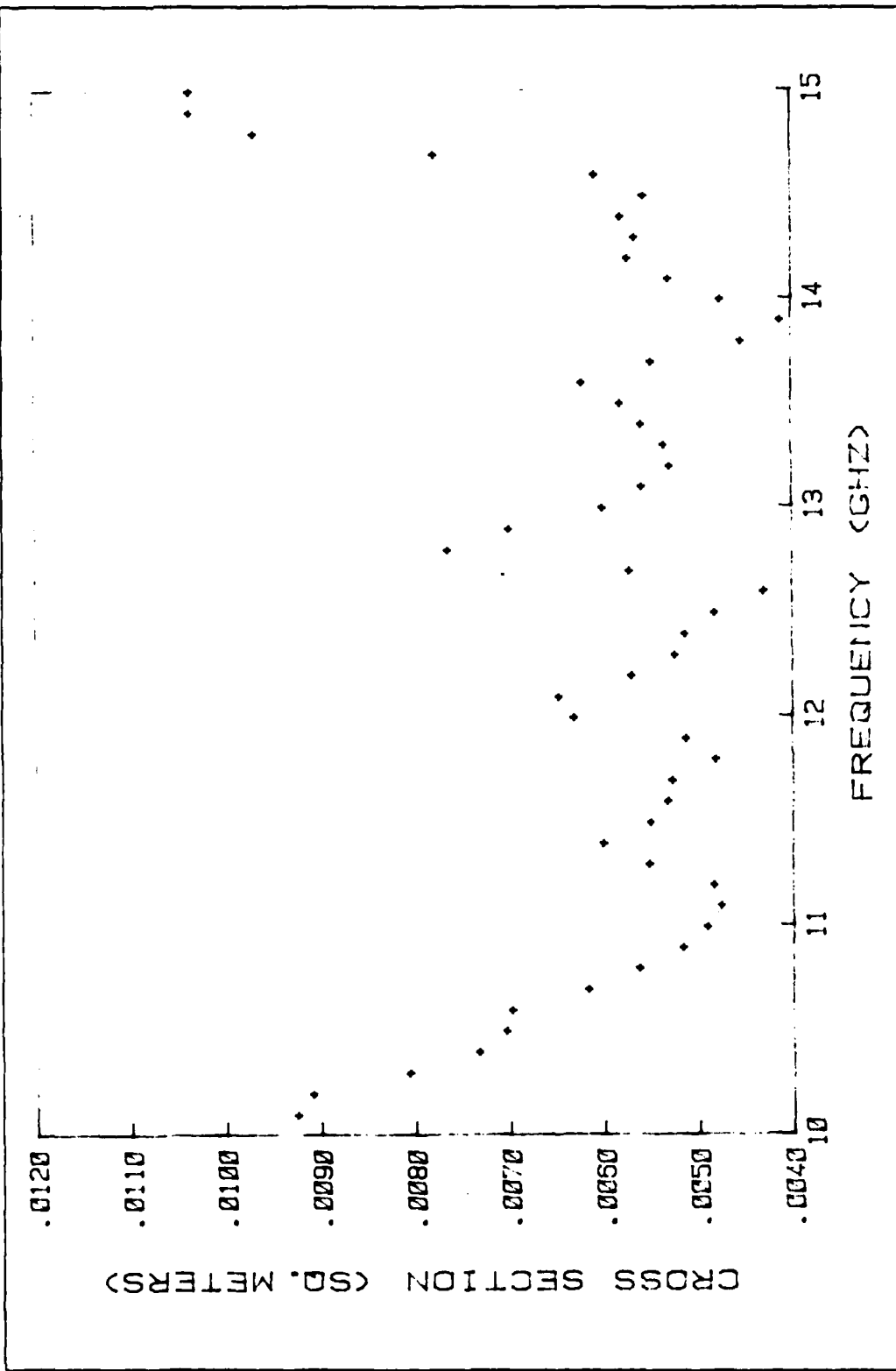


Figure 3.9 TARGET3 Cross-Section vs. Frequency

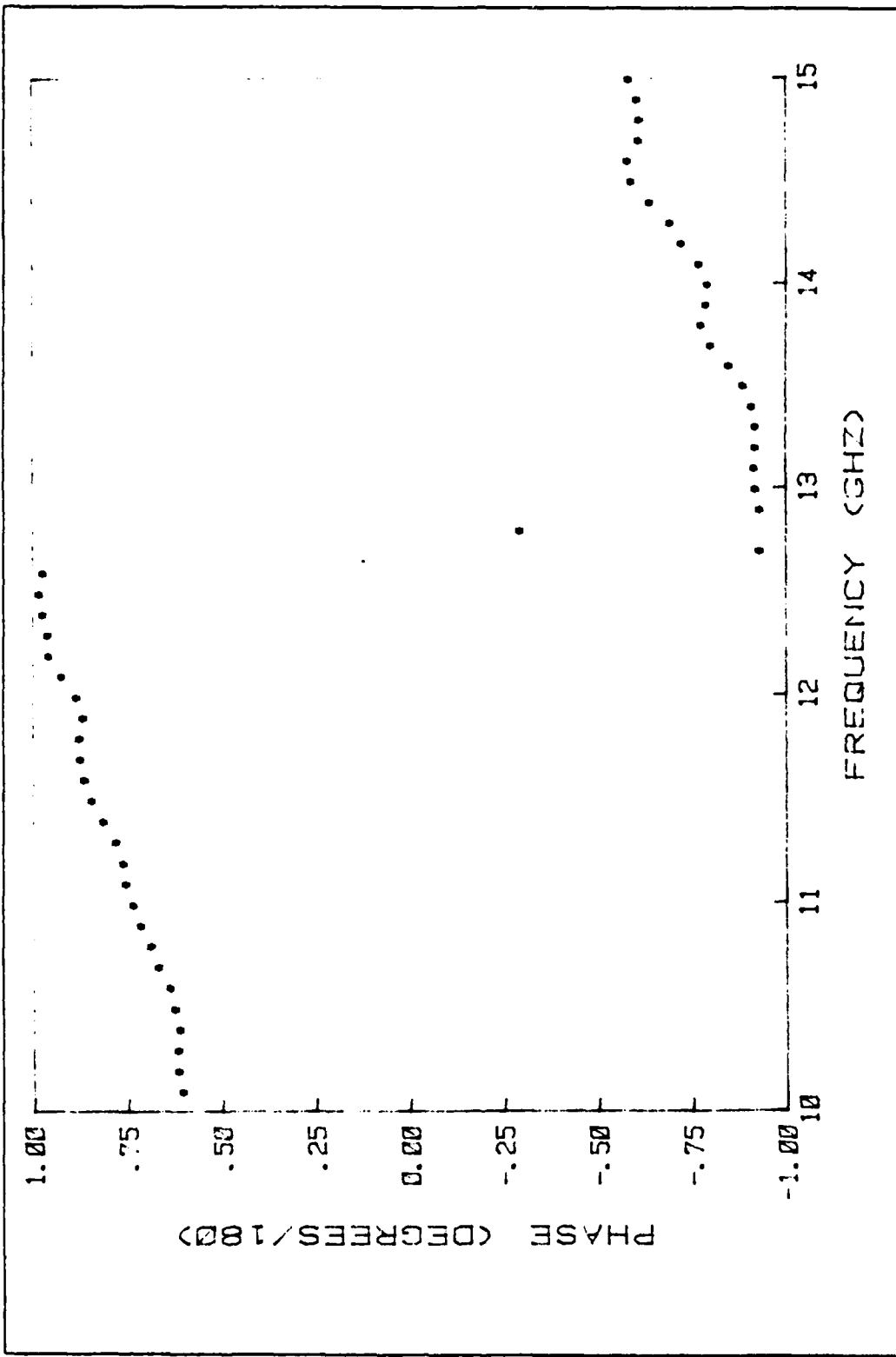


Figure 3.10 TARGET3 Phase Shift vs. Frequency

TABLE 5  
TARGET3 Measured Data

Frequency GHz	Cross-Section sq. meters	Phase Degrees/180
10.10	.00919	.59916
10.20	.00983	.60116
10.30	.00891	.60231
10.40	.00727	.59834
10.50	.00697	.61061
10.60	.00692	.62310
10.70	.00611	.65317
10.80	.00557	.67403
10.90	.00511	.70184
11.00	.00485	.72037
11.10	.00470	.74050
11.20	.00478	.74735
11.30	.00546	.76806
11.40	.00595	.80123
11.50	.00544	.83159
11.60	.00526	.85165
11.70	.00522	.86092
11.80	.00476	.86294
11.90	.00507	.85327
12.00	.00625	.87037
12.10	.00641	.91053
12.20	.00564	.94427
12.30	.00519	.94645
12.40	.00507	.96105
12.50	.00476	.96966
12.60	.00424	.96075
12.70	.00566	- .94413
12.80	.00758	- .30580
12.90	.00693	- .94393
13.00	.00594	- .93251
13.10	.00553	- .93026
13.20	.00523	- .93378
13.30	.00528	- .93329
13.40	.00553	- .92394
13.50	.00575	- .90176
13.60	.00616	- .86260
13.70	.00543	- .81444
13.80	.00447	- .78927
13.90	.00406	- .80316
14.00	.00469	- .80705
14.10	.00524	- .78351
14.20	.00567	- .73735
14.30	.00560	- .70712
14.40	.00574	- .65355
14.50	.00550	- .60520
14.60	.00601	- .59448
14.70	.00771	- .62385
14.80	.00961	- .62583
14.90	.01029	- .61821
15.00	.01029	- .59766

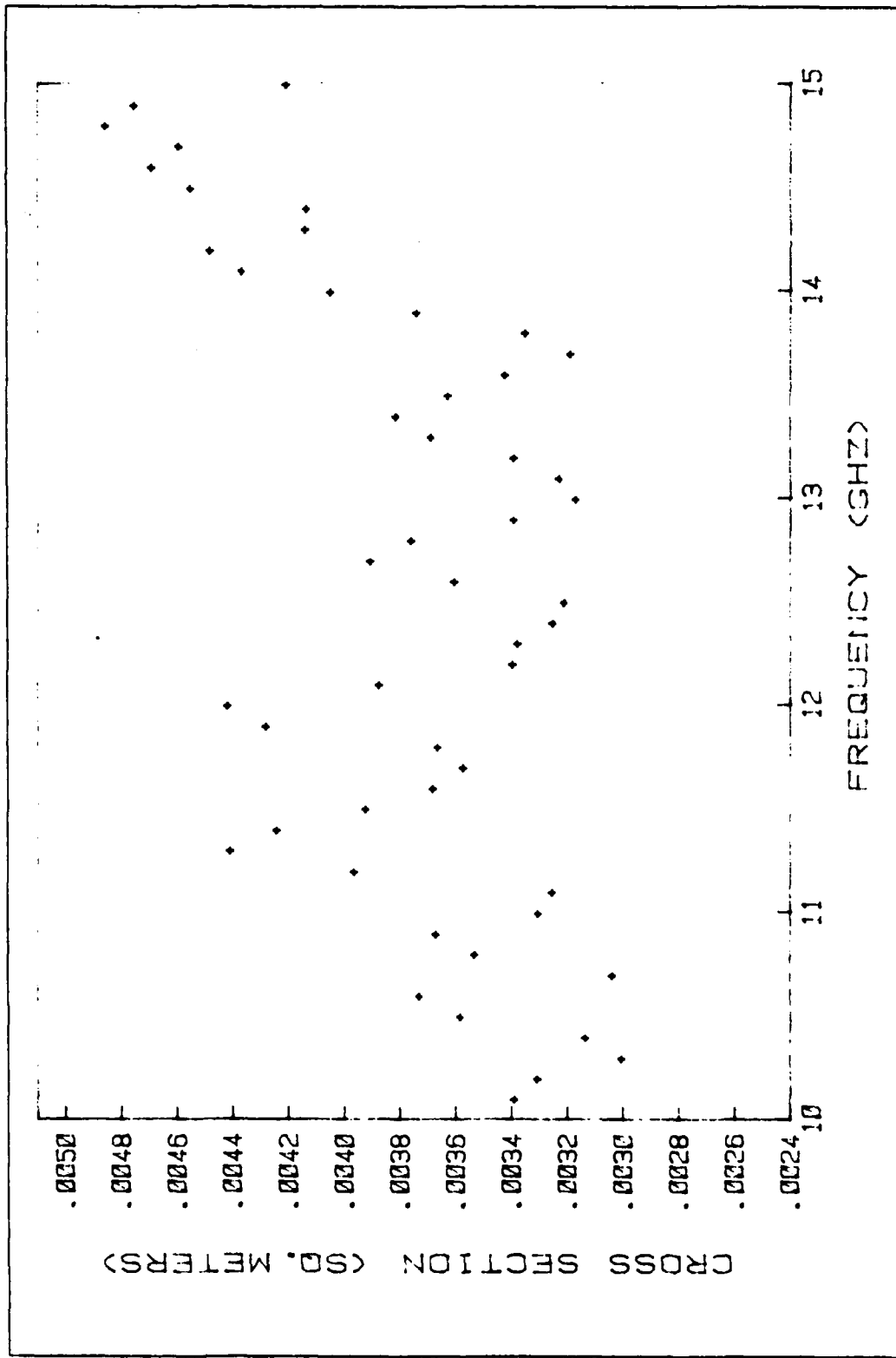


Figure 3.11 TARGET4 Cross-Section vs. Frequency

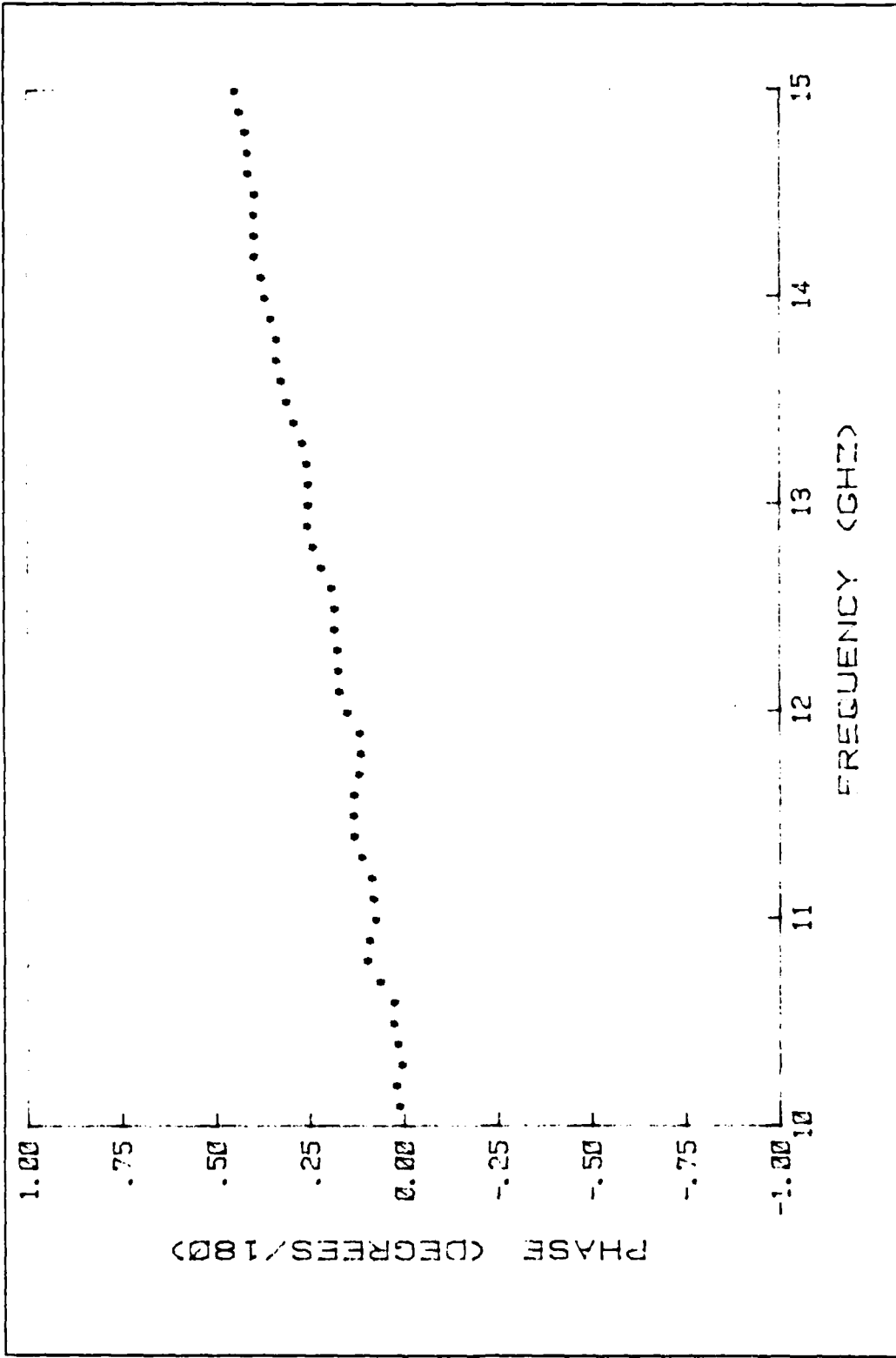


Figure 3.12 TARGET4 Phase Shift vs. Frequency

TABLE 6  
TARGET4 Measured Data

Frequency GHz	Cross-Section sq. meters	Phase Degrees/180
10.10	00337	- 00436
10.20	00329	00483
10.30	00299	- 00987
10.40	00312	- 00010
10.50	00357	01073
10.60	00371	00991
10.70	00302	04786
10.80	00351	08156
10.90	00365	07482
11.00	00329	05894
11.10	00323	06568
11.20	00394	06979
11.30	00439	09606
11.40	00422	11590
11.50	00390	11739
11.60	00366	11727
11.70	00355	10443
11.80	00365	09857
11.90	00426	10173
12.00	00440	13290
12.10	00386	15571
12.20	00338	15796
12.30	00336	16035
12.40	00323	16809
12.50	00319	16850
12.60	00359	17561
12.70	00389	20283
12.80	00374	23522
12.90	00337	23922
13.00	00315	23817
13.10	00321	23797
13.20	00337	24149
13.30	00367	25302
13.40	00380	27507
13.50	00361	29484
13.60	00340	31011
13.70	00317	32144
13.80	00333	32042
13.90	00372	33704
14.00	00403	35147
14.10	00435	36188
14.20	00446	37950
14.30	00412	37973
14.40	00412	38112
14.50	00453	37891
14.60	00467	39663
14.70	00458	39789
14.80	00484	40375
14.90	00474	41391
15.00	00419	43220

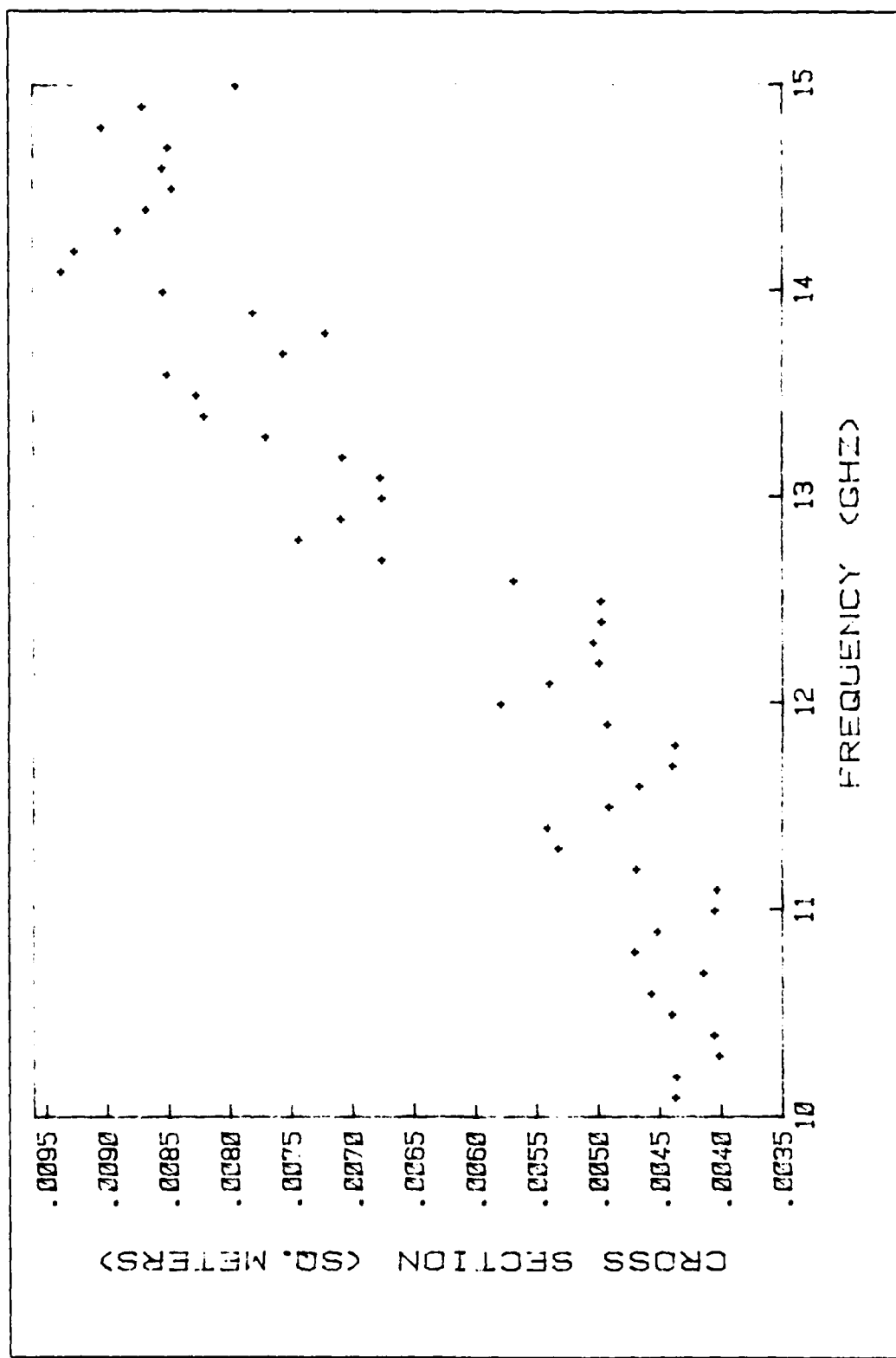


Figure 3.13 TARGET5 Cross-Section vs. Frequency

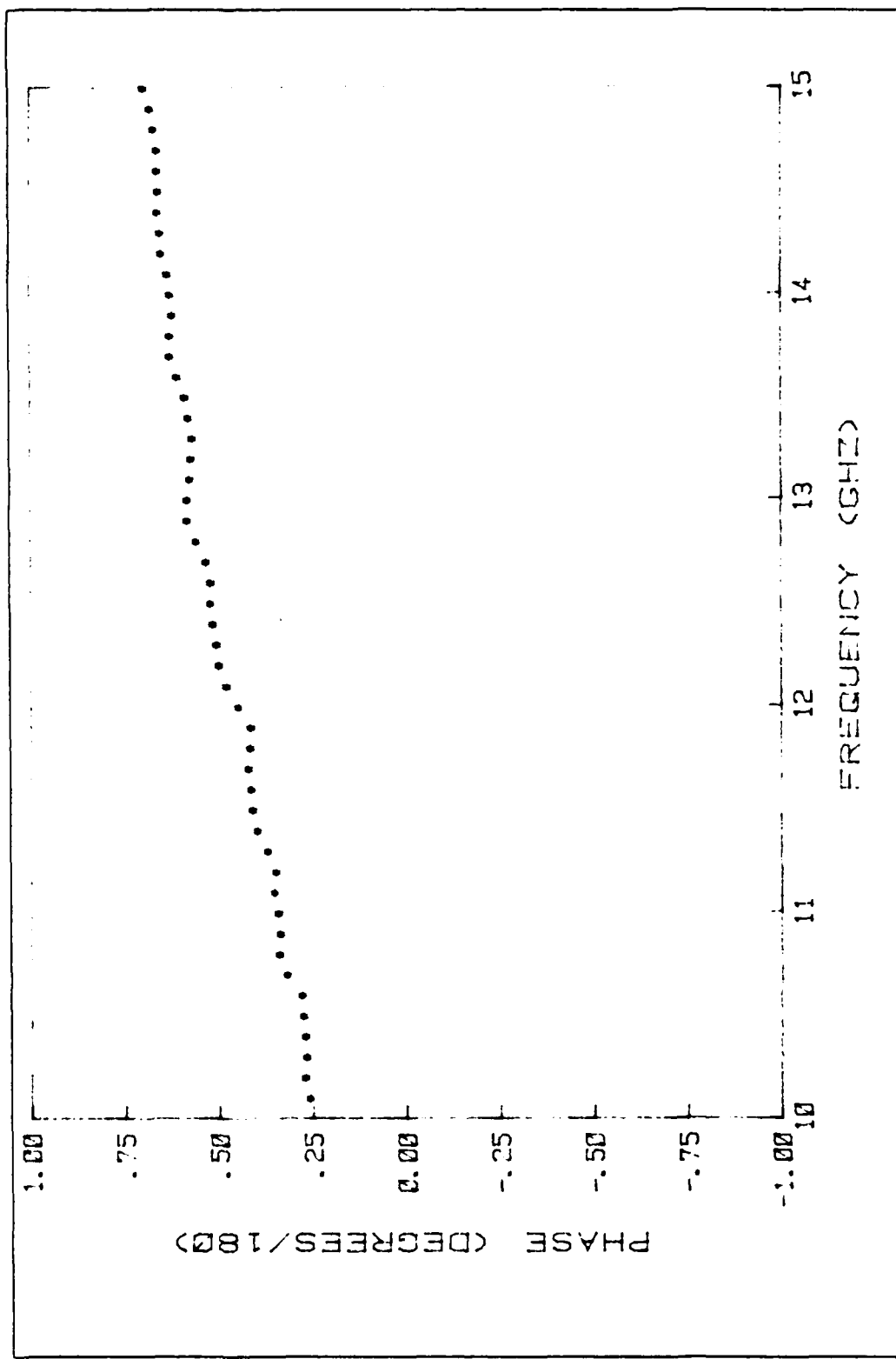


Figure 3.14 TARGET5 Phase Shift vs. Frequency

TABLE 7  
TARGET5 Measured Data

Frequency GHz	Cross-Section sq. meters	Phase Degrees/180
10.10	.00433	.24304
10.20	.00431	.25591
10.30	.00397	.25206
10.40	.00401	.25567
10.50	.00436	.26199
10.60	.00452	.26315
10.70	.00410	.30425
10.80	.00466	.32374
10.90	.00447	.32153
11.00	.00401	.32745
11.10	.00399	.33721
11.20	.00465	.33261
11.30	.00528	.35412
11.40	.00537	.38151
11.50	.00486	.39425
11.60	.00462	.39895
11.70	.00435	.40623
11.80	.00433	.40132
11.90	.00488	.39894
12.00	.00575	.43217
12.10	.00535	.46427
12.20	.00494	.48476
12.30	.00499	.49117
12.40	.00493	.50162
12.50	.00493	.50584
12.60	.00564	.50538
12.70	.00671	.51844
12.80	.00739	.54426
12.90	.00705	.56648
13.00	.00671	.56792
13.10	.00673	.56284
13.20	.00704	.55719
13.30	.00766	.55351
13.40	.00816	.56413
13.50	.00823	.57410
13.60	.00846	.59435
13.70	.00752	.61217
13.80	.00717	.61221
13.90	.00776	.60597
14.00	.00843	.61049
14.10	.00932	.61735
14.20	.00921	.63484
14.30	.00886	.63908
14.40	.00863	.64461
14.50	.00842	.64303
14.60	.00850	.64556
14.70	.00846	.64625
14.80	.00899	.65449
14.90	.00866	.66488
15.00	.00790	.68247

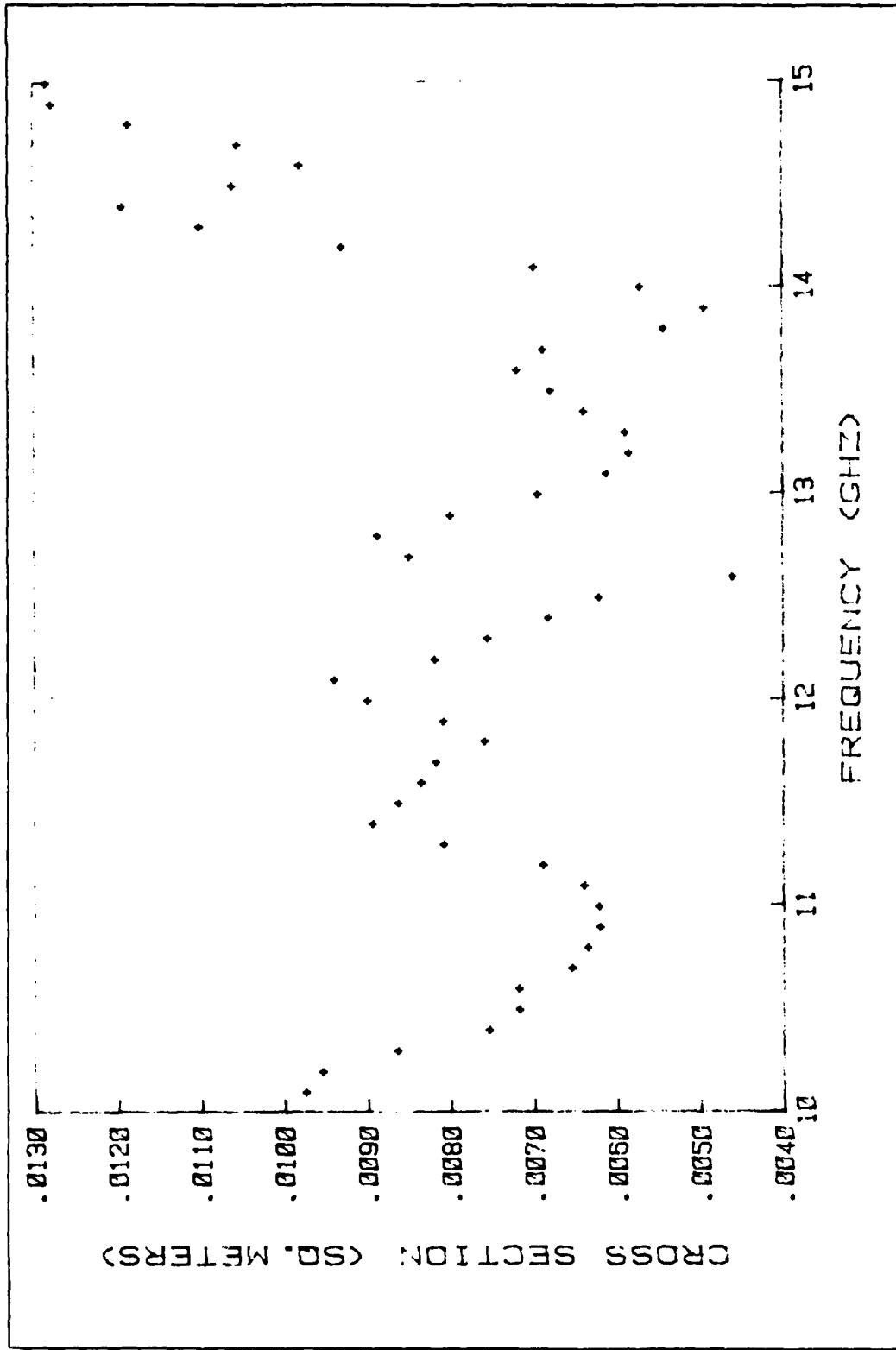


Figure 3.15 TARGET6 Cross-Section vs. Frequency

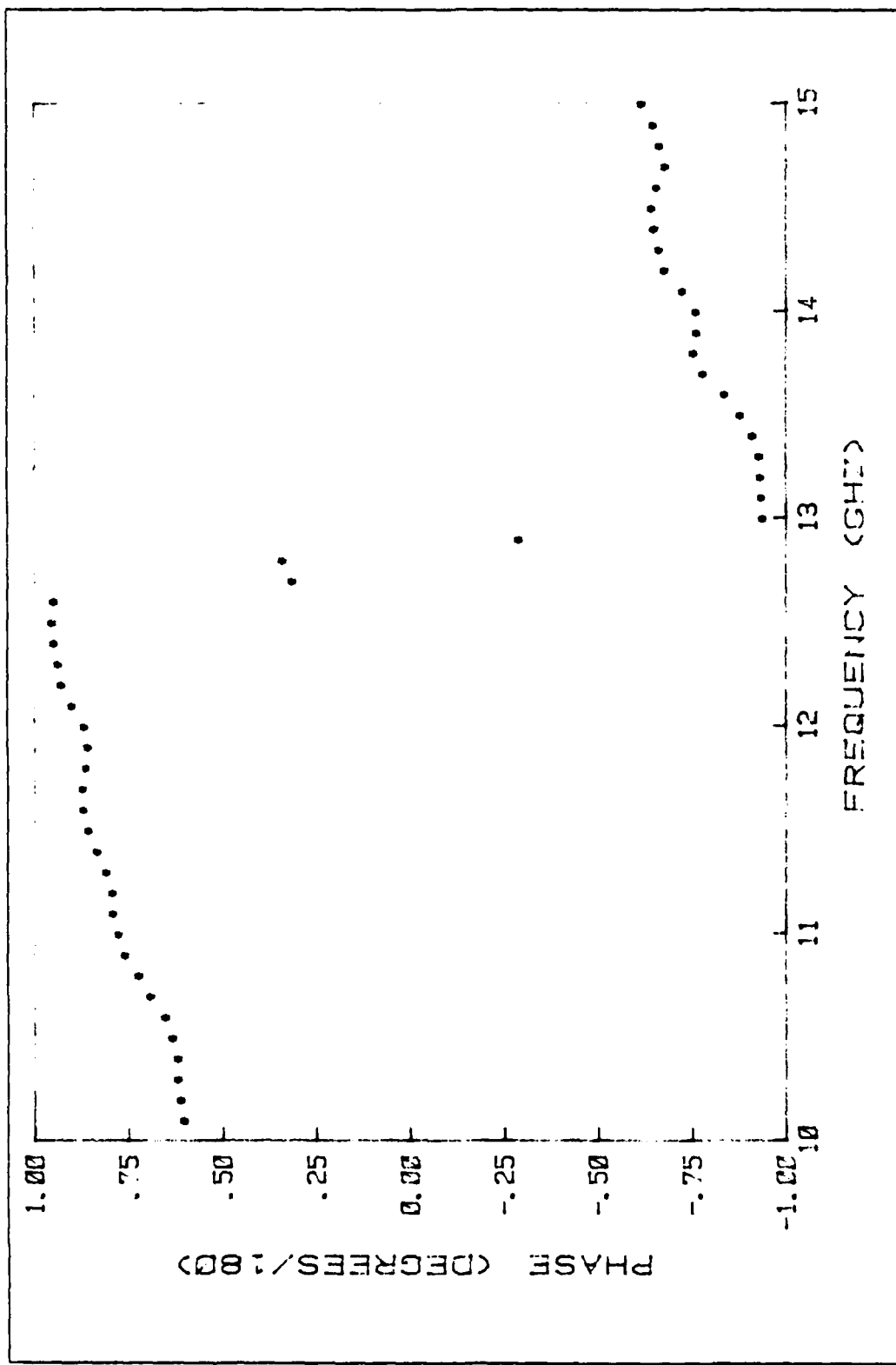


Figure 3.16 TARGET6 Phase Shift vs. Frequency

TABLE 8  
TARGET6 Measured Data

Frequency GHz	Cross-Section sq. meters	Phase Degrees/180
10.10	.00968	.58836
10.20	.00947	.59723
10.30	.00857	.69370
10.40	.00747	.60401
10.50	.00711	.61918
10.60	.00711	.63793
10.70	.00648	.67870
10.80	.00628	.70923
10.90	.00614	.74471
11.00	.00615	.76215
11.10	.00632	.77714
11.20	.00682	.77944
11.30	.00801	.79539
11.40	.00887	.81919
11.50	.00856	.84249
11.60	.00829	.85517
11.70	.00811	.85856
11.80	.00752	.85020
11.90	.00802	.84403
12.00	.00893	.85380
12.10	.00933	.88745
12.20	.00812	.91357
12.30	.00749	.92319
12.40	.00676	.93603
12.50	.00614	.93977
12.60	.00454	.93594
12.70	.00843	.30132
12.80	.00880	.32573
12.90	.00793	-.30347
13.00	.00688	-.95118
13.10	.00605	-.94729
13.20	.00577	-.94719
13.30	.00582	-.94378
13.40	.00633	-.92570
13.50	.00672	-.89385
13.60	.00712	-.85167
13.70	.00661	-.79364
13.80	.00536	-.76928
13.90	.00487	-.77640
14.00	.00565	-.77495
14.10	.00692	-.73942
14.20	.00923	-.69146
14.30	.01094	-.67695
14.40	.01186	-.66472
14.50	.01054	-.65865
14.60	.00973	-.67102
14.70	.01047	-.69307
14.80	.01179	-.67926
14.90	.01271	-.66122
15.00	.01278	-.63002

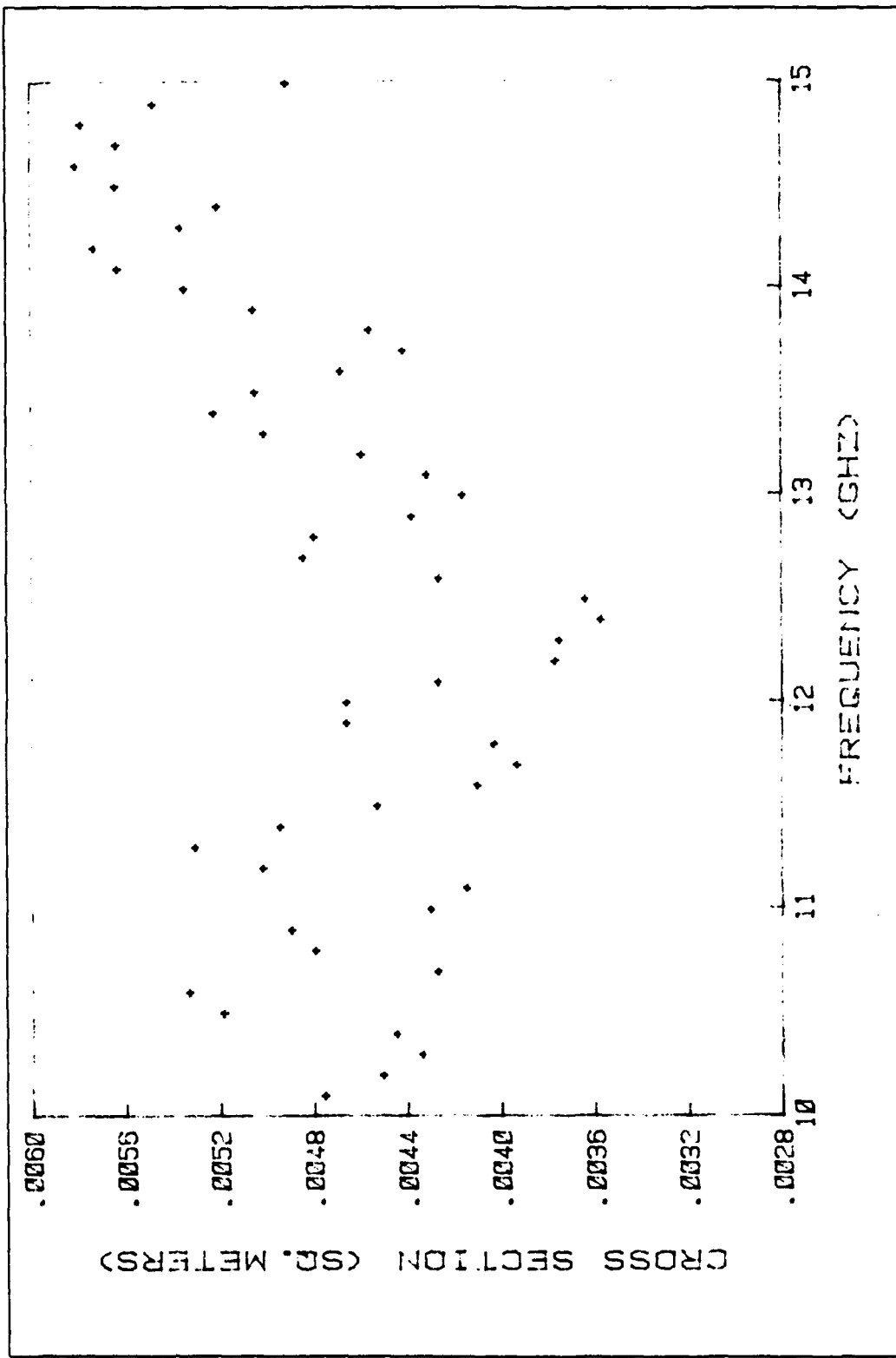


Figure 3.17 TARGET7 Cross-Section vs. Frequency

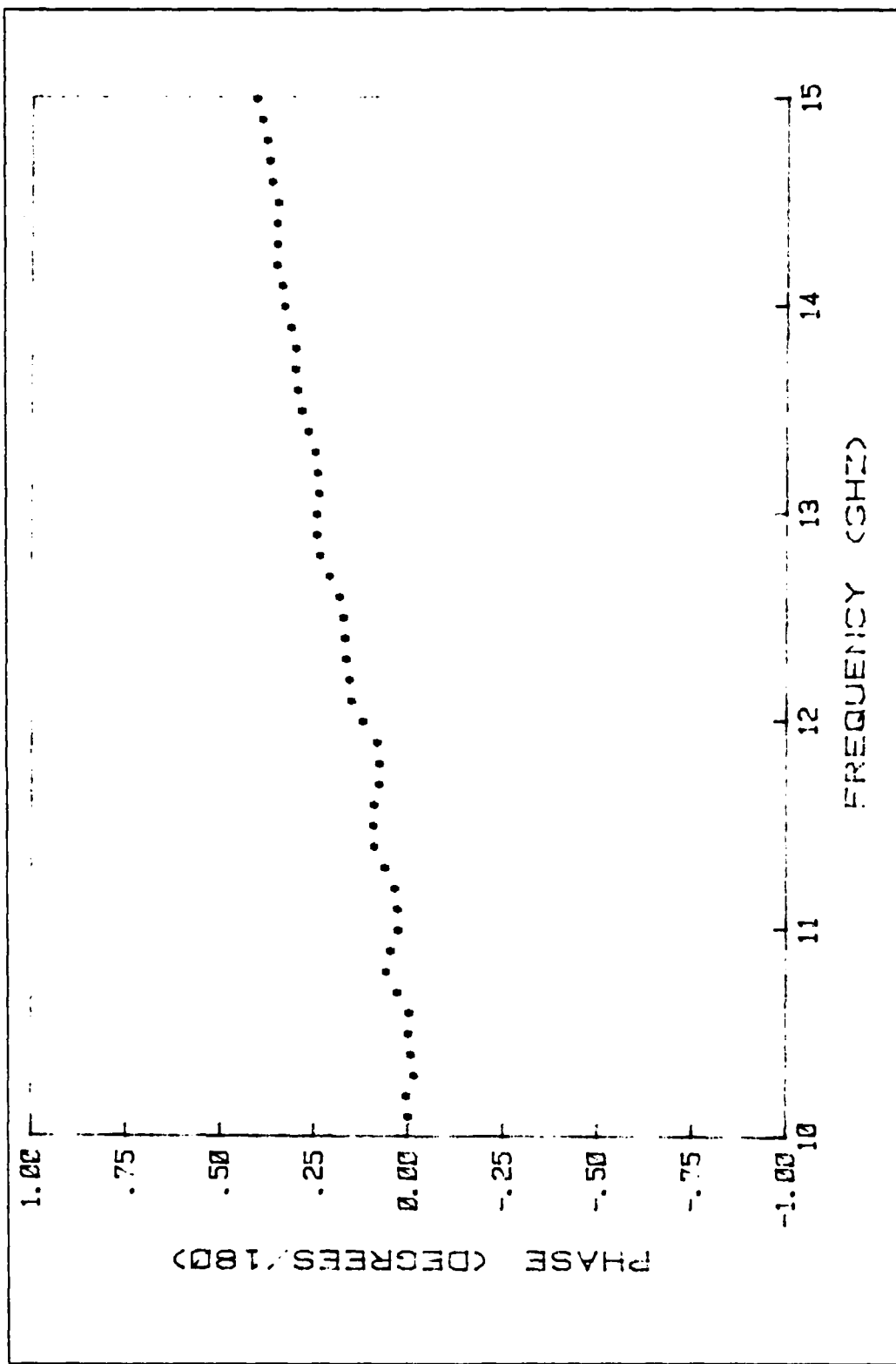


Figure 3.18 TARGET7 Phase Shift vs. Frequency

TABLE 9  
TARGET7 Measured Data

Frequency GHz	Cross-Section sq. meters	Phase Degrees/180
10.10	.00473	- .01397
10.20	.00448	- .00962
10.30	.00431	- .02948
10.40	.00442	- .02273
10.50	.00516	- .01486
10.60	.00531	- .01665
10.70	.00425	.01602
10.80	.00477	.04374
10.90	.00487	.03378
11.00	.00428	.01247
11.10	.00412	.01545
11.20	.00499	.02191
11.30	.00528	.04933
11.40	.00492	.07705
11.50	.00450	.07850
11.60	.00408	.07717
11.70	.00391	.06481
11.80	.00400	.06271
11.90	.00464	.06883
12.00	.00463	.10621
12.10	.00424	.13714
12.20	.00375	.14191
12.30	.00373	.15257
12.40	.00355	.15489
12.50	.00361	.15947
12.60	.00424	.16899
12.70	.00482	.19632
12.80	.00477	.22044
12.90	.00436	.23138
13.00	.00414	.23025
13.10	.00429	.22480
13.20	.00457	.22795
13.30	.00498	.23443
13.40	.00520	.25292
13.50	.00502	.27134
13.60	.00466	.28099
13.70	.00439	.28817
13.80	.00453	.28637
13.90	.00503	.30092
14.00	.00532	.31561
14.10	.00561	.32275
14.20	.00571	.33801
14.30	.00534	.33660
14.40	.00518	.33676
14.50	.00561	.33607
14.60	.00578	.34992
14.70	.00561	.35768
14.80	.00576	.36428
14.90	.00545	.37714
15.00	.00488	.39145

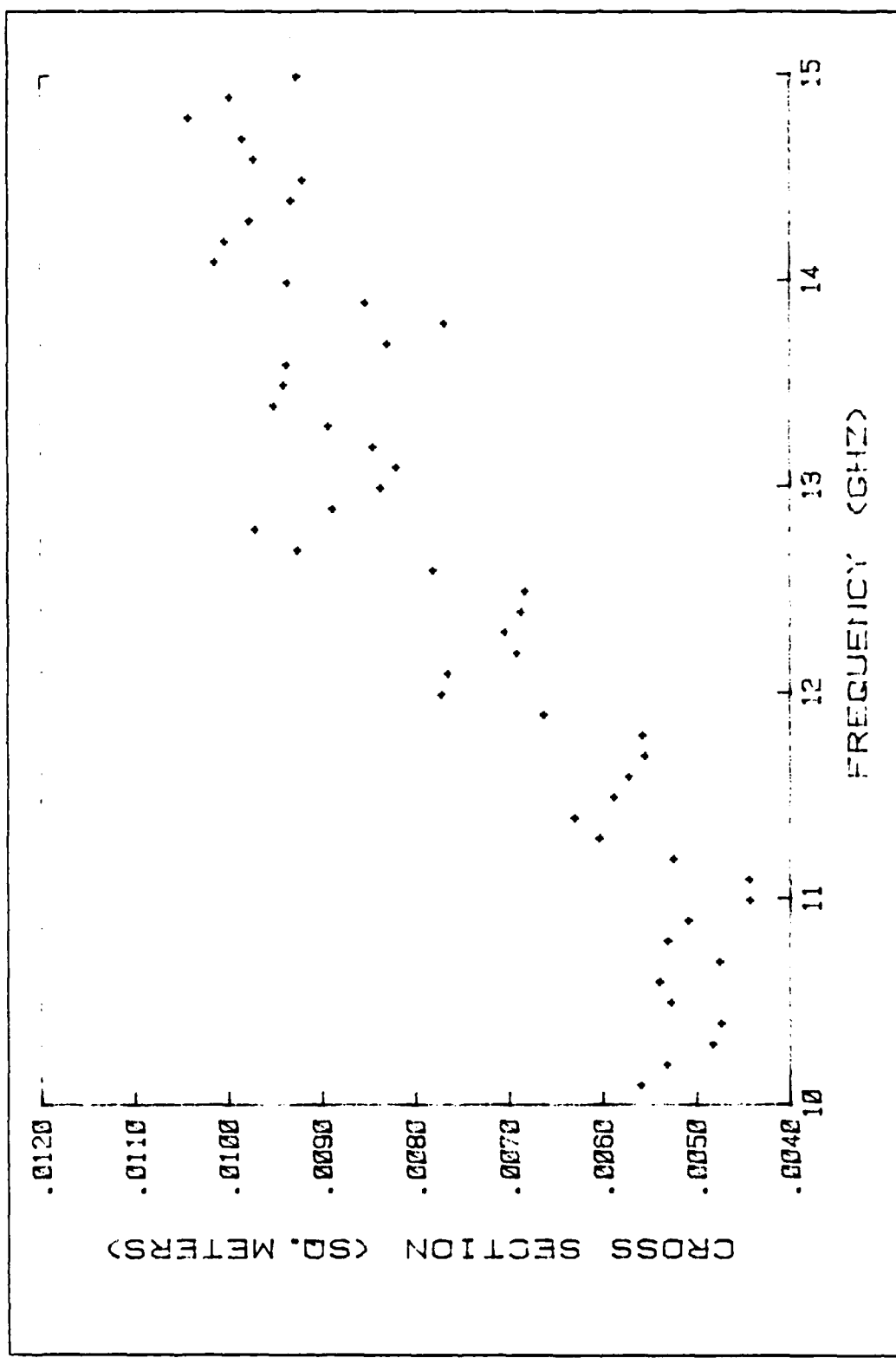


Figure 3.19 TARGET8 Cross-Section vs. Frequency

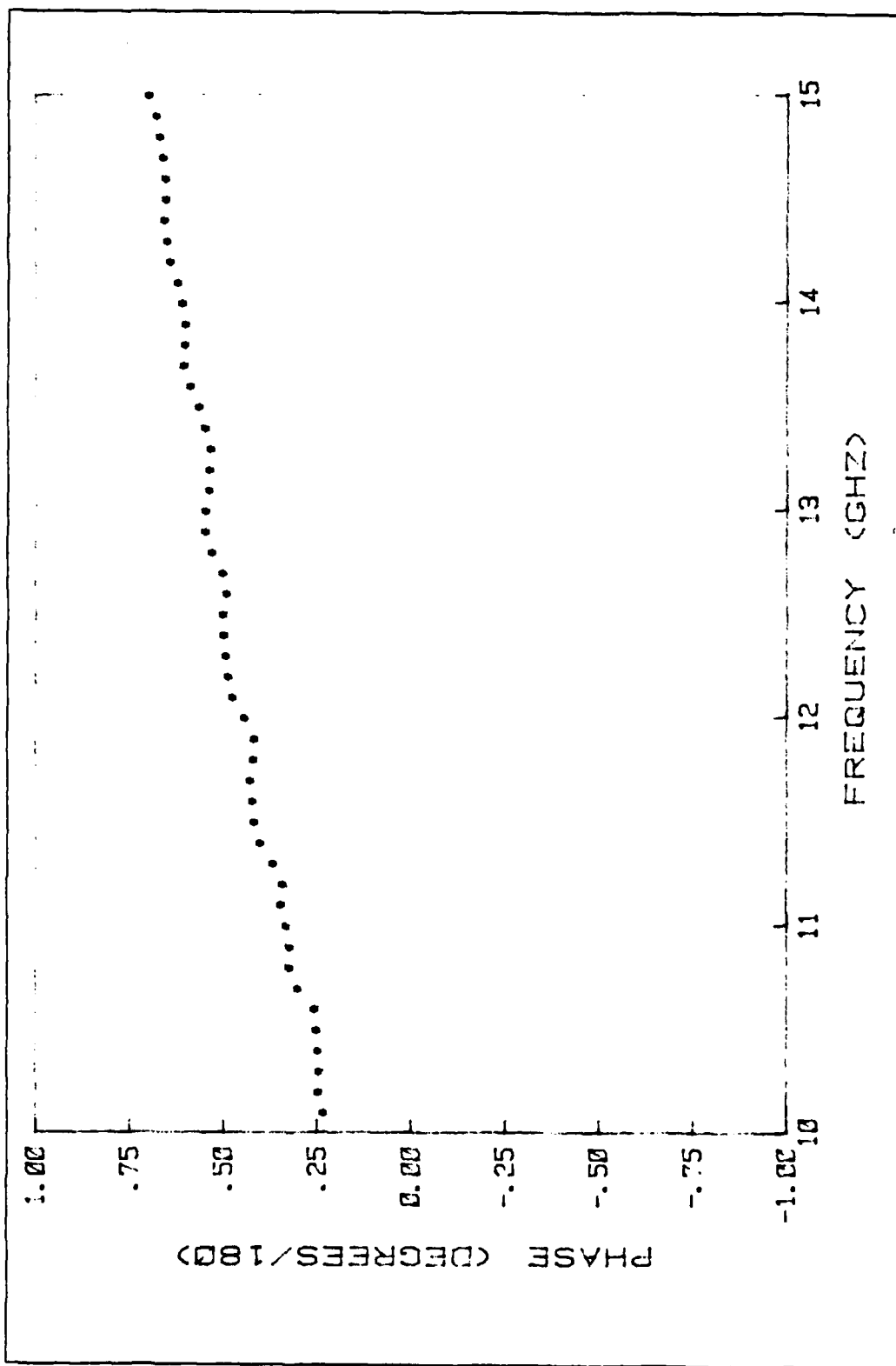


Figure 3.20 TARGET8 Phase Shift vs. Frequency

TABLE 10  
TARGET8 Measured Data

Frequency GHz	Cross-Section sq. meters	Phase Degrees/180
10.10	.00553	21832
10.20	.00526	23205
10.30	.00477	22814
10.40	.00468	23082
10.50	.00521	23691
10.60	.00534	24184
10.70	.00470	23691
10.80	.00525	30946
10.90	.00503	30844
11.00	.00437	31729
11.10	.00437	33061
11.20	.00518	32487
11.30	.00597	35357
11.40	.00624	38699
11.50	.00582	40322
11.60	.00566	40731
11.70	.00549	41455
11.80	.00552	40592
11.90	.00657	40200
12.00	.00766	42791
12.10	.00759	46060
12.20	.00686	47187
12.30	.00699	47810
12.40	.00681	48412
12.50	.00677	48710
12.60	.00775	47702
12.70	.00920	48625
12.80	.00965	51450
12.90	.00882	53275
13.00	.00832	53249
13.10	.00814	52405
13.20	.00839	52308
13.30	.00886	51987
13.40	.00945	53374
13.50	.00934	54971
13.60	.00931	57229
13.70	.00824	59173
13.80	.00763	58842
13.90	.00847	58671
14.00	.00930	59648
14.10	.01008	60688
14.20	.00997	62590
14.30	.00971	63346
14.40	.00927	64221
14.50	.00913	63841
14.60	.00966	64973
14.70	.00978	64616
14.80	.01036	65557
14.90	.00991	66344
15.00	.00920	68325

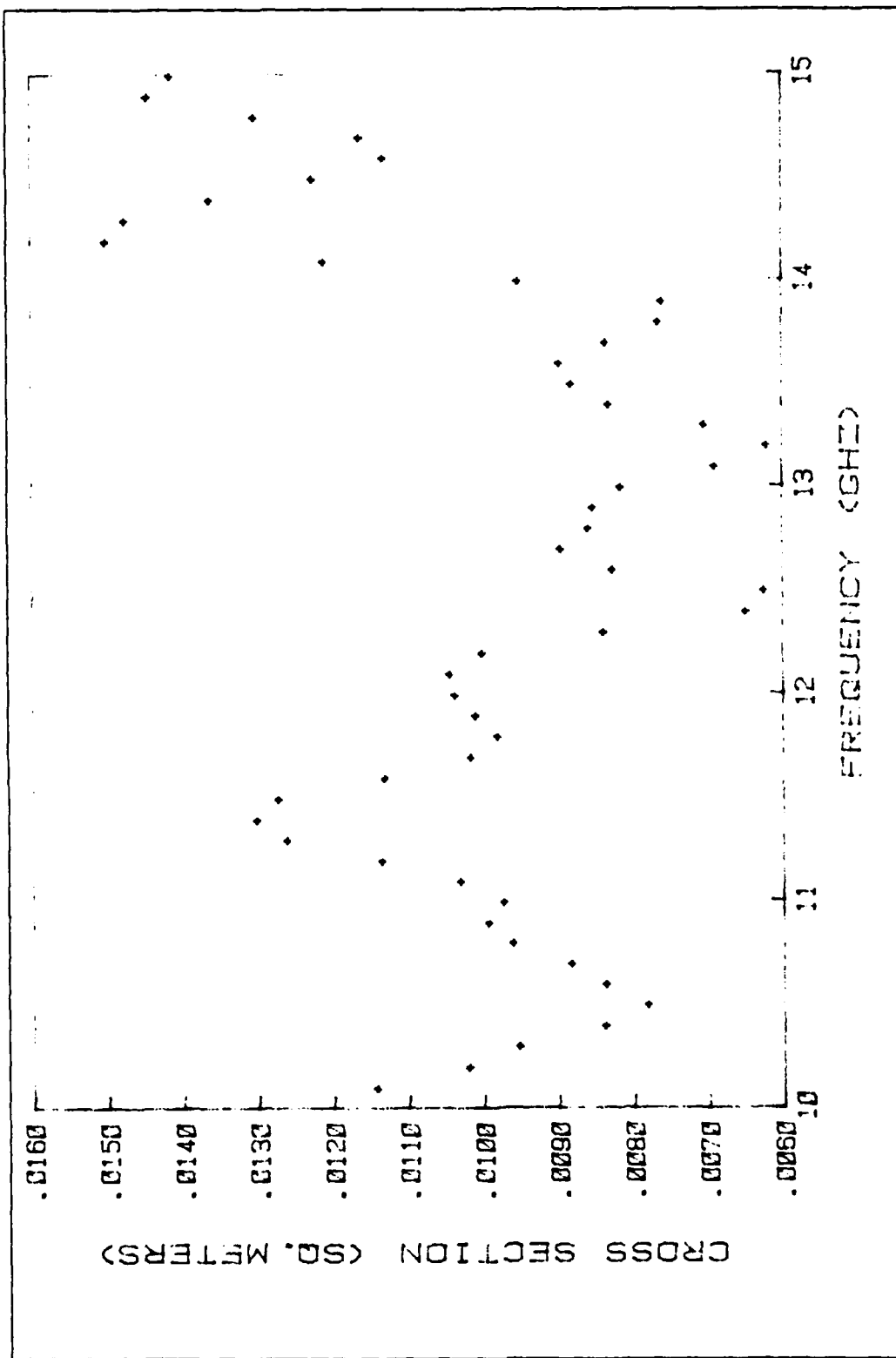


Figure 3.21 TARGET9 Cross-Section vs. Frequency

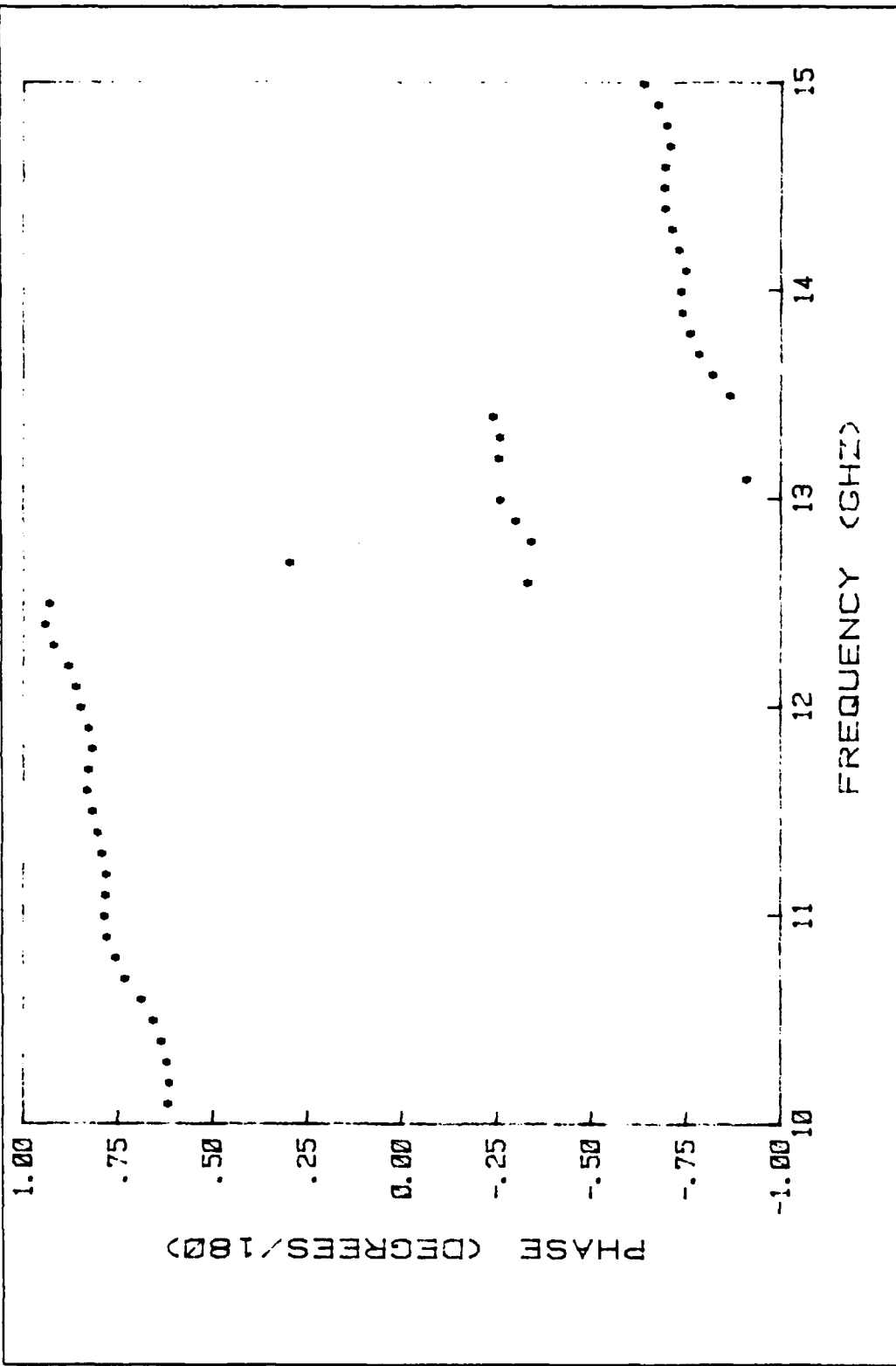


Figure 3.22 TARGET9 Phase Shift vs. Frequency

TABLE 11  
TARGET9 Measured Data

Frequency GHz	Cross-Section sq. meters	Phase Degrees/180
10.10	.01136	.60195
10.20	.01013	.59852
10.30	.00946	.60546
10.40	.00832	.62005
10.50	.00773	.64314
10.60	.00830	.67451
10.70	.00875	.71565
10.80	.00954	.73978
10.90	.00987	.76294
11.00	.00966	.77130
11.10	.01023	.76775
11.20	.01128	.76609
11.30	.01255	.77676
11.40	.01295	.78871
11.50	.01267	.80284
11.60	.01124	.81692
11.70	.01009	.81400
11.80	.00974	.80319
11.90	.01003	.81246
12.00	.01030	.83292
12.10	.01037	.84468
12.20	.00994	.86577
12.30	.00832	.90520
12.40	.00642	.92787
12.50	.00618	.91565
12.60	.00819	-.34626
12.70	.00889	.28244
12.80	.00851	-.35541
12.90	.00845	-.31401
13.00	.00808	-.27579
13.10	.00683	-.92441
13.20	.00614	-.27070
13.30	.00697	-.27350
13.40	.00823	-.25451
13.50	.00874	-.88102
13.60	.00889	-.83414
13.70	.00828	-.79897
13.80	.00757	-.77467
13.90	.00752	-.75567
14.00	.00944	-.74947
14.10	.01202	-.76533
14.20	.01493	-.74658
14.30	.01467	-.72817
14.40	.01354	-.70995
14.50	.01218	-.70593
14.60	.01123	-.70814
14.70	.01154	-.72251
14.80	.01295	-.71344
14.90	.01437	-.68823
15.00	.01405	-.65091

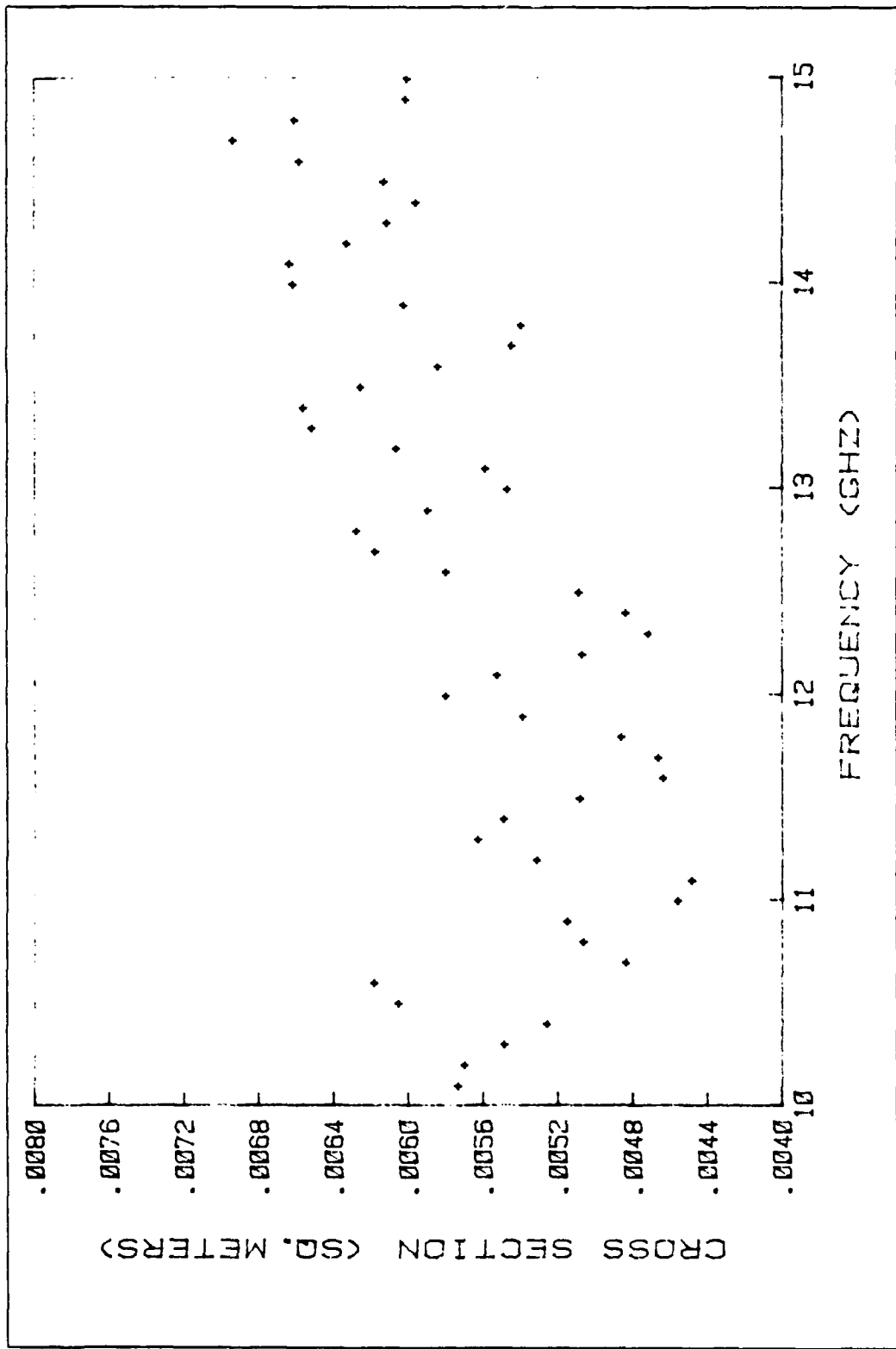


Figure 3.23 TARGET10 Cross-Section vs. Frequency

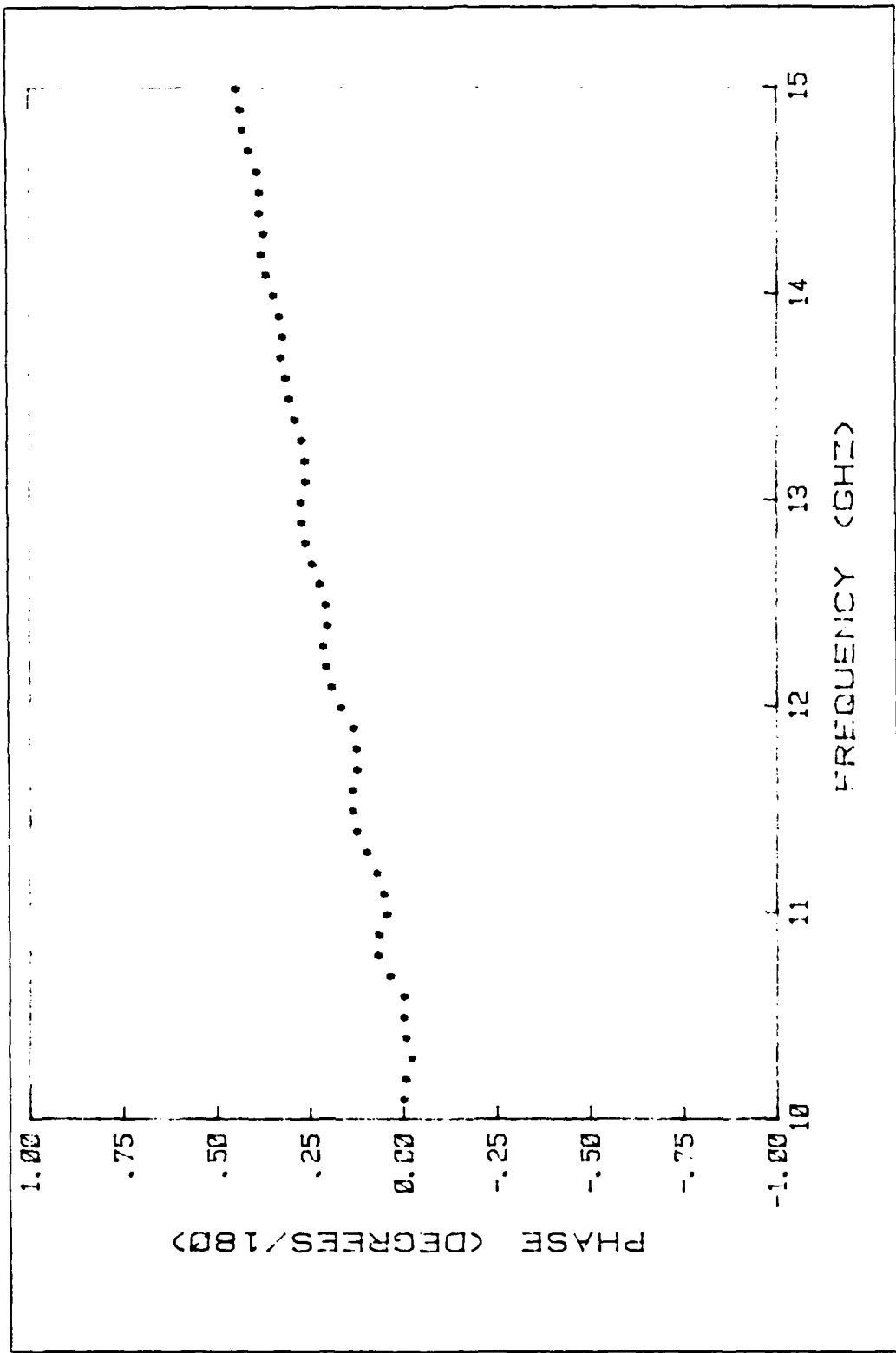


Figure 3.24 TARGET10 Phase Shift vs. Frequency

TABLE 12  
TARGET10 Measured Data

Frequency GHz	Cross-Section sq. meters	Phase Degrees/180
10.10	.00570	- .01613
10.20	.00567	- .02041
10.30	.00546	- .03873
10.40	.00523	- .02295
10.50	.00602	- .01625
10.60	.00615	- .01609
10.70	.00481	.02049
10.80	.00503	.05421
10.90	.00512	.05119
11.00	.00453	.02919
11.10	.00445	.03759
11.20	.00528	.05526
11.30	.00560	.08370
11.40	.00546	.11080
11.50	.00505	.12130
11.60	.00461	.12199
11.70	.00463	.10887
11.80	.00483	.11058
11.90	.00536	.11840
12.00	.00577	.15057
12.10	.00550	.17718
12.20	.00504	.19088
12.30	.00468	.19964
12.40	.00481	.18675
12.50	.00506	.19244
12.60	.00577	.20803
12.70	.00615	.22850
12.80	.00625	.24632
12.90	.00587	.25827
13.00	.00544	.25782
13.10	.00556	.24606
13.20	.00604	.24737
13.30	.00649	.25662
13.40	.00653	.27541
13.50	.00623	.28926
13.60	.00581	.29822
13.70	.00542	.31086
13.80	.00537	.30630
13.90	.00599	.31450
14.00	.00659	.33150
14.10	.00660	.35031
14.20	.00630	.36466
14.30	.00608	.35724
14.40	.00593	.36905
14.50	.00610	.36814
14.60	.00655	.37579
14.70	.00690	.39771
14.80	.00658	.41478
14.90	.00598	.41634
15.00	.00597	.42852

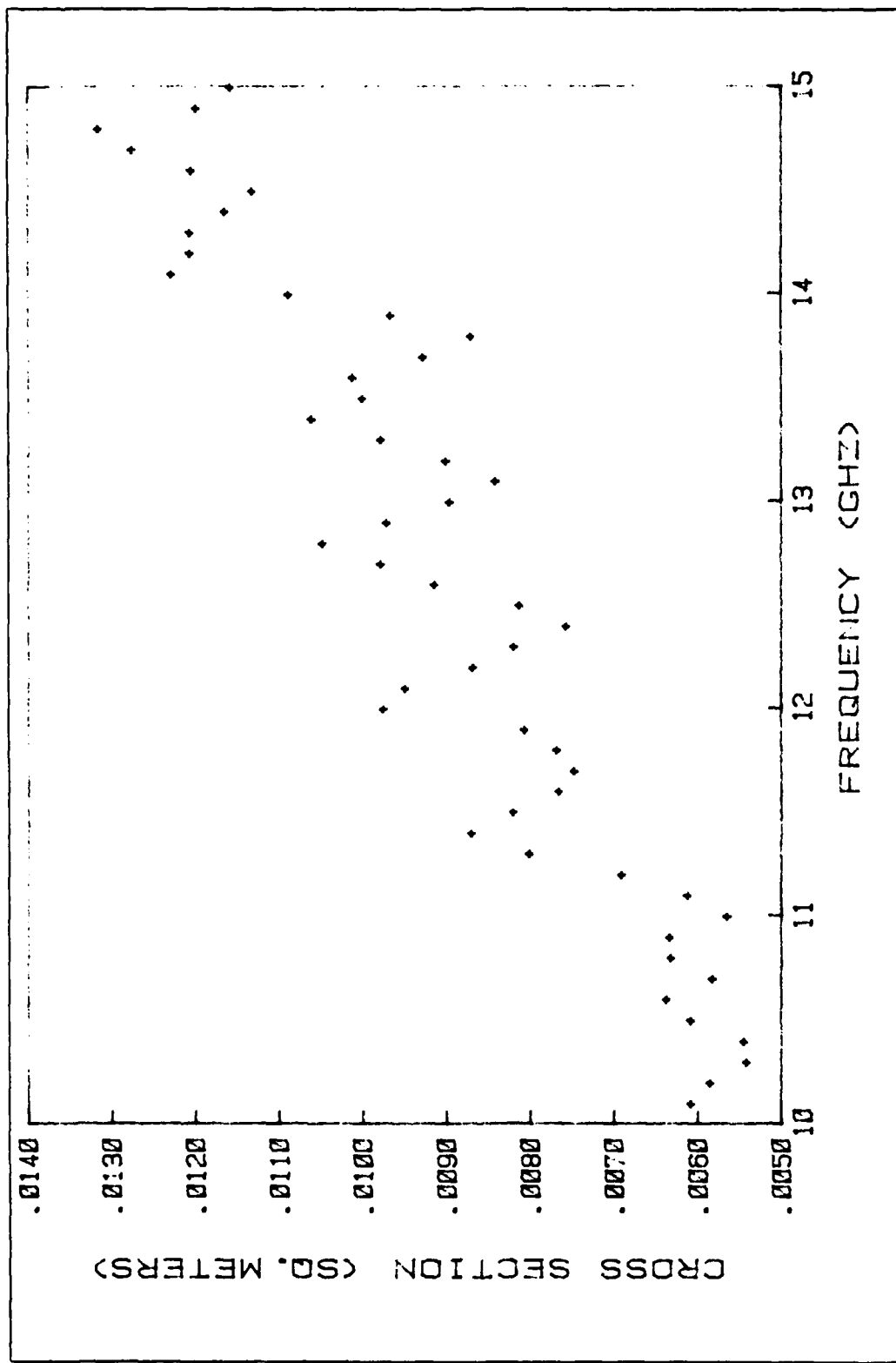


Figure 3.25 TARGET11 Cross-Section vs. Frequency

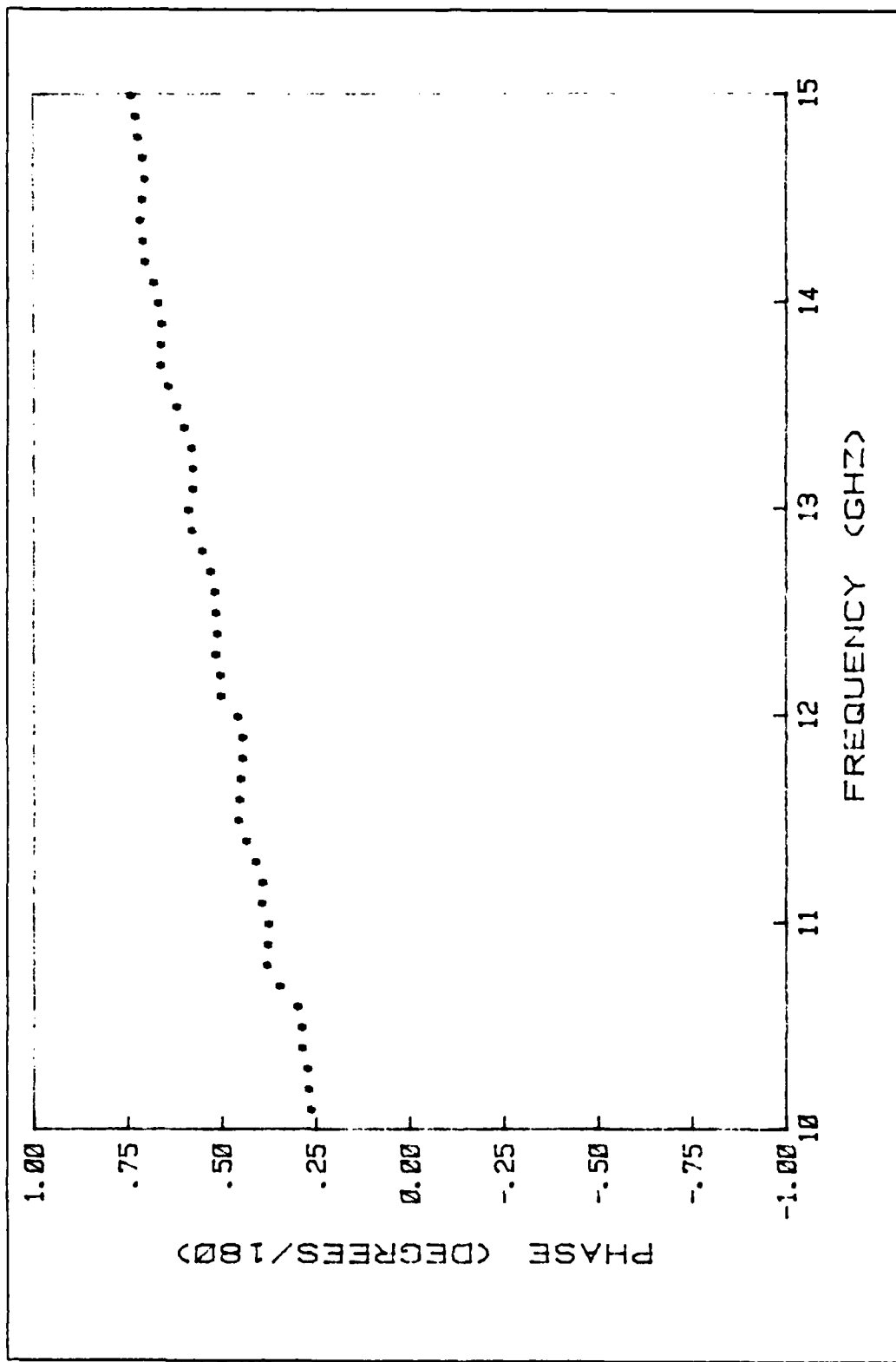


Figure 3.26 TARGET11 Phase Shift vs. Frequency

TABLE 13  
TARGET11 Measured Data

Frequency GHz	Cross-Section sq. meters	Phase Degrees/180
10.10	.00602	.24767
10.20	.00579	.25319
10.30	.00535	.25600
10.40	.00538	.27044
10.50	.00602	.27210
10.60	.00631	.28454
10.70	.00576	.33144
10.80	.00626	.36395
10.90	.00627	.36236
11.00	.00559	.36017
11.10	.00606	.37743
11.20	.00685	.37647
11.30	.00795	.39448
11.40	.00864	.41991
11.50	.00814	.44162
11.60	.00760	.43770
11.70	.00741	.43492
11.80	.00762	.42920
11.90	.00800	.42868
12.00	.00969	.44217
12.10	.00943	.48742
12.20	.00862	.48801
12.30	.00813	.50101
12.40	.00751	.49544
12.50	.00806	.49984
12.60	.00907	.50294
12.70	.00972	.51515
12.80	.01041	.53692
12.90	.00965	.56353
13.00	.00890	.57306
13.10	.00835	.56094
13.20	.00894	.55970
13.30	.00972	.56358
13.40	.01055	.58460
13.50	.00994	.60481
13.60	.01006	.62661
13.70	.00922	.64645
13.80	.00864	.64531
13.90	.00960	.64371
14.00	.01082	.65246
14.10	.01222	.66523
14.20	.01200	.68736
14.30	.01200	.69253
14.40	.01158	.69990
14.50	.01126	.69490
14.60	.01198	.68687
14.70	.01269	.69379
14.80	.01310	.70730
14.90	.01193	.71326
15.00	.01151	.72481

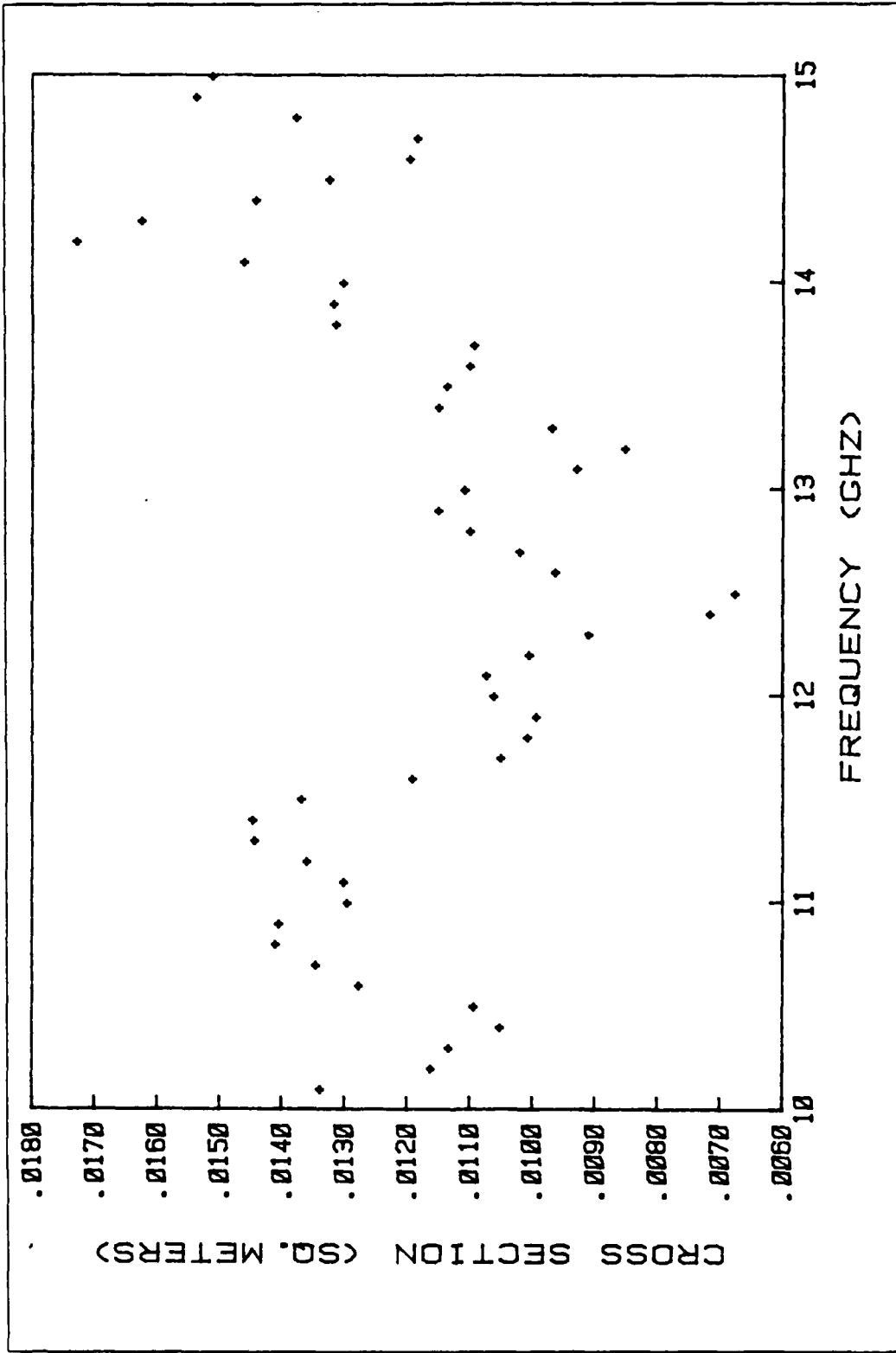


Figure 3.27 TARGET12 Cross-Section vs. Frequency

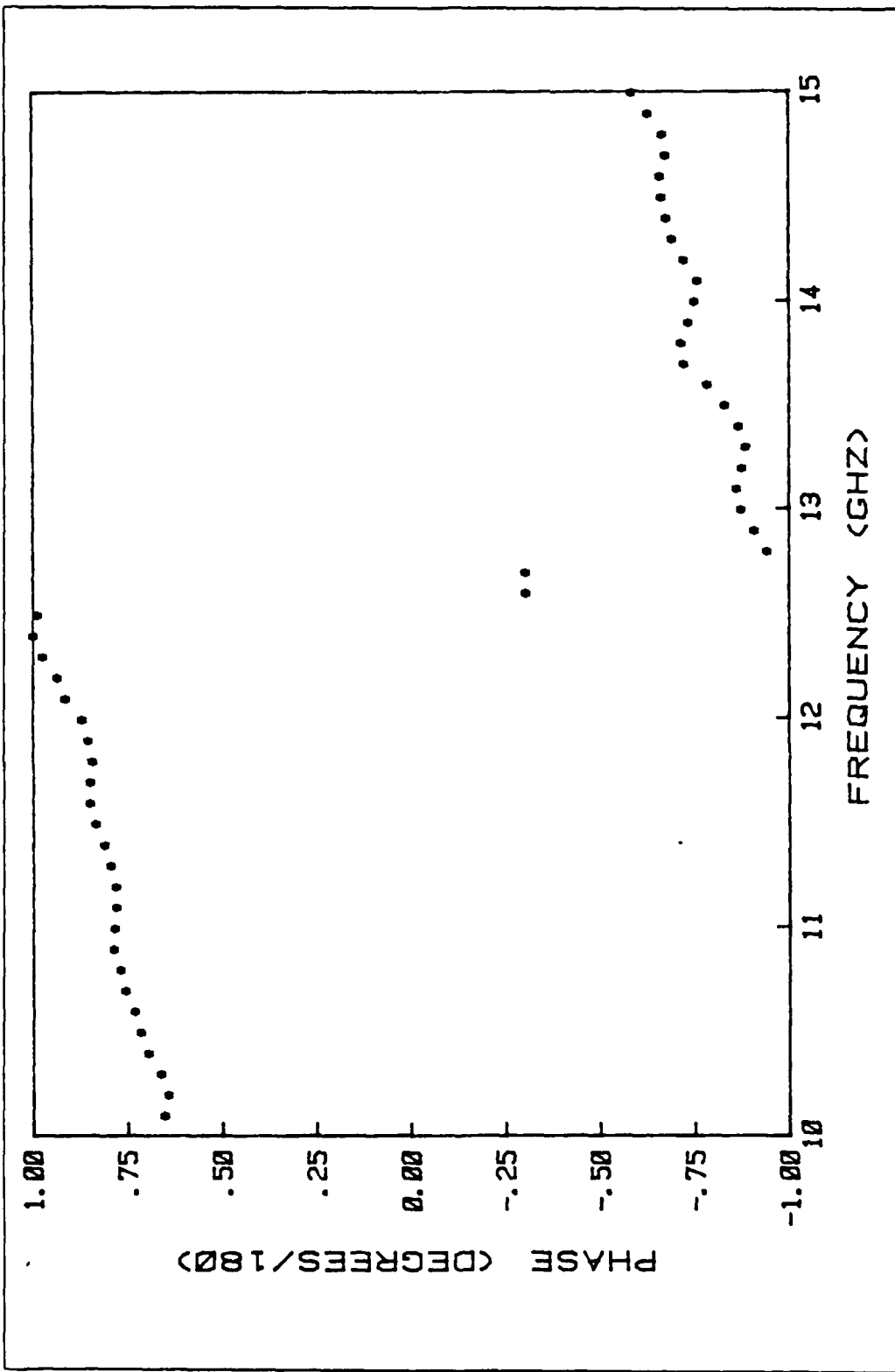


Figure 3.28 TARGET12 Phase Shift vs. Frequency

TABLE 14  
TARGET12 Measured Data

Frequency GHz	Cross-Section sq. meters	Phase Degrees/180
10.10	01329	63700
10.20	01153	62773
10.30	01124	64726
10.40	01042	68072
10.50	01084	70037
10.60	01268	71735
10.70	01337	74023
10.80	01401	75514
10.90	01396	77172
11.00	01286	77013
11.10	01291	76545
11.20	01351	76611
11.30	01435	78017
11.40	01437	79647
11.50	01361	81998
11.60	01183	83455
11.70	01041	83486
11.80	00999	82800
11.90	00984	84037
12.00	01052	85534
12.10	01064	90043
12.20	00996	92045
12.30	00900	95995
12.40	00707	98381
12.50	00667	97350
12.60	00954	- 31892
12.70	01011	- 31712
12.80	01091	- 95556
12.90	01141	- 92144
13.00	01099	- 88740
13.10	00920	- 87567
13.20	00843	- 88986
13.30	00960	- 89901
13.40	01140	- 88095
13.50	01128	- 84448
13.60	01092	- 79788
13.70	01064	- 73699
13.80	01306	- 72891
13.90	01309	- 74871
14.00	01293	- 76471
14.10	01452	- 77374
14.20	01719	- 73697
14.30	01615	- 70615
14.40	01433	- 69044
14.50	01316	- 67823
14.60	01187	- 67455
14.70	01175	- 68830
14.80	01369	- 67931
14.90	01528	- 64217
15.00	01503	- 59964

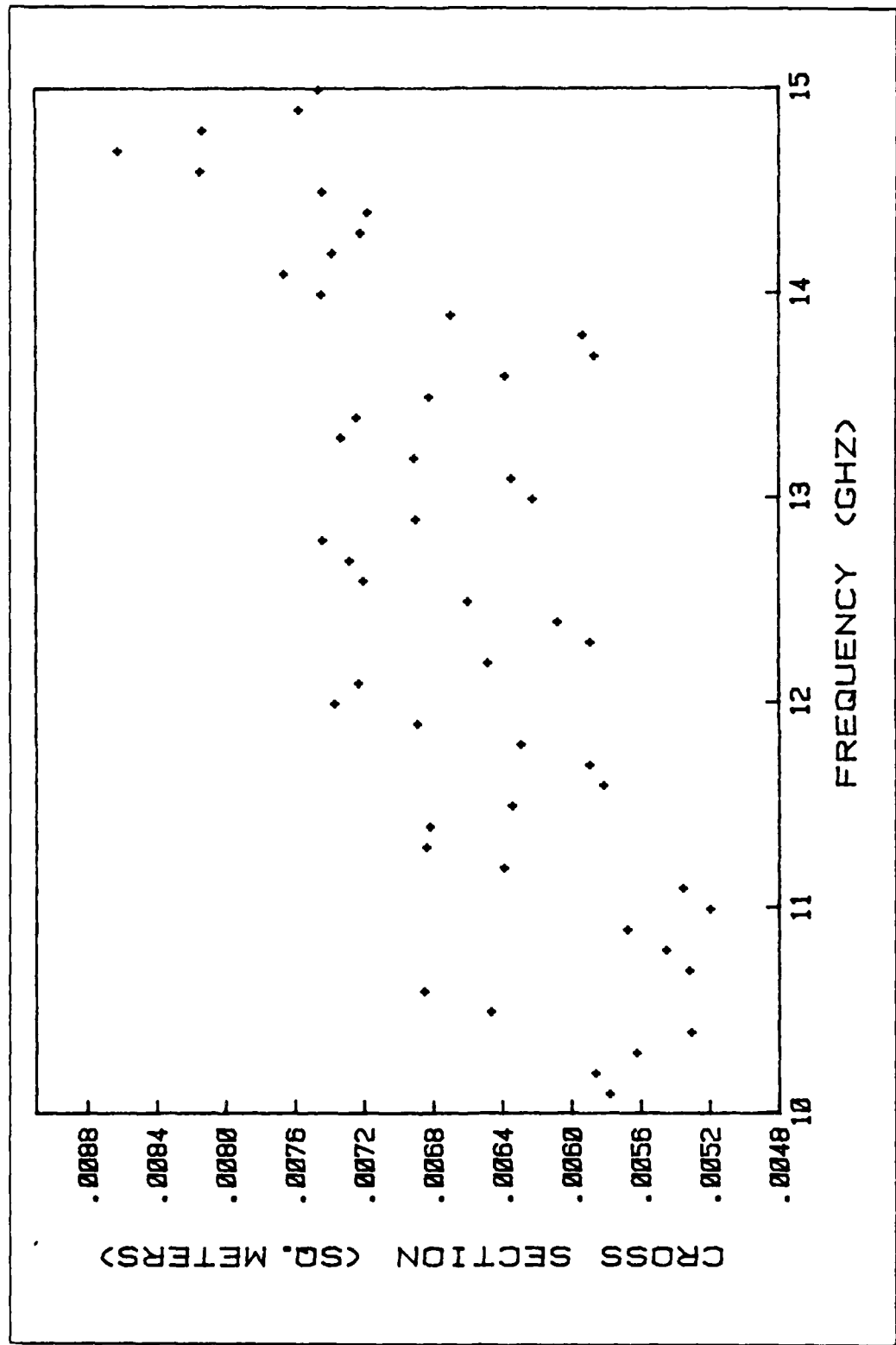


Figure 3.29 TARGET13 Cross-Section vs. Frequency

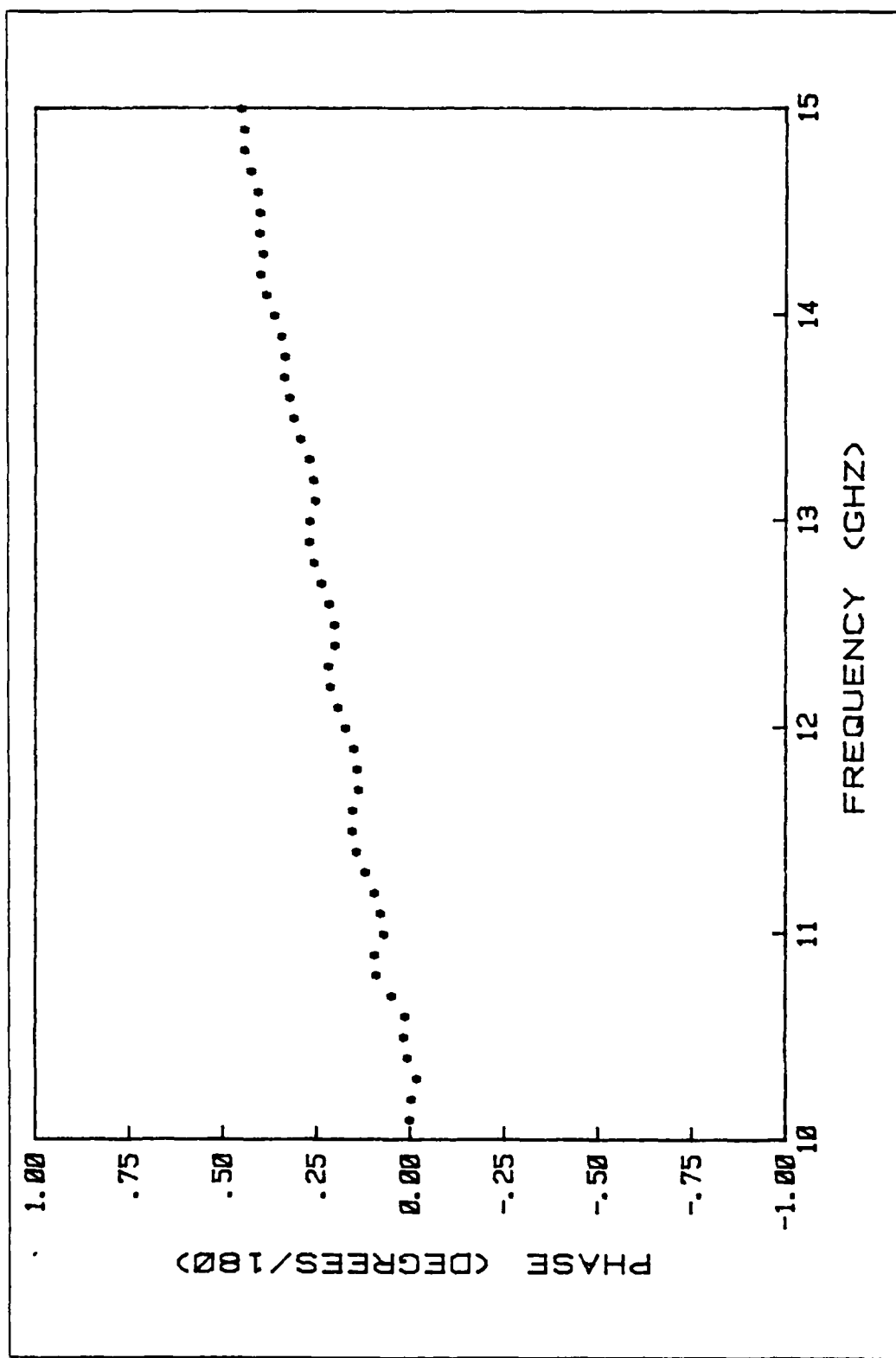


Figure 3.30 TARGET13 Phase Shift vs. Frequency

TABLE 15  
TARGET13 Measured Data

Frequency GHz	Cross-Section sq. meters	Phase Degrees/180
10.10	.00575	- .01375
10.20	.00583	- .01824
10.30	.00559	- .03205
10.40	.00527	- .00900
10.50	.00643	.00081
10.60	.00682	- .00145
10.70	.00529	.03432
10.80	.00542	.07462
10.90	.00565	.07955
11.00	.00517	.05612
11.10	.00533	.06412
11.20	.00636	.07982
11.30	.00681	.10540
11.40	.00679	.12910
11.50	.00631	.13948
11.60	.00578	.13926
11.70	.00587	.12352
11.80	.00626	.12744
11.90	.00686	.13592
12.00	.00733	.15725
12.10	.00720	.17734
12.20	.00645	.19834
12.30	.00586	.20356
12.40	.00605	.18529
12.50	.00657	.18682
12.60	.00717	.20180
12.70	.00725	.22319
12.80	.00741	.24159
12.90	.00687	.25512
13.00	.00619	.25329
13.10	.00632	.23906
13.20	.00688	.24304
13.30	.00730	.25570
13.40	.00721	.27758
13.50	.00679	.29470
13.60	.00635	.30647
13.70	.00584	.32051
13.80	.00590	.31869
13.90	.00666	.32831
14.00	.00741	.34783
14.10	.00763	.36939
14.20	.00735	.38379
14.30	.00719	.37823
14.40	.00715	.38765
14.50	.00741	.38537
14.60	.00811	.39197
14.70	.00859	.41023
14.80	.00810	.42716
14.90	.00754	.42708
15.00	.00743	.43528

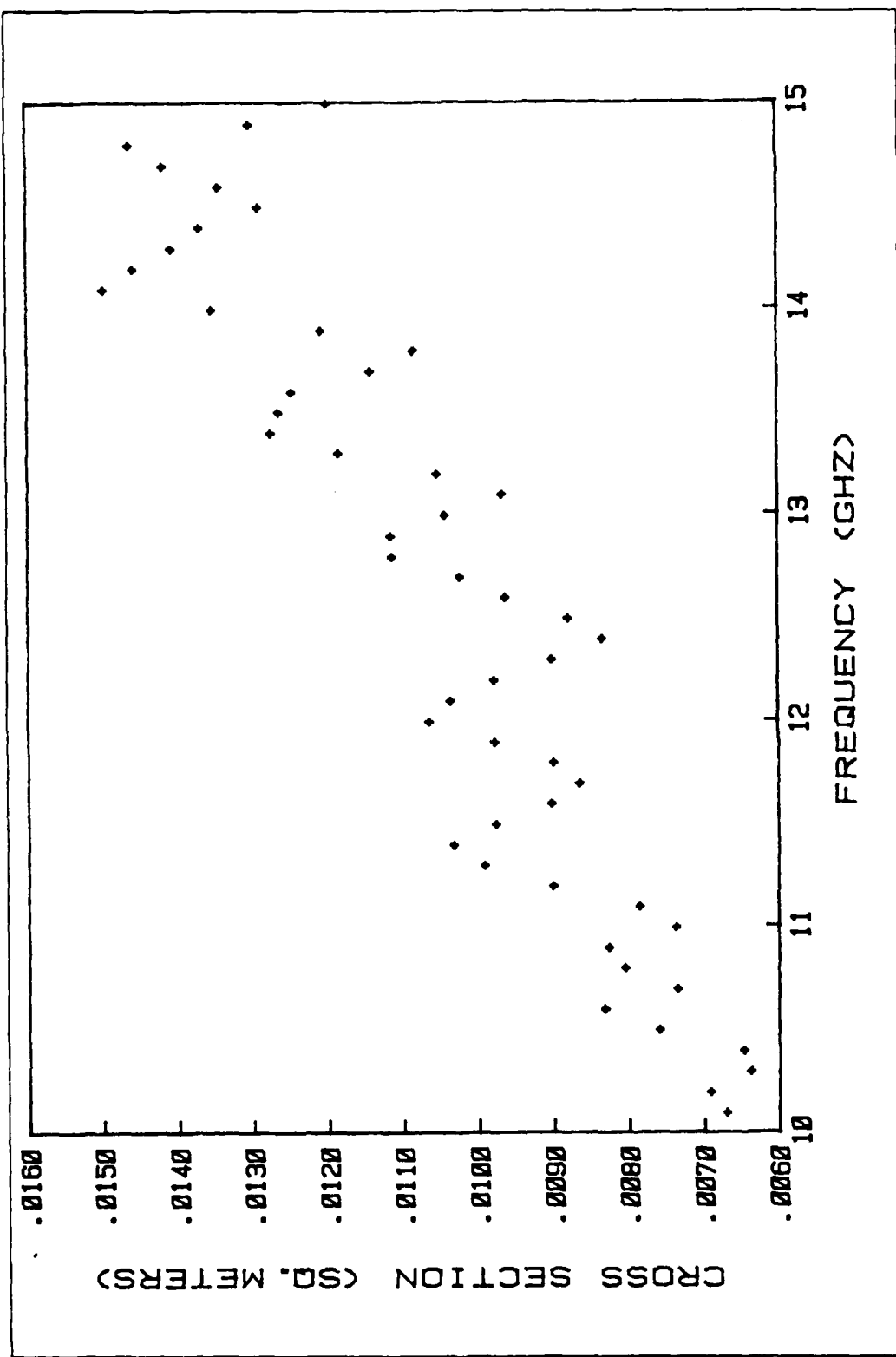


Figure 3.31 TARGET14 Cross-Section vs. Frequency

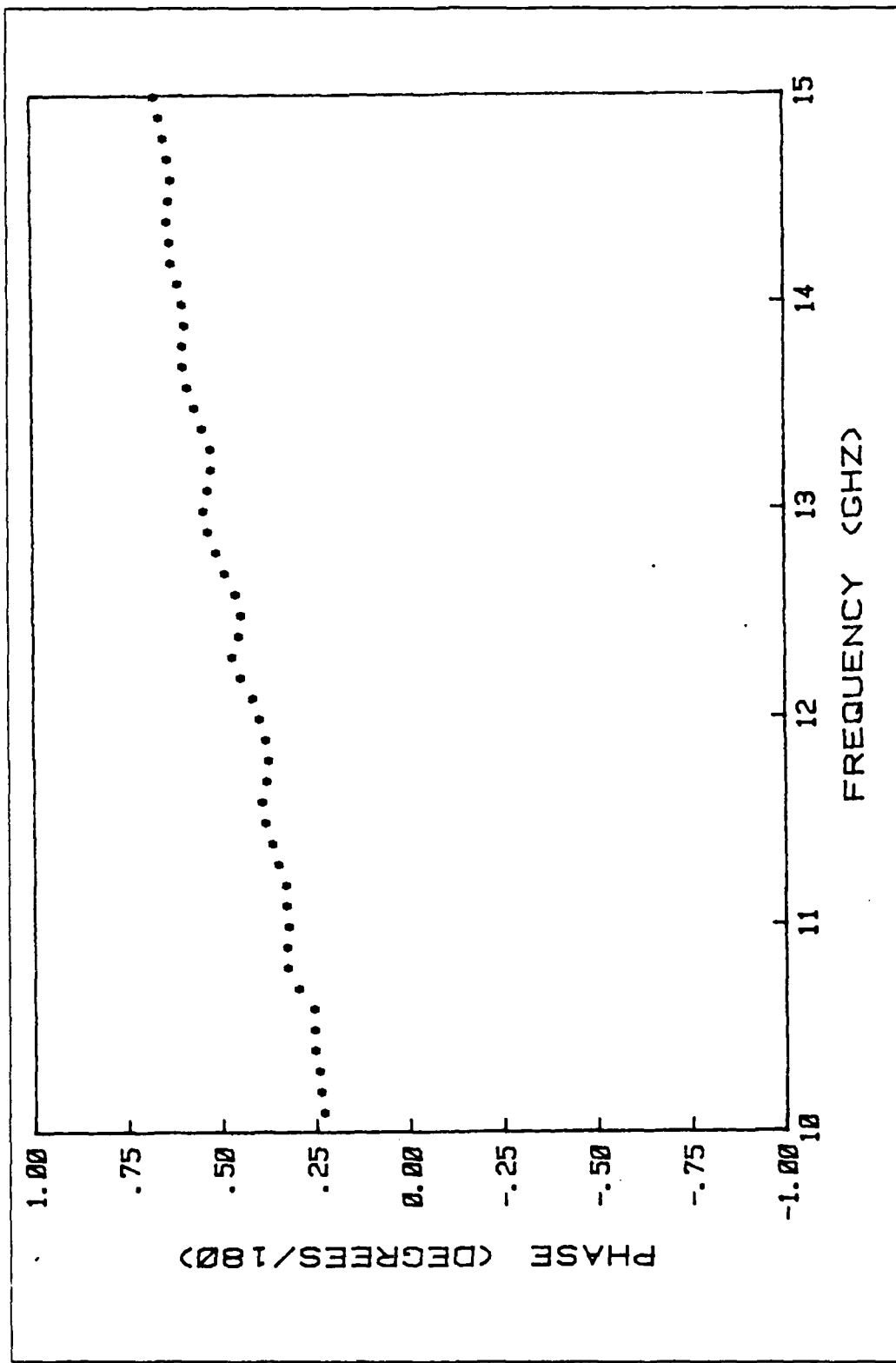


Figure 3.32 TARGET14 Phase Shift vs. Frequency

TABLE 16  
TARGET14 Measured Data

Frequency GHz	Cross-Section sq. meters	Phase Degrees/180
10.10	.00662	.21628
10.20	.00684	.22442
10.30	.00631	.22856
10.40	.00640	.24035
10.50	.00752	.24134
10.60	.00824	.24161
10.70	.00728	.28209
10.80	.00797	.31184
10.90	.00820	.31336
11.00	.00729	.30814
11.10	.00778	.31380
11.20	.00893	.31551
11.30	.00984	.33569
11.40	.01026	.35141
11.50	.00963	.36882
11.60	.00895	.37721
11.70	.00858	.36696
11.80	.00892	.36116
11.90	.00971	.36675
12.00	.01057	.38326
12.10	.01029	.40081
12.20	.00971	.43327
12.30	.00894	.45546
12.40	.00827	.43866
12.50	.00872	.43045
12.60	.00956	.44469
12.70	.01016	.47264
12.80	.01106	.49656
12.90	.01108	.51858
13.00	.01036	.52919
13.10	.00960	.51824
13.20	.01046	.50990
13.30	.01177	.51088
13.40	.01267	.53179
13.50	.01257	.55155
13.60	.01240	.57069
13.70	.01135	.58290
13.80	.01077	.58272
13.90	.01200	.57925
14.00	.01346	.58327
14.10	.01490	.59491
14.20	.01450	.61334
14.30	.01399	.61522
14.40	.01361	.62257
14.50	.01283	.61685
14.60	.01336	.61190
14.70	.01410	.61984
14.80	.01454	.63250
14.90	.01294	.64160
15.00	.01130	.65430

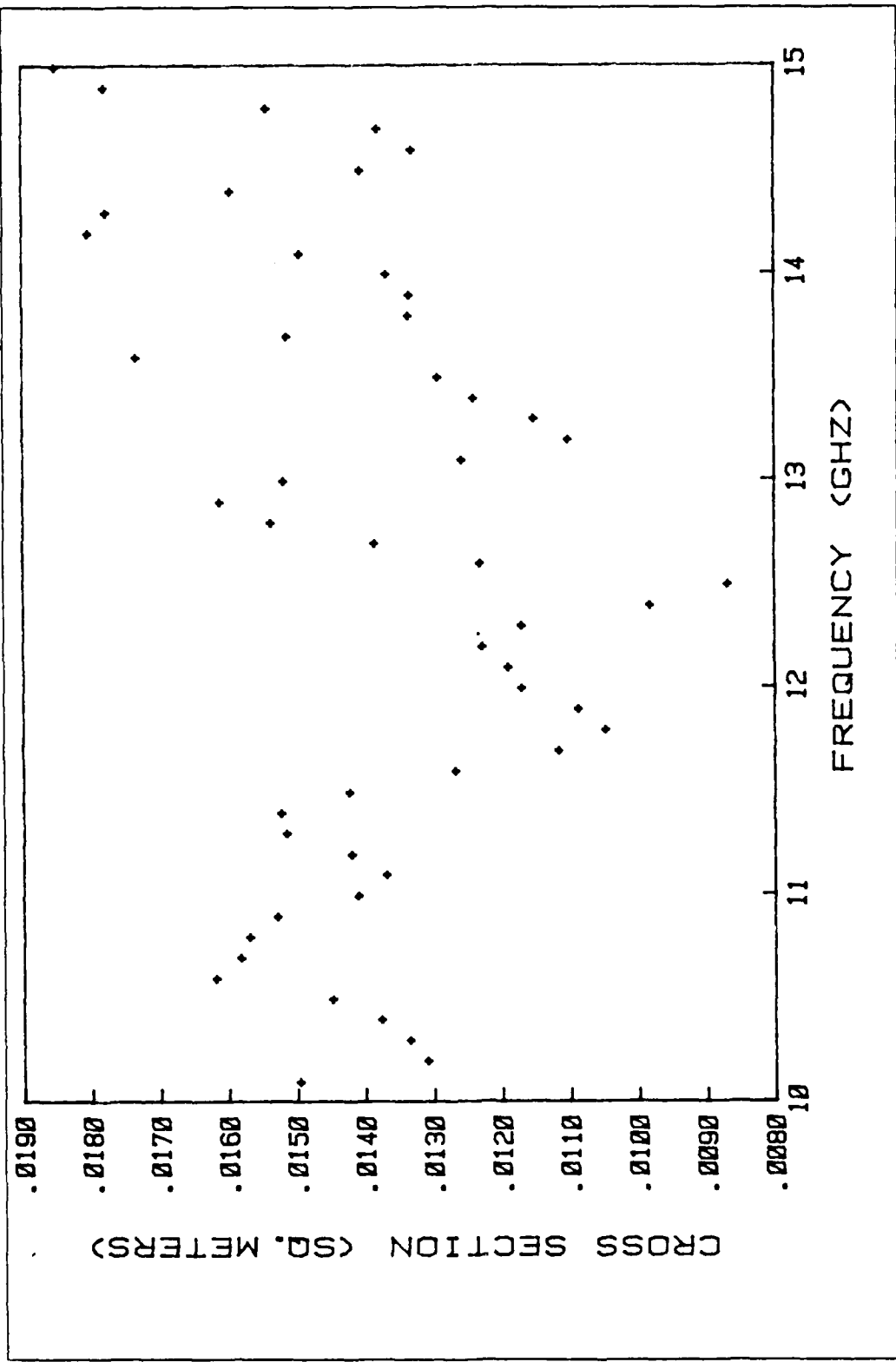


Figure 3.33 TARGET15 Cross-Section vs. Frequency

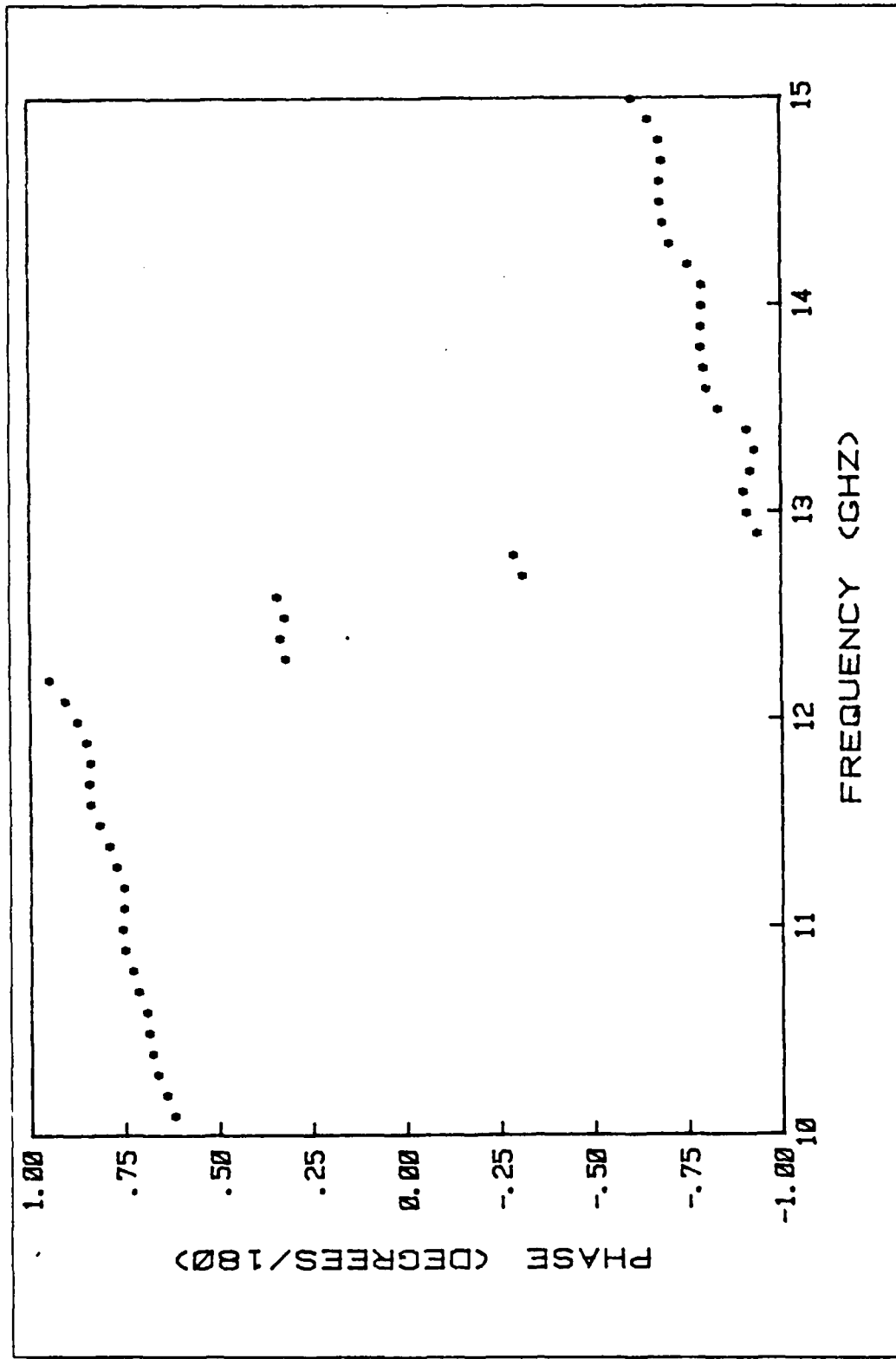


Figure 3.34 TARGET15 Phase Shift vs. Frequency

TABLE 17  
TARGET15 Measured Data

Frequency GHz	Cross-Section sq. meters	Phase Degrees/180
10.10	.01488	.60414
10.20	.01301	.62459
10.30	.01326	.64849
10.40	.01368	.66312
10.50	.01440	.67060
10.60	.01610	.67599
10.70	.01574	.69815
10.80	.01562	.71483
10.90	.01520	.73574
11.00	.01402	.73973
11.10	.01360	.73646
11.20	.01411	.73698
11.30	.01508	.75581
11.40	.01514	.77496
11.50	.01415	.80163
11.60	.01260	.82415
11.70	.01108	.82799
11.80	.01040	.82444
11.90	.01079	.83556
12.00	.01163	.85912
12.10	.01182	.89129
12.20	.01219	.93103
12.30	.01162	.30434
12.40	.00974	.31929
12.50	.00860	.30507
12.60	.01222	.32517
12.70	.01377	-.32655
12.80	.01529	-.30402
12.90	.01603	-.95134
13.00	.01511	-.92413
13.10	.01250	-.91309
13.20	.01094	-.93352
13.30	.01144	-.94571
13.40	.01231	-.92487
13.50	.01284	-.84693
13.60	.01725	-.81656
13.70	.01505	-.81043
13.80	.01327	-.80265
13.90	.01325	-.80197
14.00	.01359	-.80388
14.10	.01485	-.80439
14.20	.01795	-.76921
14.30	.01769	-.72022
14.40	.01586	-.70249
14.50	.01396	-.69516
14.60	.01321	-.69304
14.70	.01371	-.69835
14.80	.01533	-.69215
14.90	.01771	-.66405
15.00	.01843	-.61856

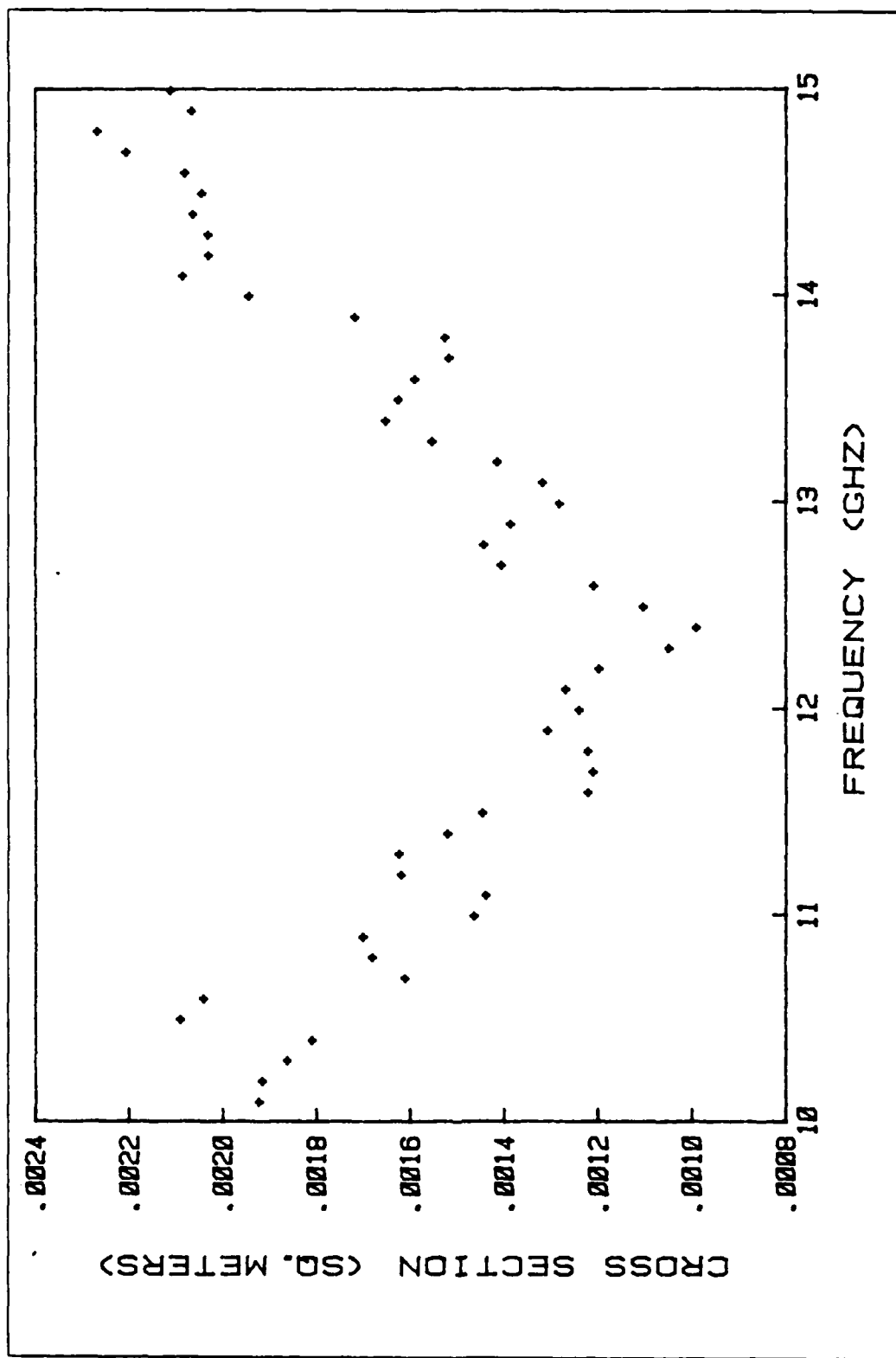


Figure 3.35 TARGET16 Cross-Section vs. Frequency

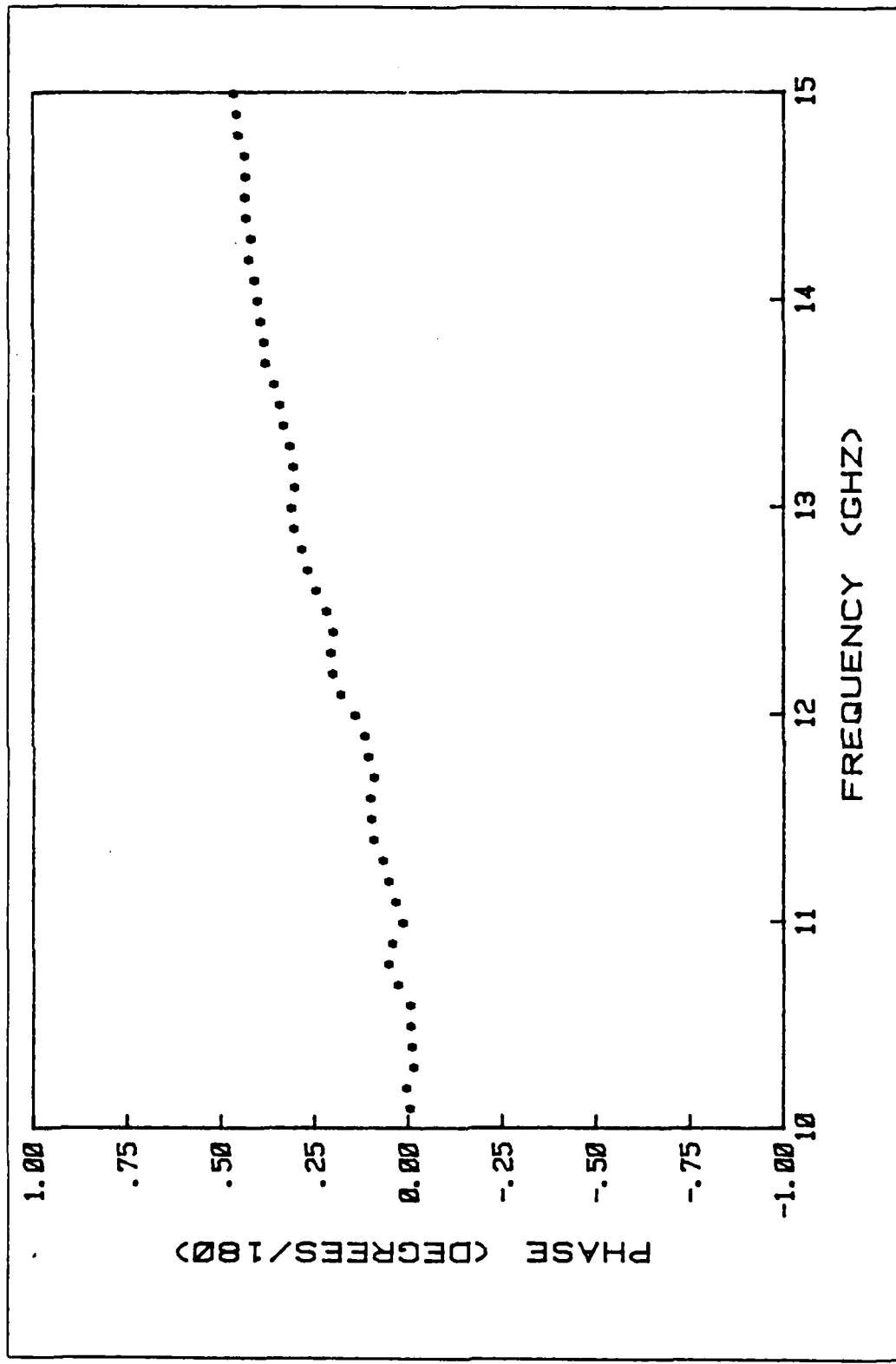


Figure 3.36 TARGET16 Phase Shift vs. Frequency

TABLE 18  
TARGET16 Measured Data

Frequency GHz	Cross-Section sq. meters	Phase Degrees/180
10.10	.00191	- .01981
10.20	.00190	- .01043
10.30	.00185	- .02846
10.40	.00180	- .02513
10.50	.00208	- .02143
10.60	.00203	- .01960
10.70	.00160	.01329
10.80	.00167	.03816
10.90	.00169	.02650
11.00	.00145	- .00047
11.10	.00143	.01843
11.20	.00161	.03776
11.30	.00161	.05299
11.40	.00151	.07801
11.50	.00143	.08473
11.60	.00121	.08665
11.70	.00120	.07786
11.80	.00121	.09312
11.90	.00130	.09945
12.00	.00123	.12639
12.10	.00126	.16458
12.20	.00119	.18565
12.30	.00104	.19985
12.40	.00098	.18504
12.50	.00109	.20305
12.60	.00120	.23177
12.70	.00139	.25334
12.80	.00143	.26984
12.90	.00138	.28878
13.00	.00127	.29633
13.10	.00131	.28705
13.20	.00140	.29187
13.30	.00154	.30142
13.40	.00164	.31797
13.50	.00161	.32802
13.60	.00158	.34364
13.70	.00151	.36658
13.80	.00152	.37135
13.90	.00171	.37675
14.00	.00193	.38538
14.10	.00207	.39298
14.20	.00202	.40854
14.30	.00202	.40296
14.40	.00205	.41617
14.50	.00203	.41932
14.60	.00207	.41850
14.70	.00219	.42041
14.80	.00226	.43807
14.90	.00205	.44164
15.00	.00210	.44929

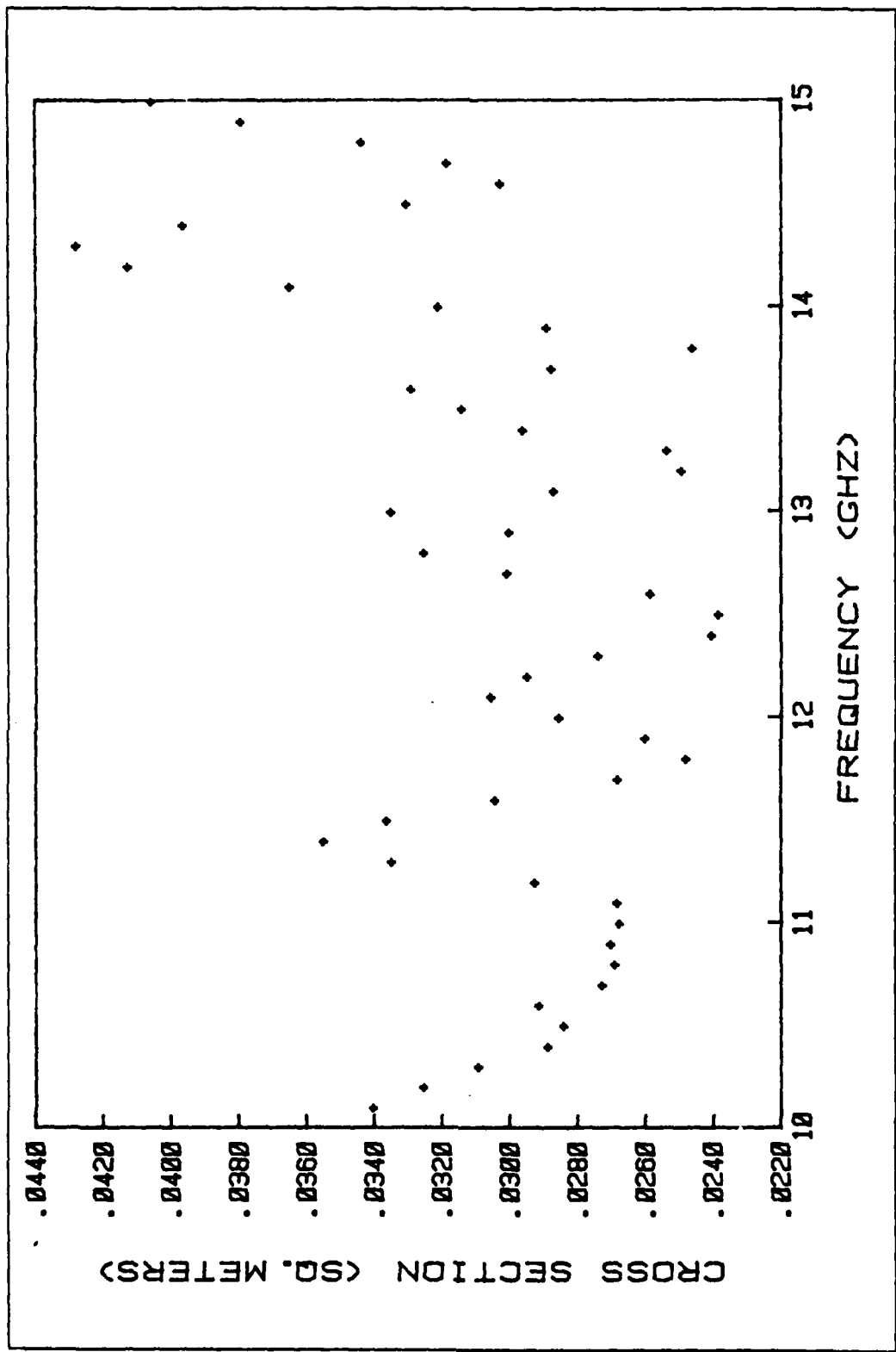


Figure 3.37 TARGET17 Cross-Section vs. Frequency

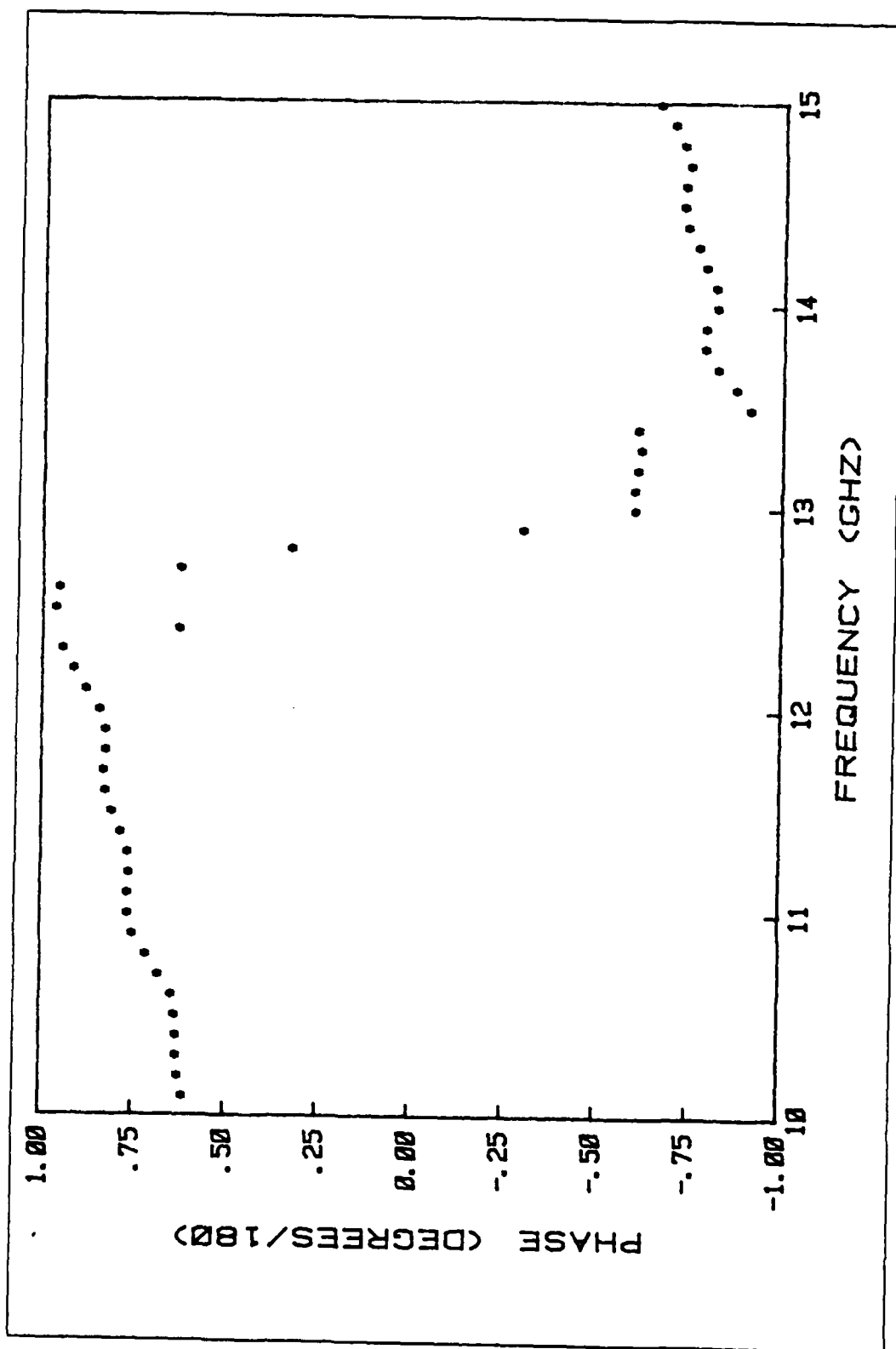


Figure 3.38 TARGET17 Phase Shift vs. Frequency

TABLE 19  
TARGET17 Measured Data

Frequency GHz	Cross-Section sq. meters	Phase Degrees/180
10.10	.03388	.59630
10.20	.03238	.60864
10.30	.03077	.61456
10.40	.02872	.61390
10.50	.02826	.61828
10.60	.02899	.62889
10.70	.02711	.66596
10.80	.02674	.70048
10.90	.02688	.73402
11.00	.02661	.74786
11.10	.02667	.74859
11.20	.02910	.74542
11.30	.03333	.75021
11.40	.03534	.77020
11.50	.03348	.79461
11.60	.03027	.81224
11.70	.02666	.81737
11.80	.02465	.81165
11.90	.02584	.81189
12.00	.02839	.82825
12.10	.03042	.86668
12.20	.02933	.89934
12.30	.02724	.93012
12.40	.02389	.61479
12.50	.02369	.94946
12.60	.02570	.94207
12.70	.02992	.61165
12.80	.03237	.31203
12.90	.02986	-.31636
13.00	.03335	-.61746
13.10	.02855	-.61522
13.20	.02477	-.62329
13.30	.02519	-.63267
13.40	.02946	-.62304
13.50	.03124	-.92602
13.60	.03273	-.88636
13.70	.02861	-.83729
13.80	.02446	-.80036
13.90	.02876	-.80314
14.00	.03196	-.83425
14.10	.03633	-.83013
14.20	.04111	-.90359
14.30	.04263	-.78172
14.40	.03948	-.75217
14.50	.03289	-.74045
14.60	.03012	-.74376
14.70	.03170	-.75679
14.80	.03421	-.74094
14.90	.03777	-.71410
15.00	.04040	-.67494

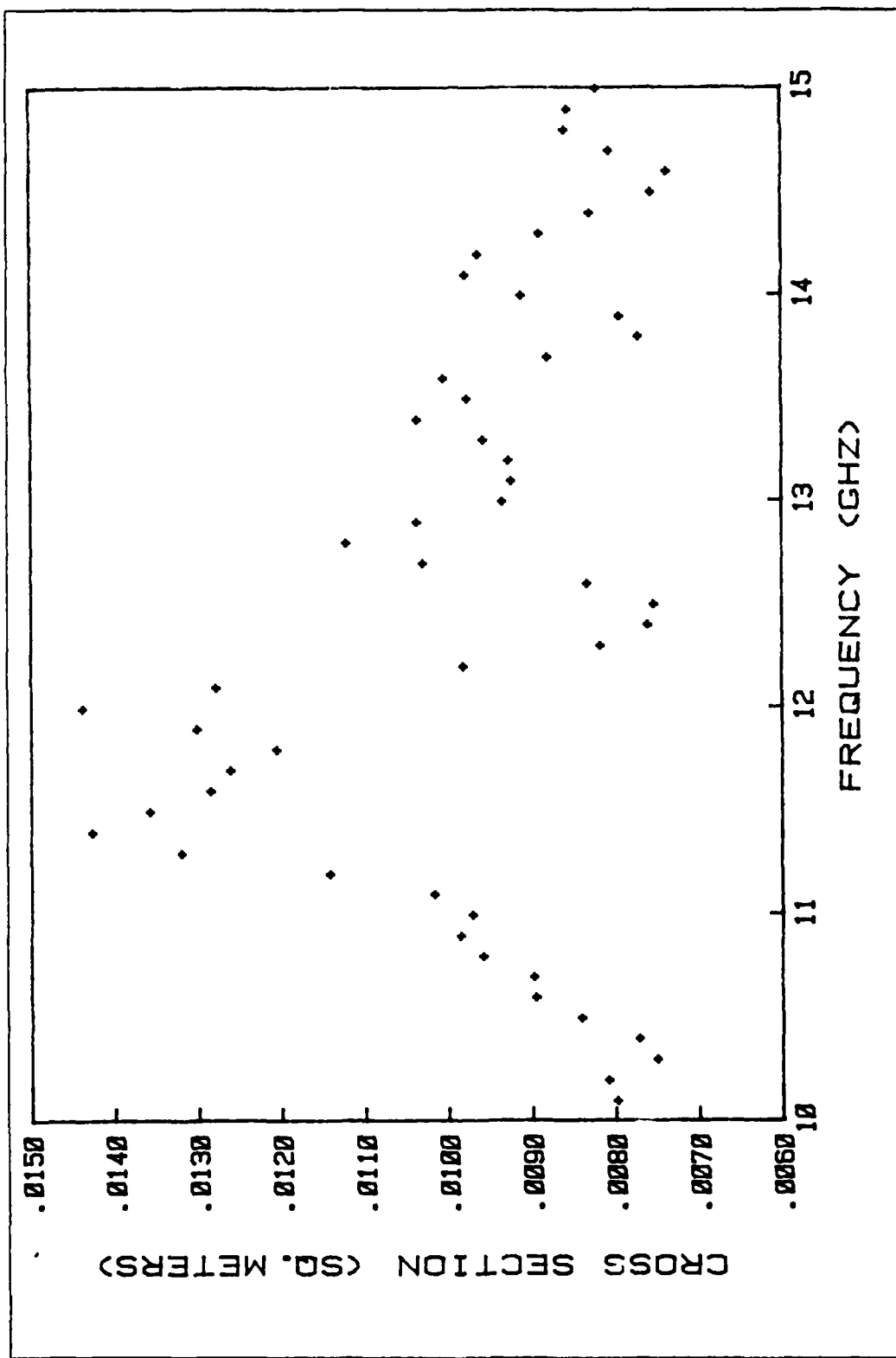


Figure 3.39 TARGET18 Cross-Section vs. Frequency

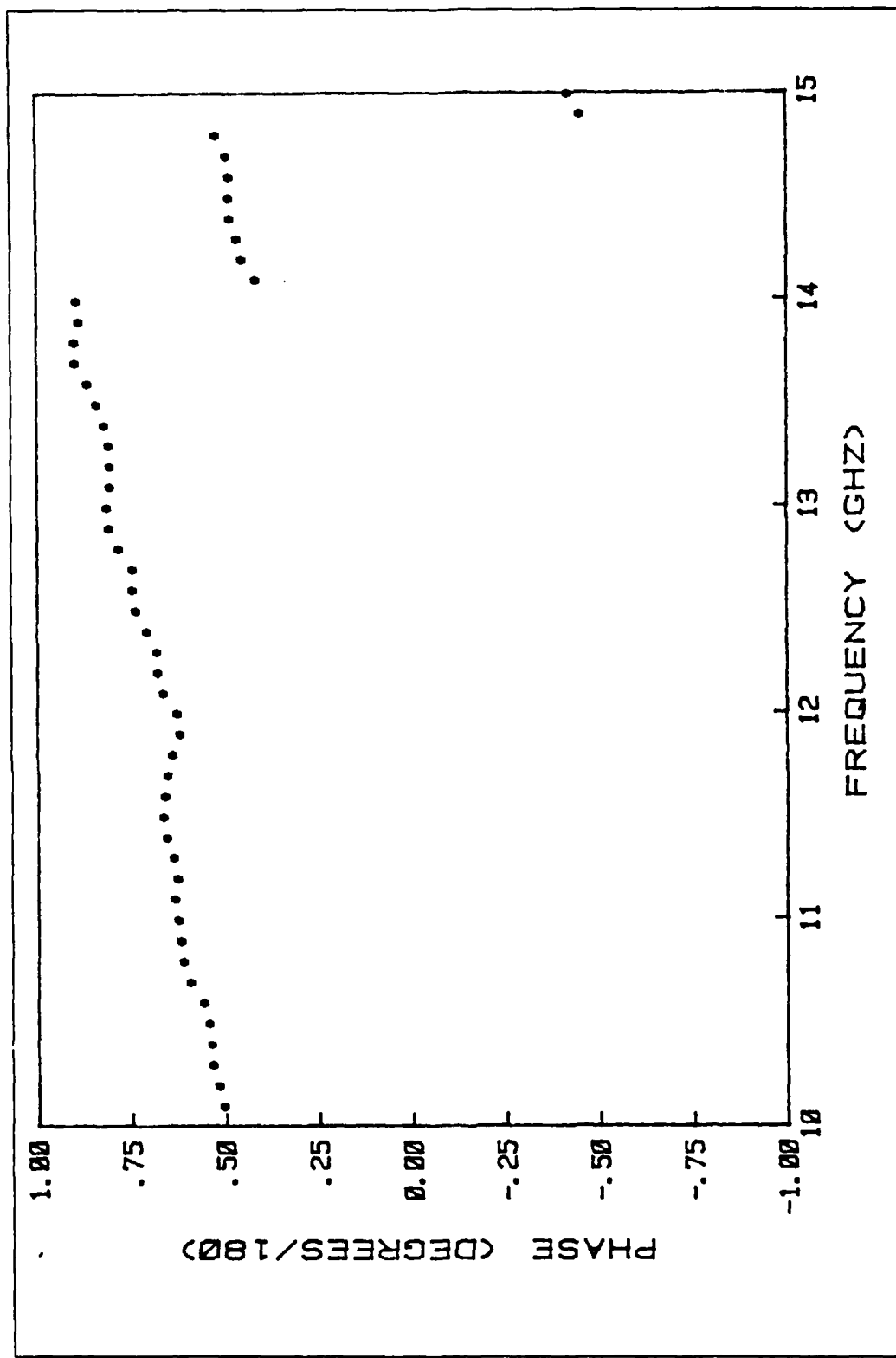


Figure 3.40 TARGET18 Phase Shift vs. Frequency

TABLE 20  
TARGET18 Measured Data

Frequency GHz	Cross-Section sq. meters	Phase Degrees/180
10.10	.00792	.49006
10.20	.00802	.50306
10.30	.00743	.51995
10.40	.00765	.52051
10.50	.00835	.52888
10.60	.00889	.54330
10.70	.00891	.58054
10.80	.00952	.59758
10.90	.00979	.60511
11.00	.00965	.61175
11.10	.01010	.62009
11.20	.01136	.61254
11.30	.01313	.62358
11.40	.01420	.64120
11.50	.01351	.65096
11.60	.01278	.64641
11.70	.01254	.64803
11.80	.01199	.62488
11.90	.01294	.60546
12.00	.01431	.61338
12.10	.01271	.65064
12.20	.00975	.66407
12.30	.00812	.66759
12.40	.00754	.69225
12.50	.00747	.72220
12.60	.00827	.73127
12.70	.01023	.73148
12.80	.01115	.76808
12.90	.01031	.79457
13.00	.00928	.79839
13.10	.00917	.79078
13.20	.00921	.79003
13.30	.00951	.79290
13.40	.01030	.80617
13.50	.00969	.82647
13.60	.00998	.85067
13.70	.00873	.88347
13.80	.00765	.88351
13.90	.00787	.87301
14.00	.00904	.87832
14.10	.00972	.40112
14.20	.00957	.43689
14.30	.00883	.45085
14.40	.00822	.45688
14.50	.00749	.47060
14.60	.00731	.46955
14.70	.00800	.47799
14.80	.00853	.50338
14.90	.00849	-.46492
15.00	.00814	-.43260

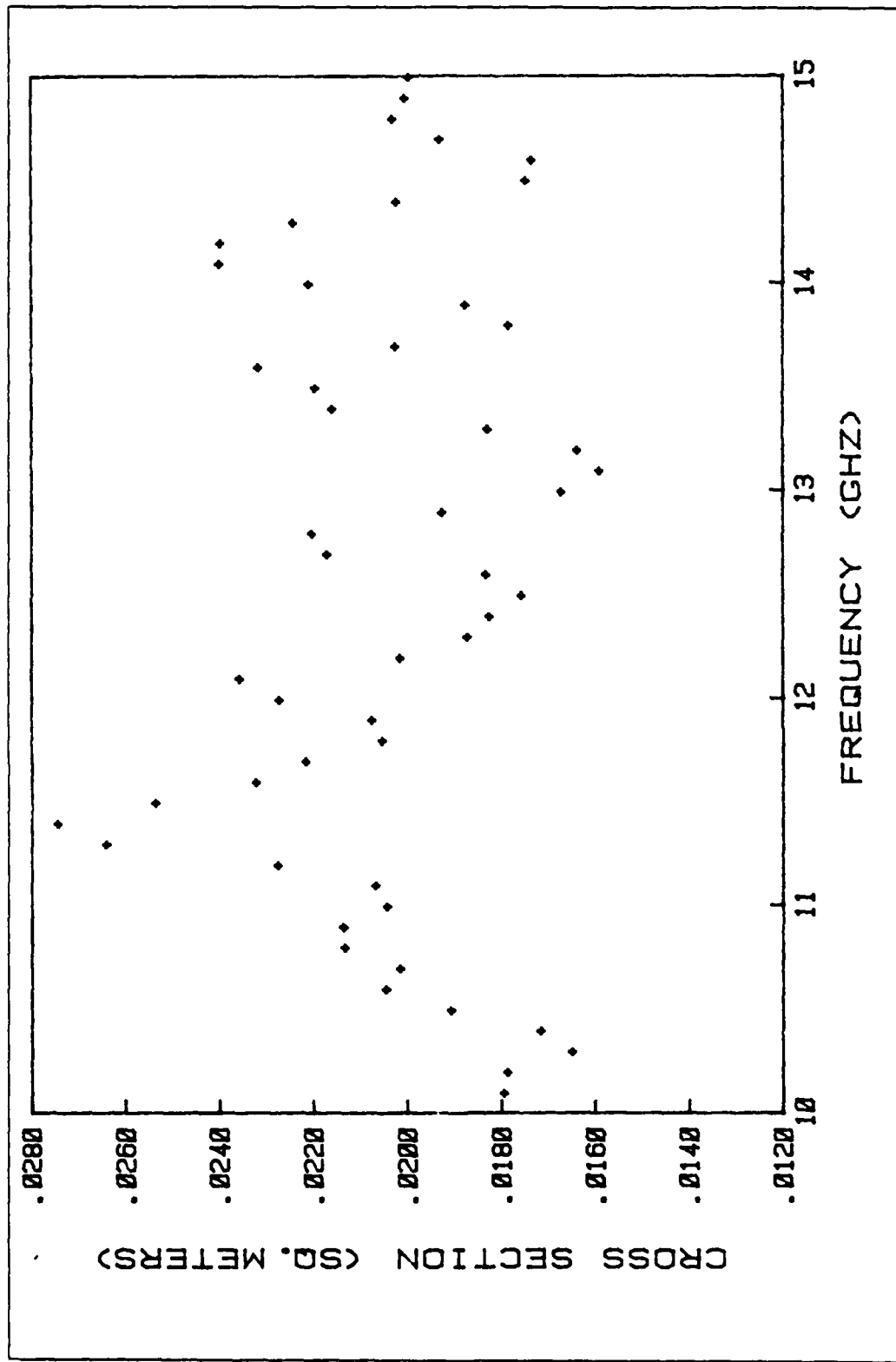


Figure 3.41 TARGET19 Cross-Section vs. Frequency

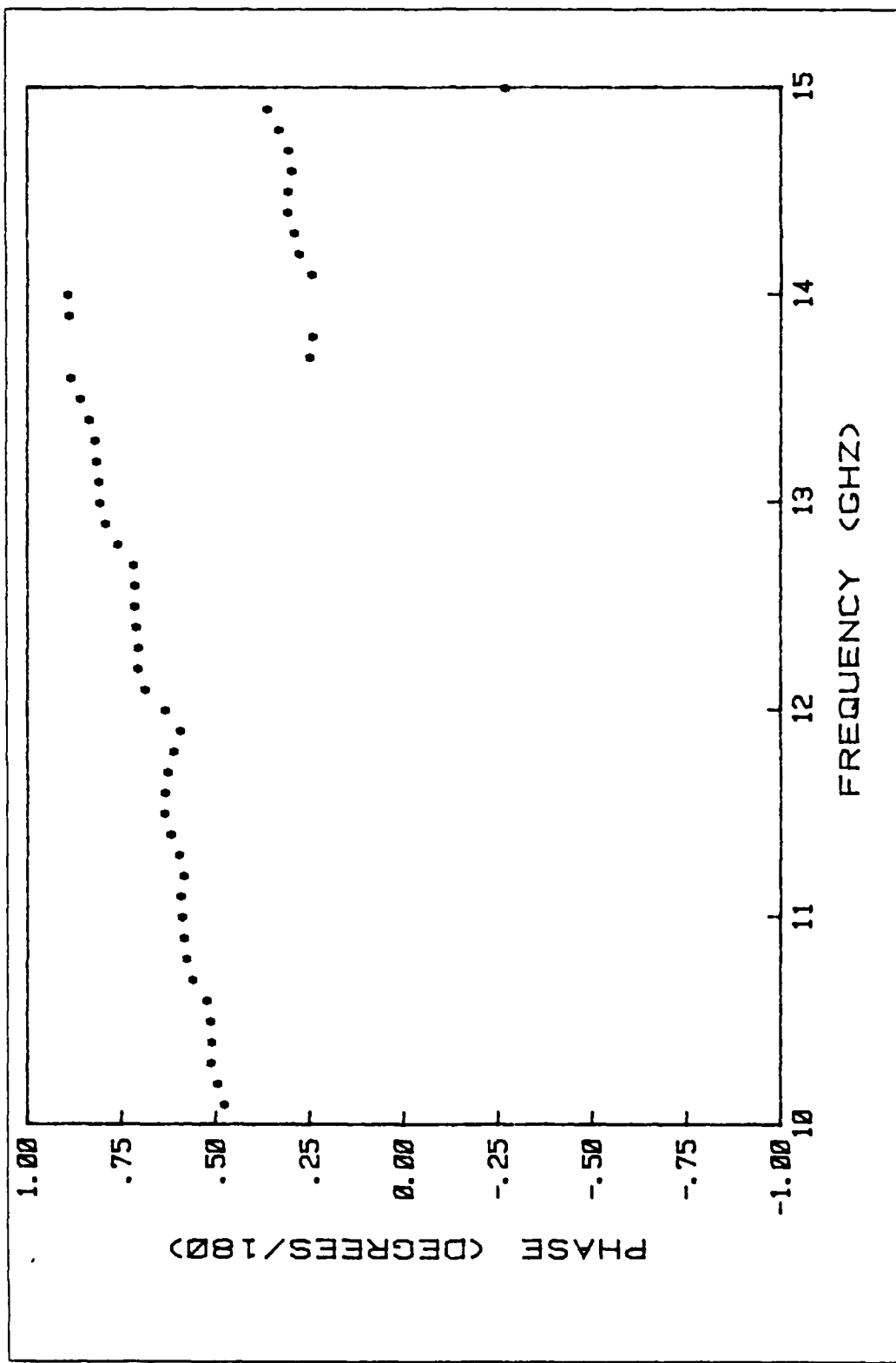


Figure 3.42 TARGET19 Phase Shift vs. Frequency

TABLE 21  
TARGET19 Measured Data

Frequency GHz	Cross-Section sq. meters	Phase Degrees/180
10.10	01783	46155
10.20	01774	47869
10.30	01638	49631
10.40	01704	49497
10.50	01895	49709
10.60	02034	50843
10.70	02063	54543
10.80	02121	56201
10.90	03125	56931
11.00	02032	57261
11.10	02056	57723
11.20	02264	56814
11.30	02629	58113
11.40	02732	60324
11.50	02524	61907
11.60	02310	61904
11.70	02205	61175
11.80	02042	59585
11.90	02063	57811
12.00	02261	61738
12.10	02345	67181
12.20	02004	69085
12.30	01861	68954
12.40	01813	68586
12.50	01746	69959
12.60	01820	70003
12.70	02159	70243
12.80	02190	74464
12.90	01914	77743
13.00	01860	79158
13.10	01578	79453
13.20	01626	80063
13.30	01817	80553
13.40	02148	82103
13.50	02183	84263
13.60	02305	87006
13.70	02014	23459
13.80	01772	22744
13.90	01864	87457
14.00	02197	87667
14.10	02387	23076
14.20	02384	26251
14.30	02230	27554
14.40	02011	29318
14.50	01736	29159
14.60	01723	28308
14.70	01919	29101
14.80	02019	31760
14.90	01993	34735
15.00	01984	- 28466

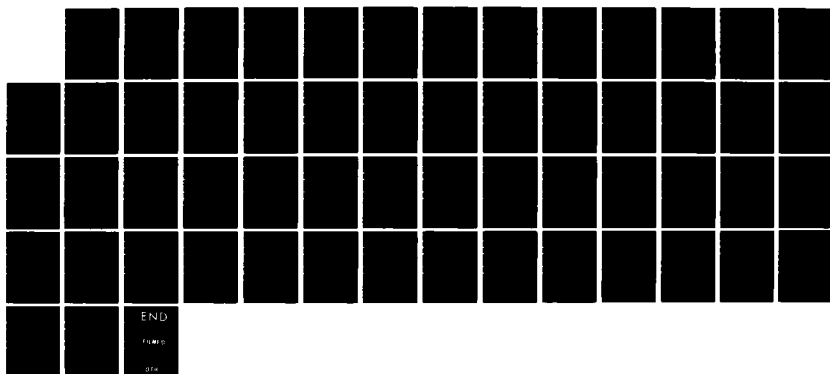
AD-A155 739 BROADSIDE SCATTERING OF A TUBULAR CYLINDER FOR  
EVALUATION OF TARGET IDENTIFICATION(U) NAVAL  
POSTGRADUATE SCHOOL MONTEREY CA B HAFLAY MAR 85

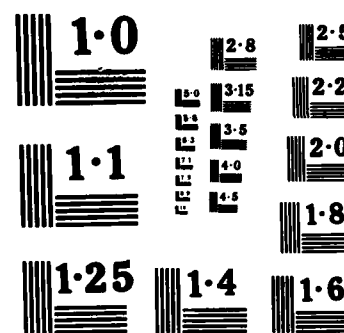
2/2

UNCLASSIFIED

F/G 17/9

NL





NATIONAL BUREAU OF STANDARDS  
MICROCOPY RESOLUTION TEST CHART

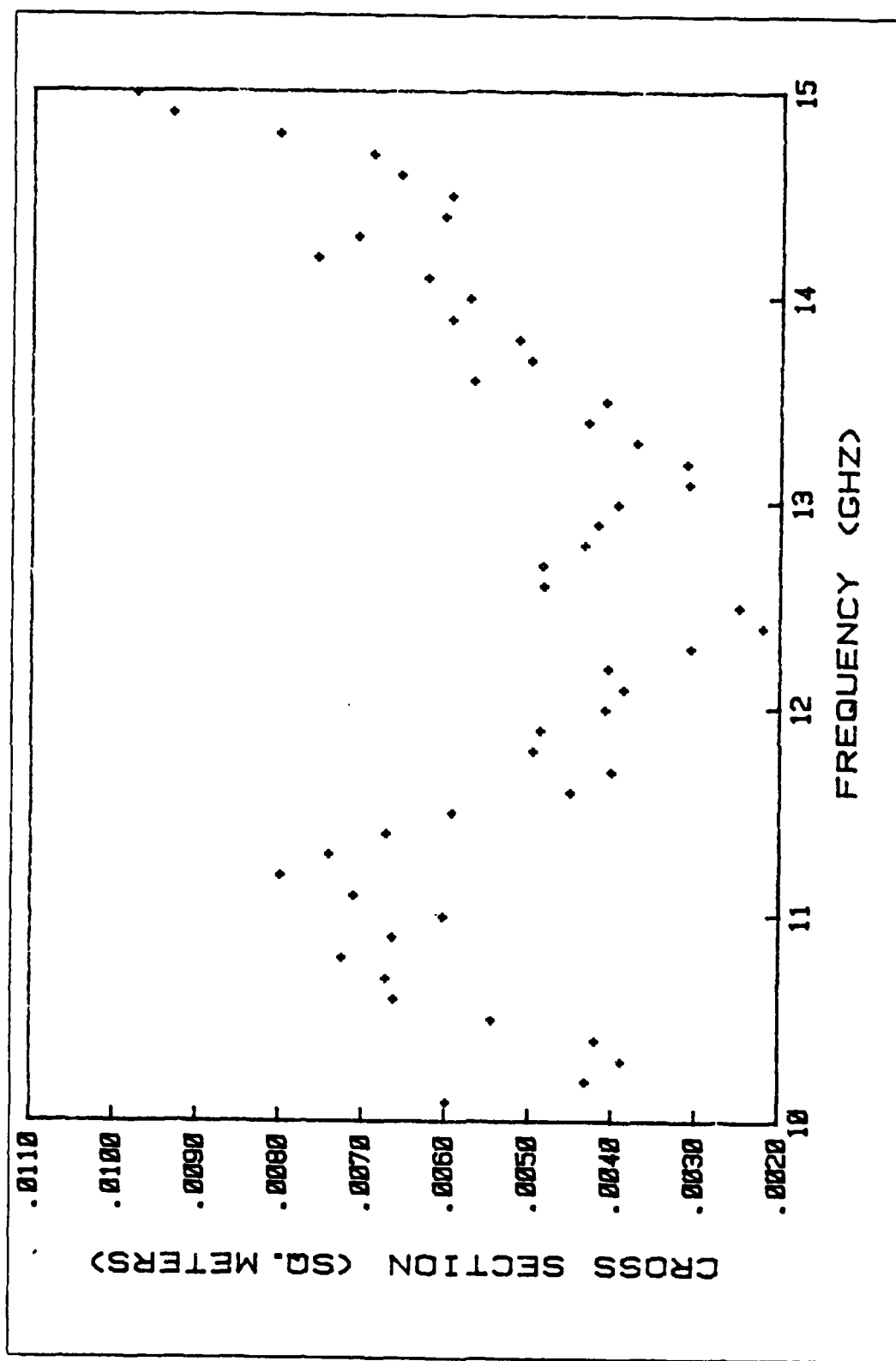


Figure 3.43 TARGET20 Cross-Section vs. Frequency

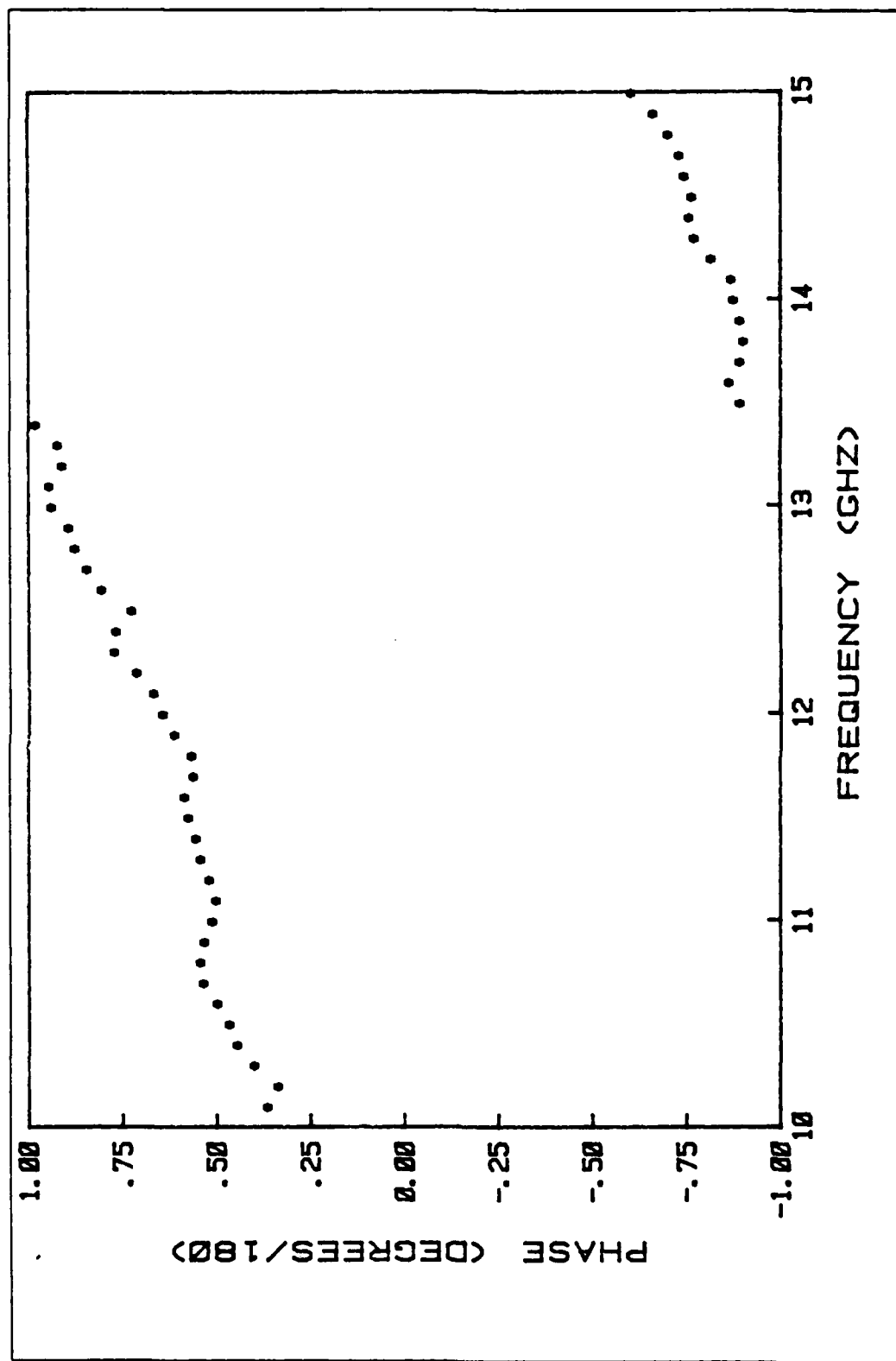


Figure 3.44 TARGET20 Phase Shift vs. Frequency

TABLE 22  
TARGET20 Measured Data

Frequency GHz	Cross-Section sq. meters	Phase Degrees/180
10.10	.00592	.34969
10.20	.00425	.32158
10.30	.00382	.38386
10.40	.00413	.43098
10.50	.00538	.45171
10.60	.00655	.48329
10.70	.00665	.52071
10.80	.00717	.52879
10.90	.00657	.51834
11.00	.00597	.49649
11.10	.00704	.48646
11.20	.00792	.50464
11.30	.00734	.52759
11.40	.00665	.53942
11.50	.00586	.55987
11.60	.00444	.56960
11.70	.00395	.54635
11.80	.00489	.54966
11.90	.00480	.59912
12.00	.00402	.62885
12.10	.00380	.65289
12.20	.00399	.69847
12.30	.00299	.75723
12.40	.00213	.75326
12.50	.00242	.71088
12.60	.00477	.79151
12.70	.00478	.83069
12.80	.00428	.86141
12.90	.00412	.87804
13.00	.00389	.92379
13.10	.00303	.92955
13.20	.00306	.89495
13.30	.00366	.90670
13.40	.00424	.96667
13.50	.00402	-.90790
13.60	.00561	-.87820
13.70	.00493	-.90765
13.80	.00508	-.91694
13.90	.00588	-.90704
14.00	.00567	-.89028
14.10	.00618	-.88433
14.20	.00751	-.83079
14.30	.00702	-.78607
14.40	.00597	-.77294
14.50	.00590	-.77987
14.60	.00652	-.76032
14.70	.00684	-.74685
14.80	.00797	-.71762
14.90	.00925	-.67590
15.00	.00969	-.61797

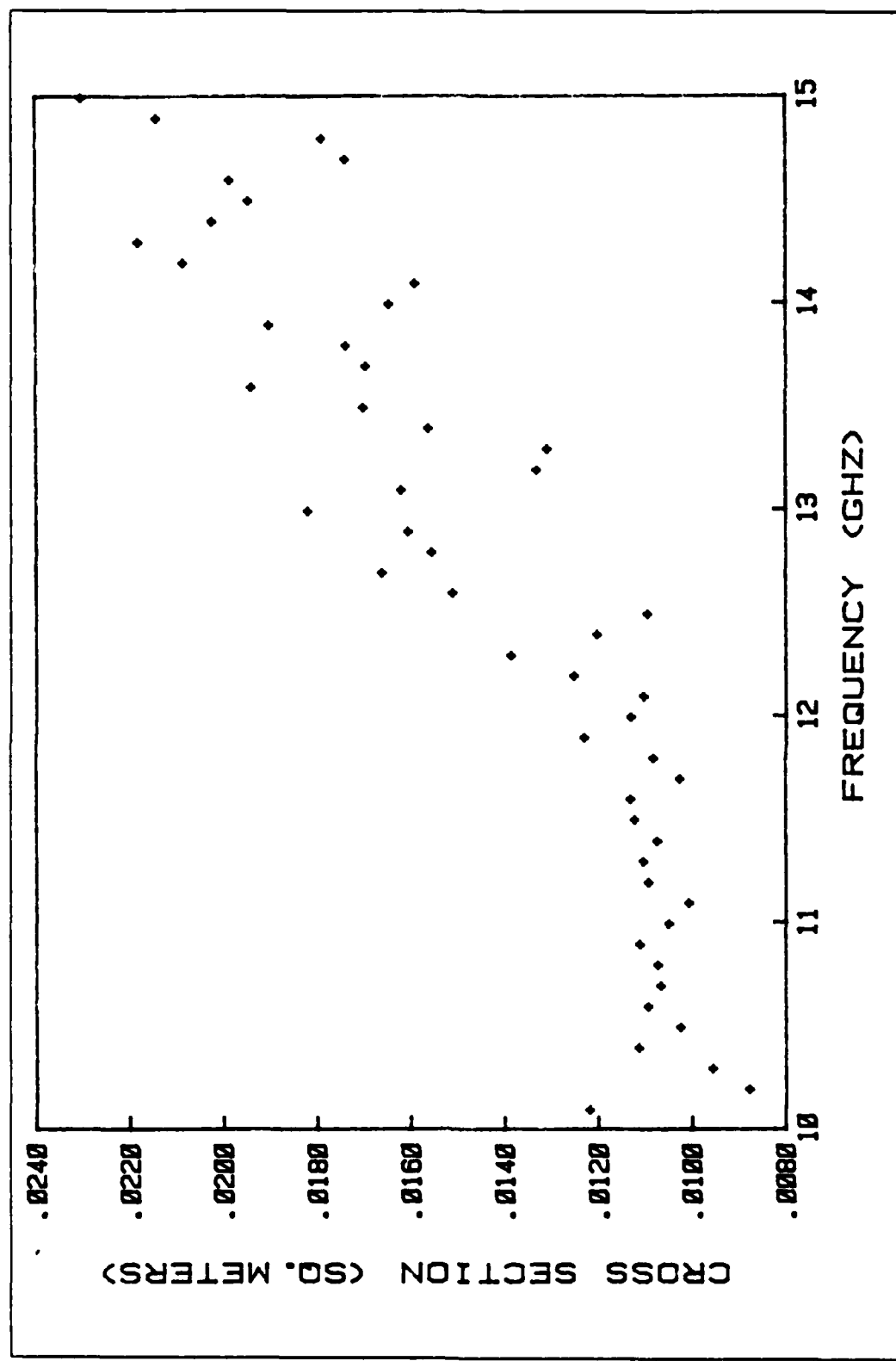


Figure 3.45 TARGET21 Cross-Section vs. Frequency

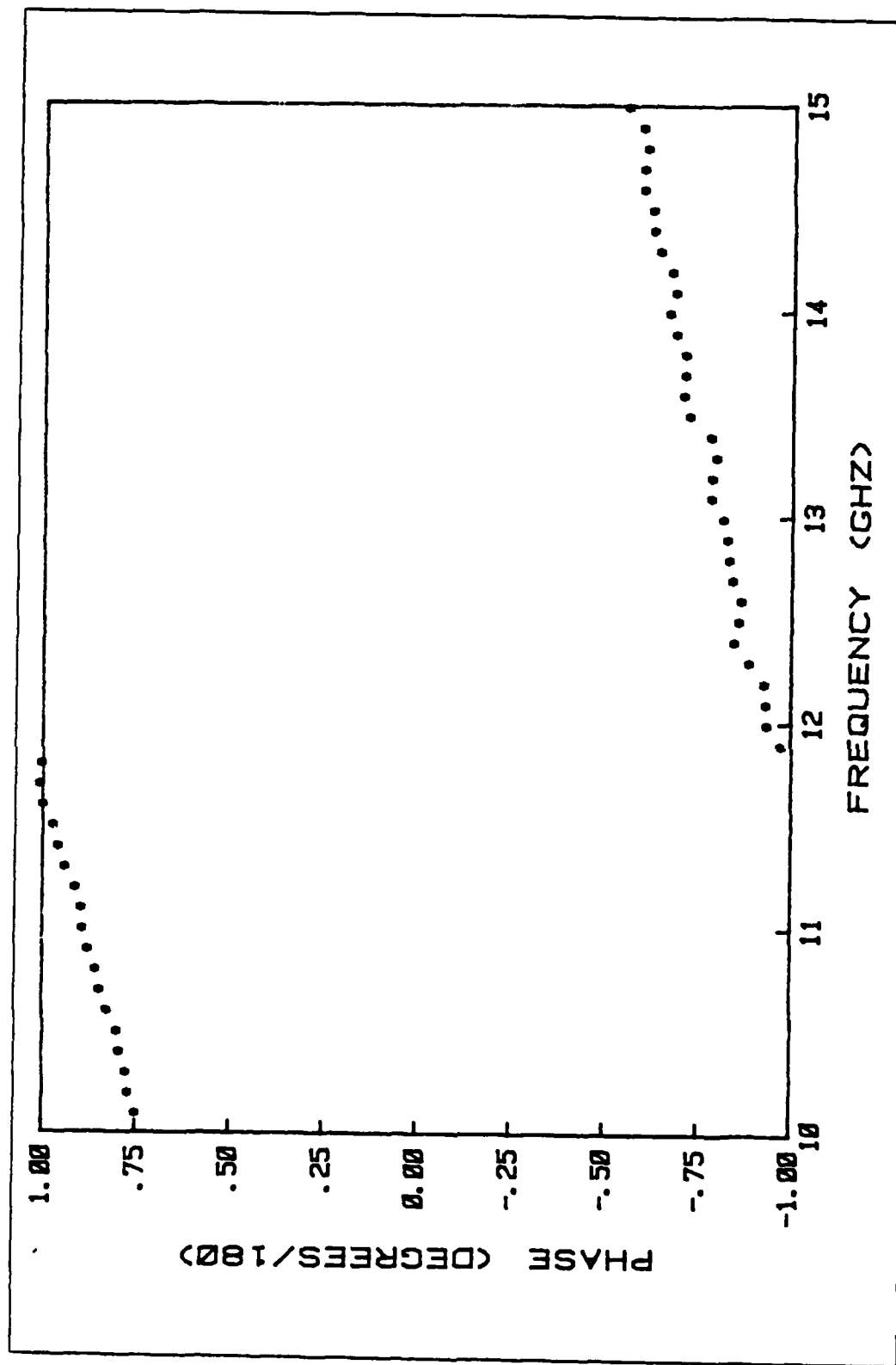


Figure 3.46 TARGET21 Phase Shift vs. Frequency

TABLE 23  
TARGET21 Measured Data

Frequency GHz	Cross-Section sq. meters	Phase Degrees/180
10.10	.01206	.73561
10.20	.00866	.75538
10.30	.00944	.76087
10.40	.01101	.77910
10.50	.01012	.78630
10.60	.01081	.81097
10.70	.01054	.83066
10.80	.01060	.84228
10.90	.01099	.86339
11.00	.01037	.87750
11.10	.00995	.88143
11.20	.01081	.89719
11.30	.01092	.92596
11.40	.01062	.94367
11.50	.01110	.95768
11.60	.01119	.98364
11.70	.01013	.99392
11.80	.01070	.98934
11.90	.01219	-.98821
12.00	.01119	-.94993
12.10	.01091	-.94692
12.20	.01240	-.94244
12.30	.01374	-.90184
12.40	.01191	-.86166
12.50	.01082	-.87250
12.60	.01498	-.88010
12.70	.01649	-.85741
12.80	.01544	-.84620
12.90	.01593	-.84336
13.00	.01808	-.82983
13.10	.01608	-.79775
13.20	.01319	-.80921
13.30	.01296	-.81179
13.40	.01549	-.79727
13.50	.01688	-.73962
13.60	.01928	-.72404
13.70	.01684	-.72684
13.80	.01726	-.72723
13.90	.01889	-.70348
14.00	.01633	-.68427
14.10	.01578	-.70022
14.20	.03073	-.68936
14.30	.02168	-.65751
14.40	.02010	-.63941
14.50	.01934	-.63719
14.60	.01973	-.61530
14.70	.01726	-.61382
14.80	.01776	-.62422
14.90	.02129	-.61064
15.00	.02289	-.57067

## IV. DATA ANALYSIS

### A. ANALYSIS OF EXPERIMENTAL DATA

The experimental data on the back scattered cross section of a tubular cylinder obtained in the Scattering Laboratory as described in Chapter III are analyzed. The cross section under the circumstances described in Chapter III is a function of three parameters:

- (1) The length of the cylinder ( $2h$ )
- (2) The diameter of the cylinder ( $2a$ ).
- (3) The frequency of the incident wave ( $f$ ).

This is shown in equation 4.1

$$\sigma = G(a, h, f) \quad (4.1)$$

The experimental data as shown in Figures 3.5 to 3.46 shows the dependence of the cross section on frequency for cylinders of fixed lengths and diameters.

To isolate the dependence of the back scattering cross section on the length of a cylinder, the constant parameters should be the cylinder diameter and the frequency. This was achieved by using five cylinders with the same diameter and taking the cross section of each one of them at the same frequency. Table 24 shows the targets used for each diameter.

The frequencies checked were 10.1, 11, 12, 13, 14 and 15 GHz and the results are given at the end of this chapter in Figures 4.1, 4.2, 4.3 .

In Figure 4.1 for  $2a=0.375"$ , one can see that the curve has tilt at  $f=10.1$  when  $2h=2.7$ ; for  $f=11$  the tilt occurs at  $2h=2.5$  and for  $f=12$  this happens at  $2h=2.25$ . The line seems

TABLE 24  
Targets with Constant 2a

2h 2a	0.375"	0.5"	0.75"
2.0	TARGET1	TARGET2	TARGET3
2.25	TARGET4	TARGET5	TARGET6
2.5	TARGET7	TARGET8	TARGET9
2.75	TARGET10	TARGET11	TARGET12
3.0	TARGET13	TARGET14	TARGET15

to have the same slope in all these graphs near this point. The same phenomenon appears for  $2h=2.75$  at  $f=11$ ;  $2h=2.5$  at  $f=12$  and  $2h=2.25$  at  $f=13$ . In Figure 4.2 for  $2a=0.5"$  the same phenomenon occurs at  $2h=2.75$  and  $f=12$ ,  $2h=2.5$  and  $f=13$  and  $2h=2.25$  and  $f=14$ . For  $2a=0.75"$  in Figure 4.3 this occurs at  $2h=2.75$ ,  $f=11$  and  $2h=2.4$ ,  $f=12$ ; and another at  $2h=2.5$ ,  $f=13$  and  $2h=2.25$ ,  $f=14$ .

This phenomenon leads to the assumption that the back scattering cross section of a tubular cylinder has a dependence not on  $h$  by itself but on combination of  $f$  and  $h$ . For those points mentioned above, the product  $2hf$  is shown in Table 25.

Thus the cross section of a tubular cylinder can be written as a function of  $hf$  or  $kh$  where  $k=2\pi f/c$  and is shown in equation 4.2 which is identical to equation 4.1.

$$\sigma = G_1(a, f, hf) = G_2(a, k, kh) \quad (4.2)$$

#### B. COMPARISON BETWEEN MEASUREMENTS AND THEORY

From equations 2.30 one can see that  $\sigma$ , when properly normalized, (e.g. divided by  $ah$  or multiplied by  $k^2$ ) depends only on two variables which are combinations of  $a$ ,  $h$  and  $k$ . This dependence is shown in equation 4.3, where  $l_1=kh$  and  $l_2=ka$ . This equation can also be written as 4.4.

TABLE 25  
2hf for Discontinuity Points

2a	f	2h	2hf
0.375	10.1	2.7	27.25
	11	2.5	27.5
	12	2.25	27.0
0.375	11	2.75	30.25
	12	2.5	30.0
	13	2.25	29.25
0.5	12	2.75	30.25
	12	2.75	30.0
	13	2.25	29.25
0.75	11	2.75	30.25
	12	2.4	28.8
0.75	13	2.5	52.5
	14	2.25	31.5

$$\sigma/ah = F(l_1, l_2) \quad (4.3)$$

$$\sigma/ah = F_1(l_1, l_2/l_1) = F_1(ka, h/a) \quad (4.4)$$

For cylinders with a constant  $h/a$ ,  $\sigma/ah$  can be plotted as a function of  $ka$  on the same graph. This effectively expands the frequency range over which data can be obtained using a cylinder. Table 26 shows the targets used for this purpose.

TABLE 26  
Cylinders with the Same h/a

Target name	Length	Diameter	h/a
TARGET16	1.5"	0.375"	4
TARGET2	2"	0.5"	4
TARGET18	2.5"	0.625"	4
TARGET15	3"	0.75"	4
<hr/>			
TARGET4	2.25"	0.375"	6
TARGET14	3"	0.5"	6
TARGET19	3.75"	0.625"	6
TARGET17	4.5"	0.75"	6
<hr/>			

Figure 4.4 is the graph for  $h/a=4$  and Figure 4.5 for  $h/a=6$ .  
The  $ka$  range covered by each target is shown on Table 27 .

TABLE 27  
ka Range Covered by Each Target

Target Name	h/a	minimum ka	maximum ka
TARGET16	4	1.01	1.50
TARGET2	4	1.34	2.00
TARGET18	4	1.68	2.49
TARGET15	4	2.01	2.99
<hr/>			
TARGET4	6	1.01	2.00
TARGET14	6	1.34	2.00
TARGET19	6	1.68	2.49
TARGET17	6	2.01	2.99

The overlapping points as shown on these graphs show that the experimental data are in agreement with the overall

shape. However, the small variations in the overlapping regions do not seem to fall at the same places. The reason for this discrepancy were discussed as measurement errors in Chapter III.

The overall shape is used to compare with theoretical predictions obtained by Professor Lee at the Naval Postgraduate School through solving equations 2.30 and 2.31 [Ref. 13]. This data is shown in Figure 4.6 for  $h/a=4$  and in Figure 4.7 for  $h/a=6$ . Theoretical values and experimental data are plotted together in Figures 4.8 and 4.9. In this figures one can see that there is very good agreement up to the point where  $ka$  is about 1.9. From that point to  $ka$  equal approximately 2.5 the minima and maxima of the experimental curve is shifted in  $ka$  by about 0.08.

The reason for the shifting and the disagreement at these points can be explained by the fact that there is wall thickness in the measured targets while the theory assumes infinitesimal thickness. The points of  $ka=1.9$  and  $ka=2.5$  are special because they correspond to the first two cutoff frequencies for the cylindrical waveguide modes:  $ka=1.8415$  is the cutoff point for  $H_{11}$  mode and  $ka=2.4046$  is the cutoff point for  $E_{01}$  mode [Ref. 14]. At  $ka=1.8415$  the wave starts to propagate without attenuation inside the cylinder. Since this value is determined by the inner diameter of the cylinder, the wall thickness cause the phenomenon to occur at a higher frequency and so produces the shift in the minima and maxima. Above  $ka=2.4$ ,  $E_{01}$  mode adds to the  $H_{11}$  mode and the total field inside the cylinder is the vectoral sum of those two modes. These effects were included in the theoretical calculation but the wall thickness was not.

The measured phase shift is shown in Figures 4.10 and 4.11 and the theoretical phase shift is given in Figures 4.12 and 4.13. The comparison as shown in Figures 4.14 and 4.15 shows agreement between the theory and the experiment.

The constant phase shift in the overall curve is due to the calibration of the system. It was done with a 3.187" sphere while the targets are 0.375" to 0.75" in diameter. That caused small phase shift because the targets were not at the same height as the calibration sphere. At  $ka=2.75$  where the phase shift is near  $\pm 180$  degrees, the average of  $\pm 180$  degrees produced the data points near  $180(m-2n)/m$  degrees which appear in Figures 4.14 and 4.15. Here  $0 \leq n \leq m$  and  $m$  is the number of averages taken.

The comparison between the theory and the measured data leads to conclusions that can be used for future work in this project, that will discussed in Chapter V.

#### C. RESULTS FOR CYLINDERS WITH FINS

As the first step for future work on employing target identification scheme through the cross section as a function of the frequency, two cylinders with fins attached have been measured (TARGET20 and TARGET21). The results as shown in Figure 3.43 and 3.44 are compared with the cylinder of the same length and diameter, TARGET15. The fins are like reflectors in TARGET20 and like corner reflectors in TARGET21. The comparison shows that the back scattered cross section of TARGET20 is much smaller than TARGET15. The reason might be that the axial current that flow on the fins cause field that add vectorally to the field created by the current flowing on the cylinder and in this spatial case it happens to be added destructively. A detailed study on the surface current distribution on the cylinder without fins may lead to explanations about how the fins change the surface current flow on the cylinder.

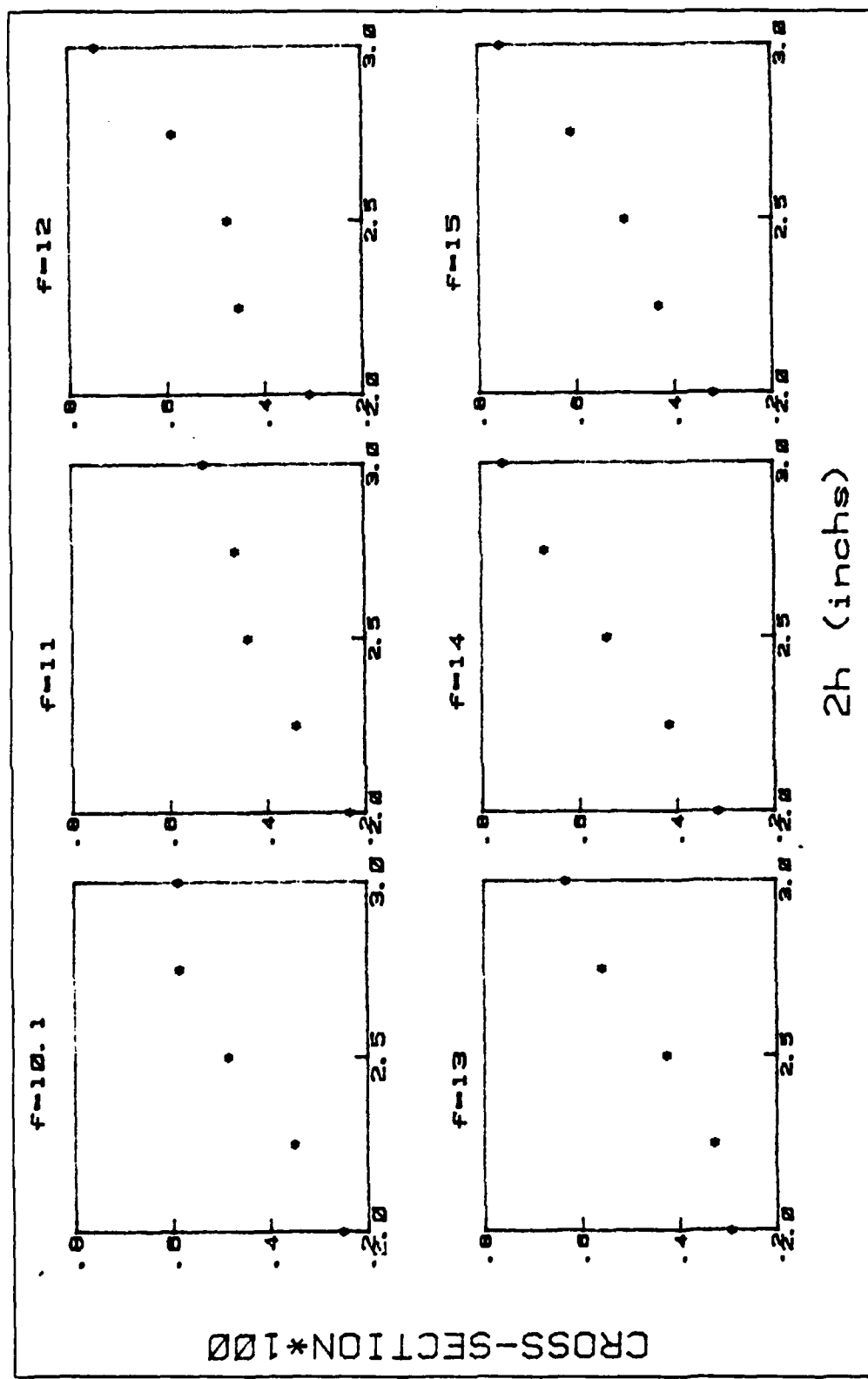


Figure 4.1 Length Dependence of Cross Section  
for  $2a = 0.375$ .

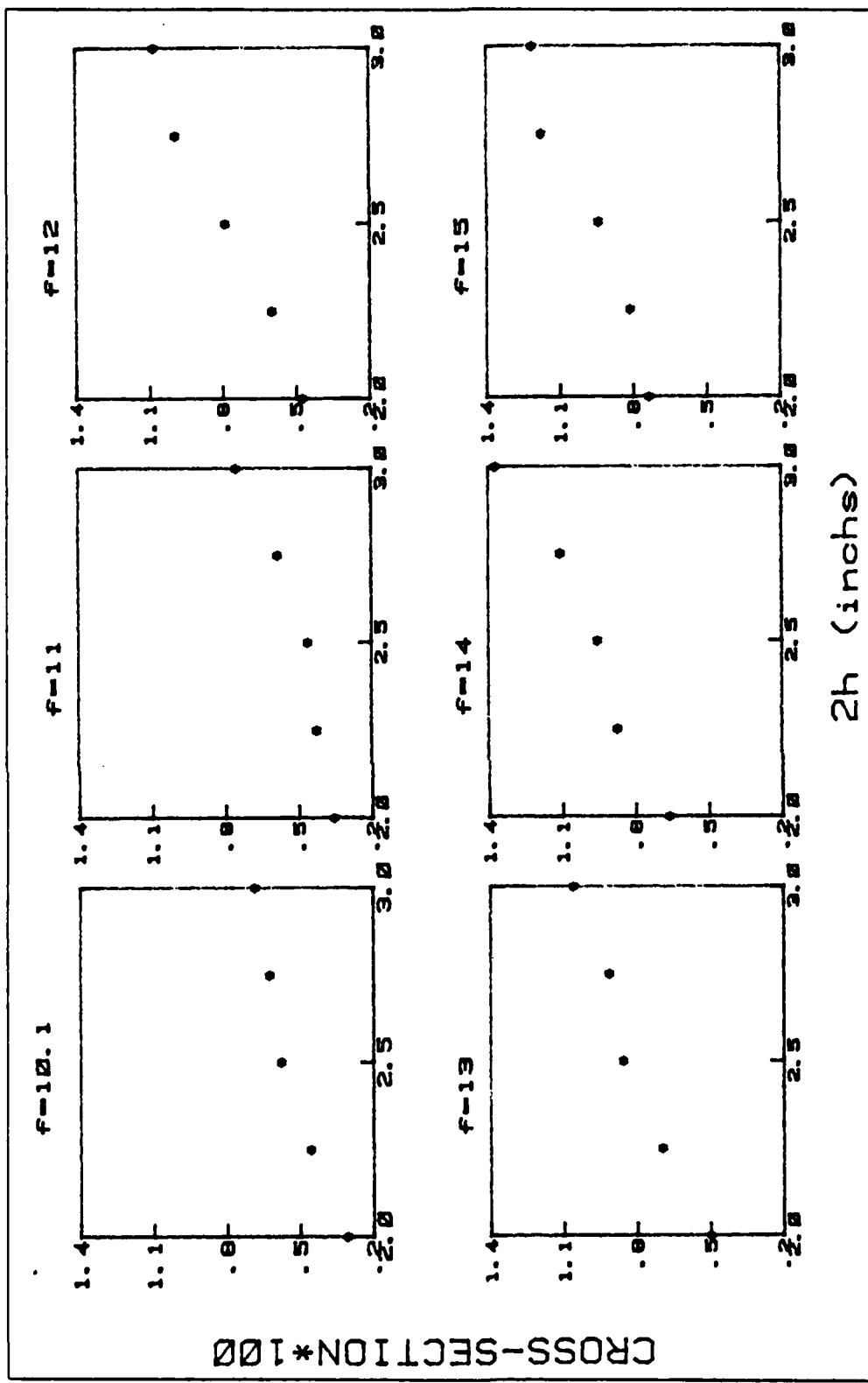


Figure 4.2 Length Dependence of Cross Section  
for  $2a=0.5$ .

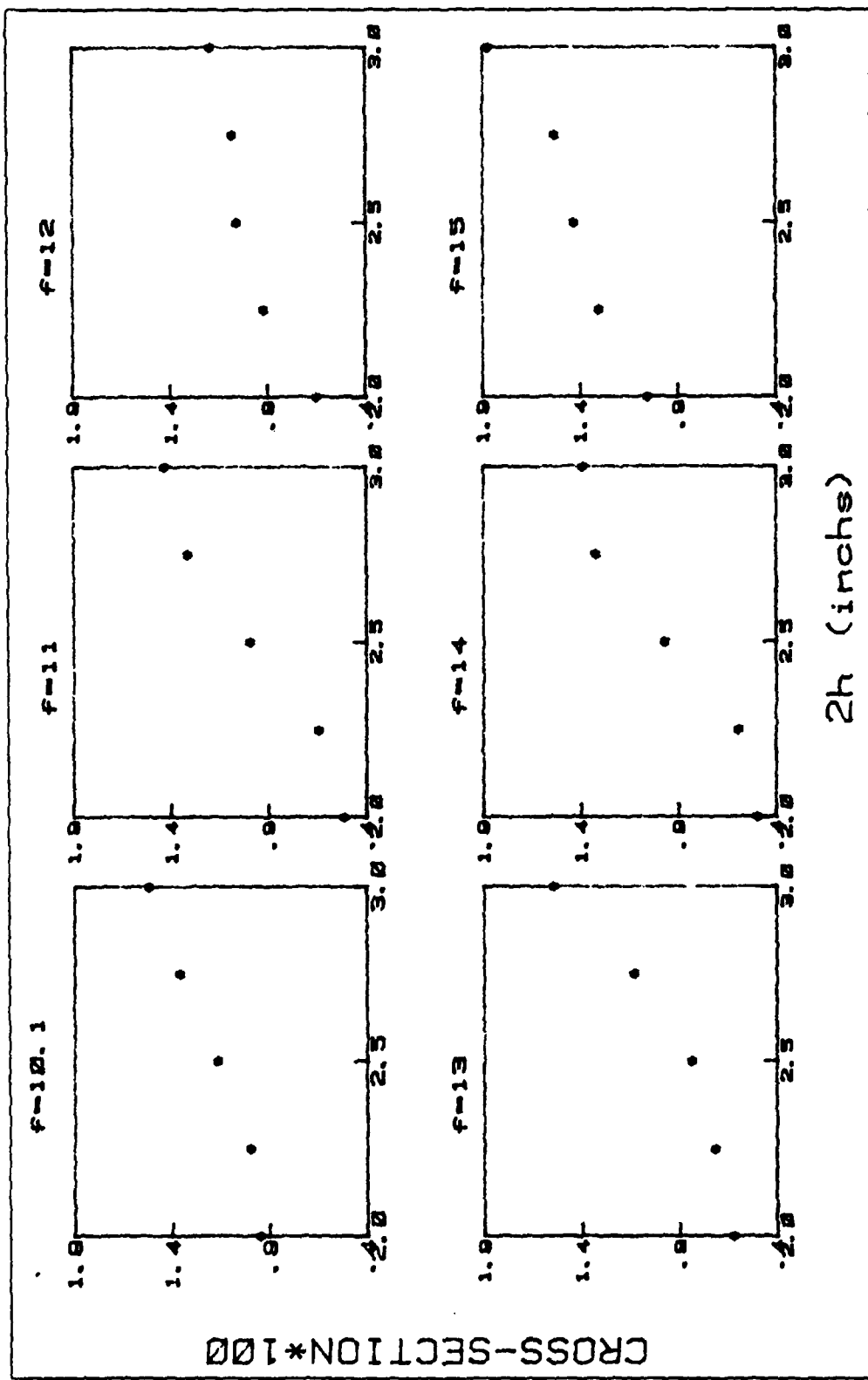


Figure 4.3 Length Dependence of Cross Section  
for  $2a=0.75$ .

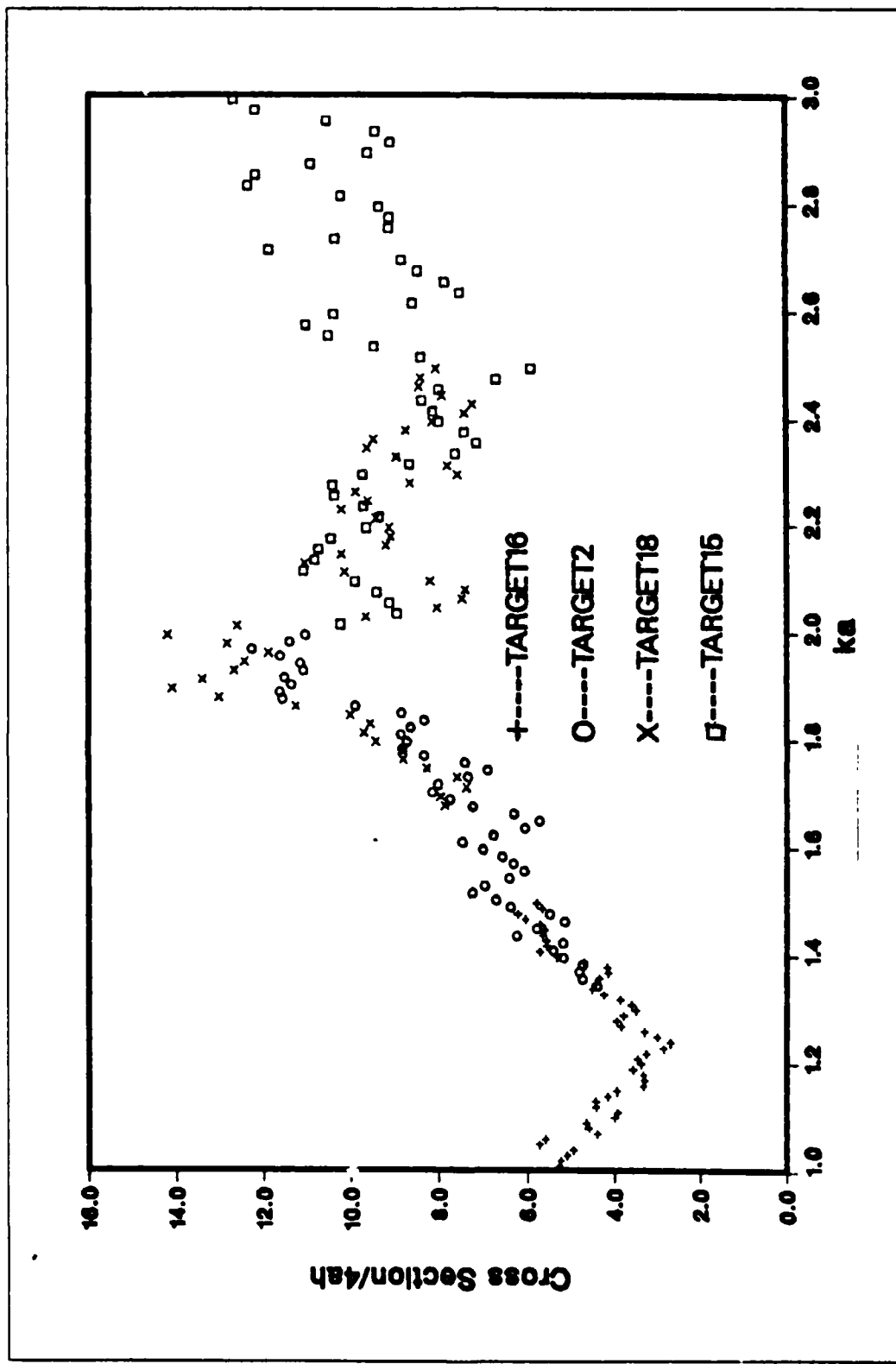


Figure 4.4 Measured Cross Section/4ah vs.  $ka$  for  $h/a=4$

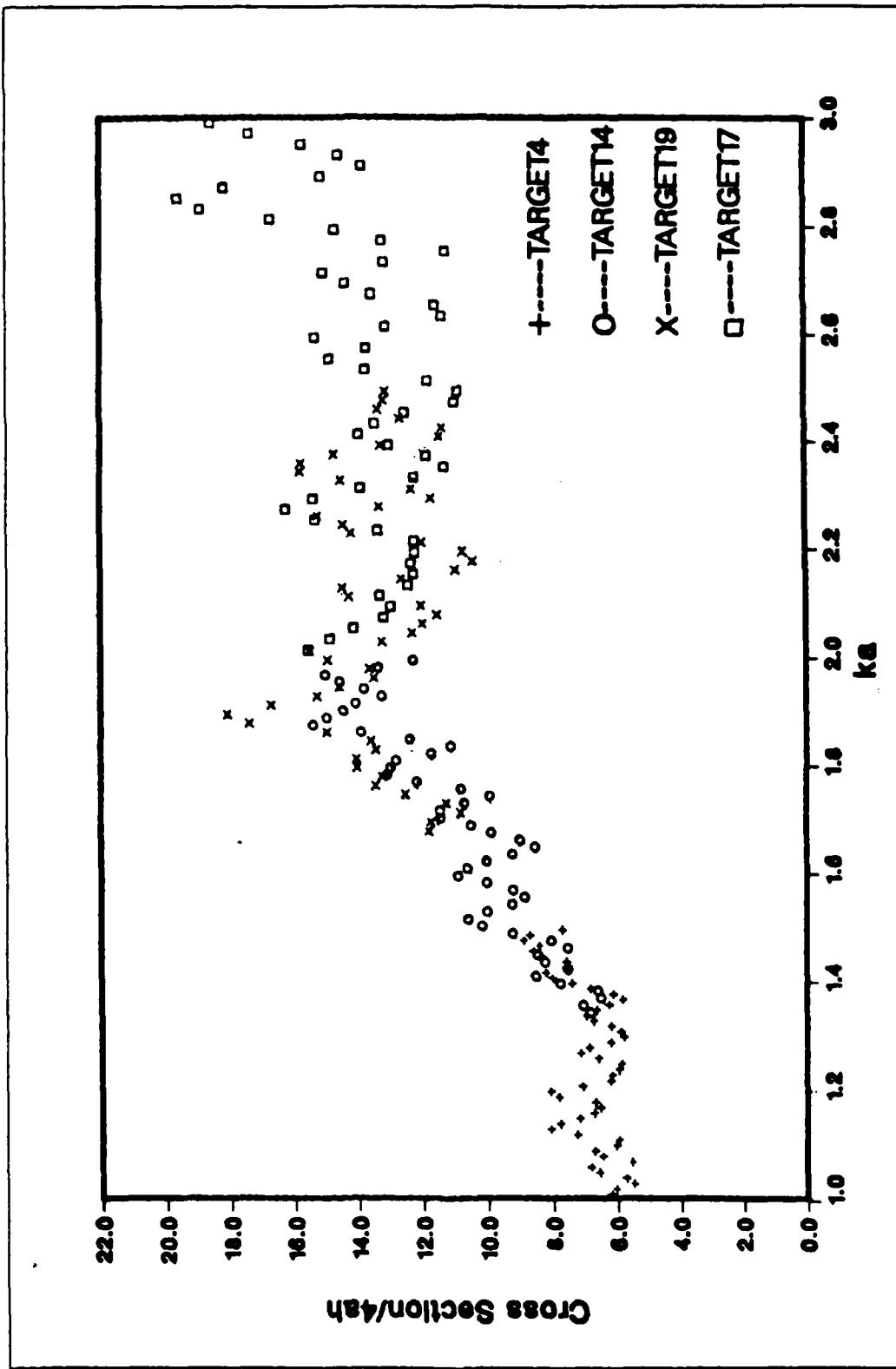


Figure 4.5 Measured Cross Section/4ah vs. ka for  $h/a=6$

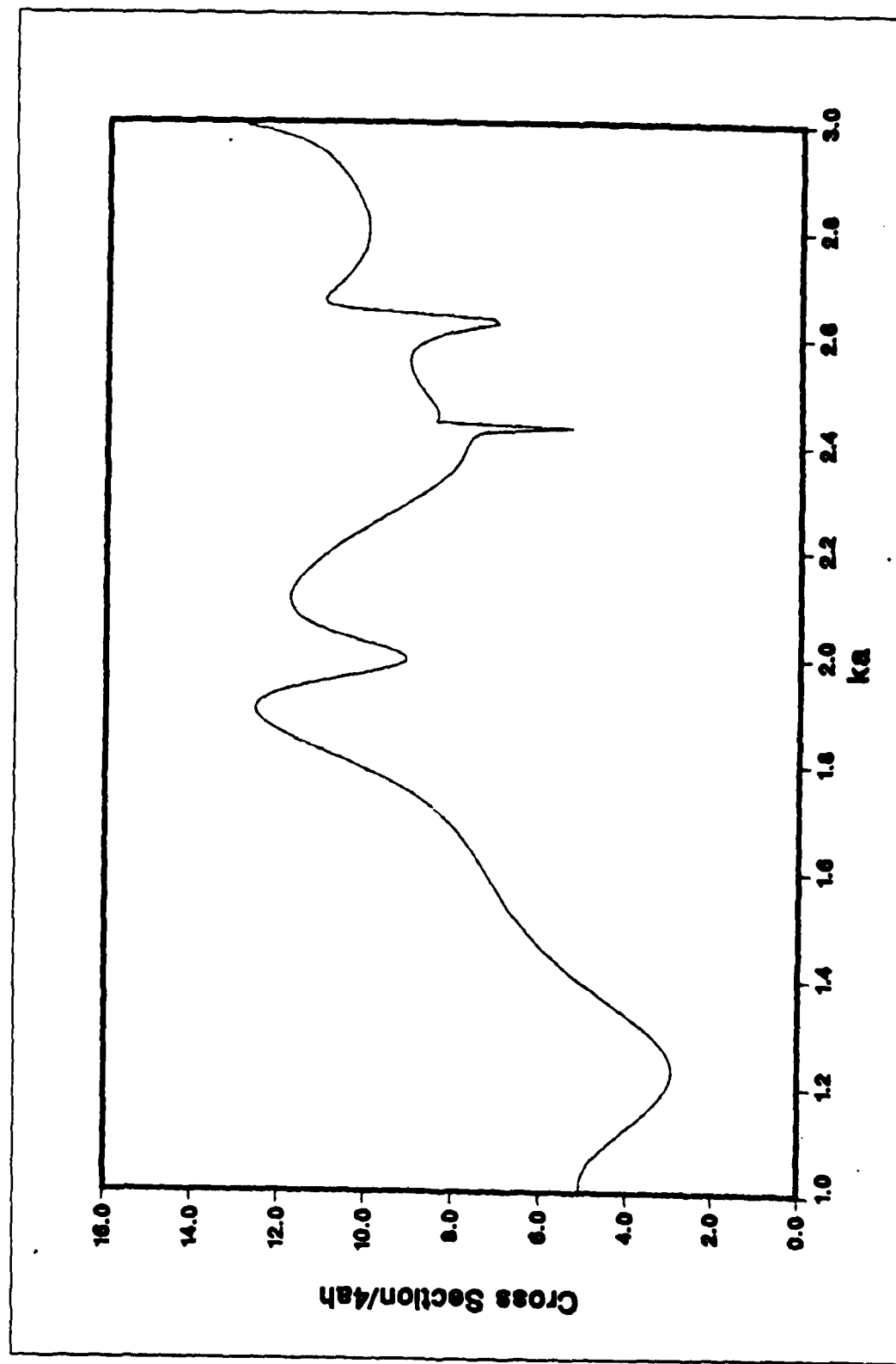


Figure 4.6 Theoretical Cross Section for  $h/a=4$

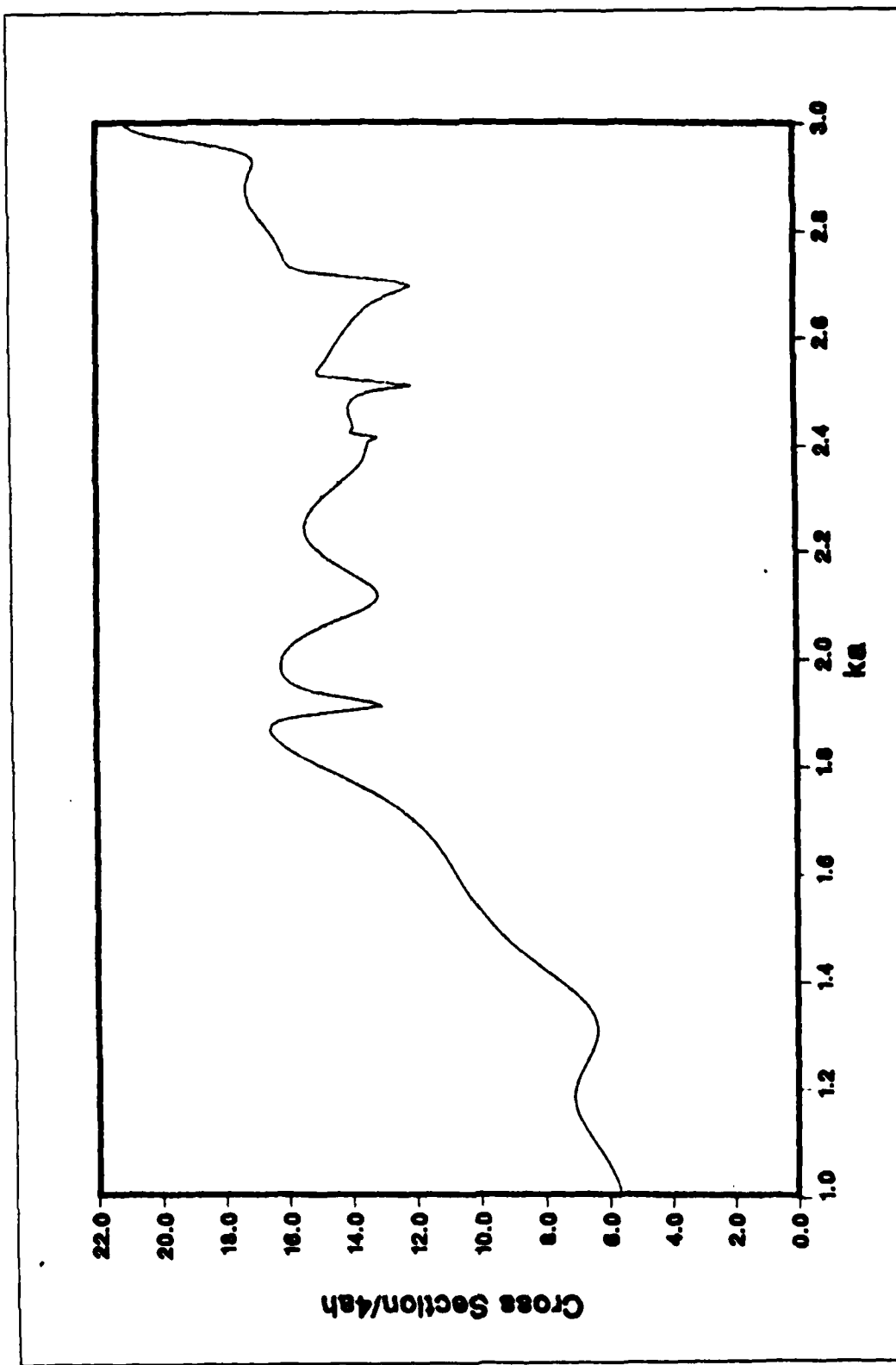


Figure 4.7 Theoretical Cross Section for  $h/a=6$

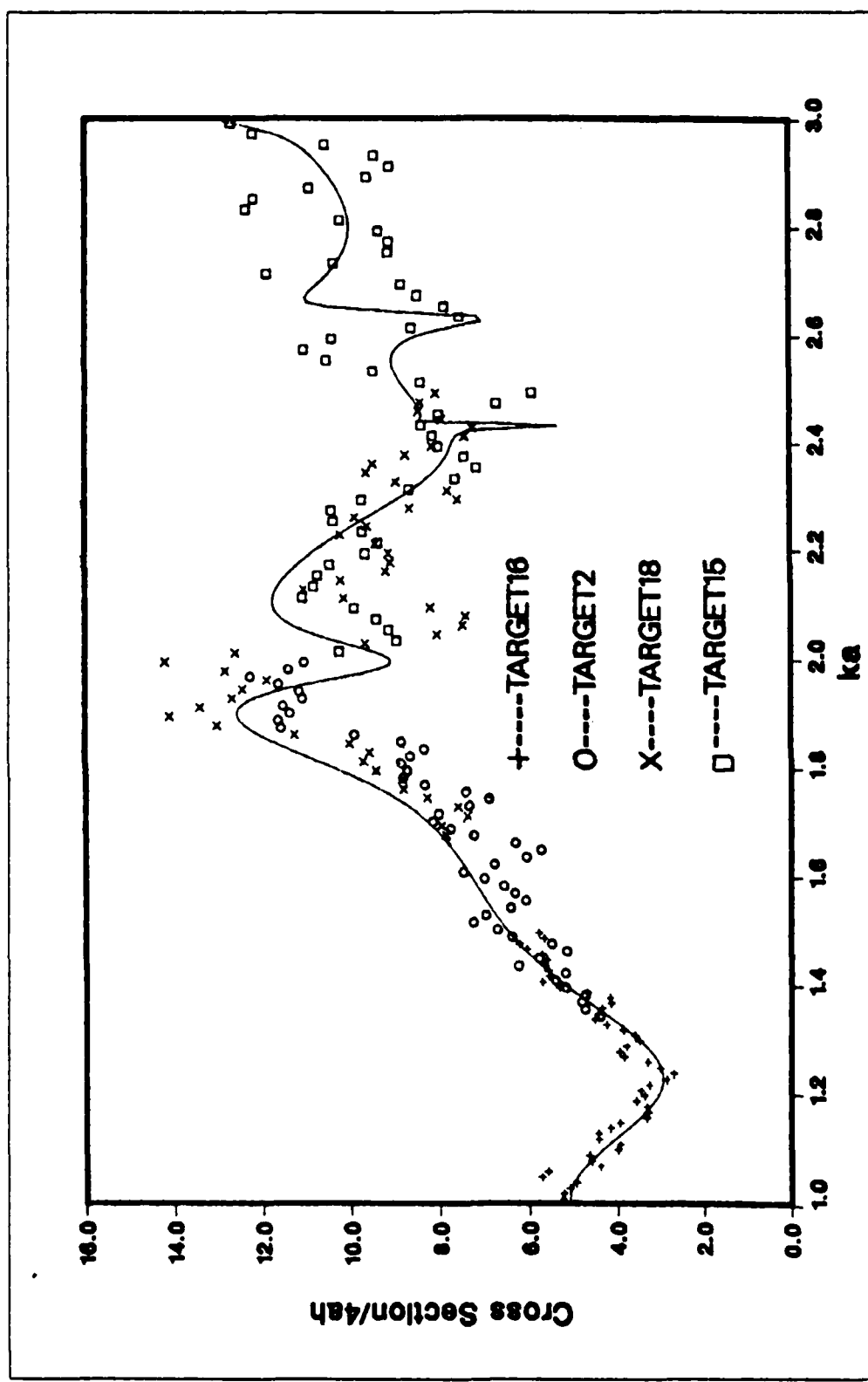


Figure 4.8 Comparison of Cross Section Between Theoretical & Experimental Data for  $h/a=4$ .

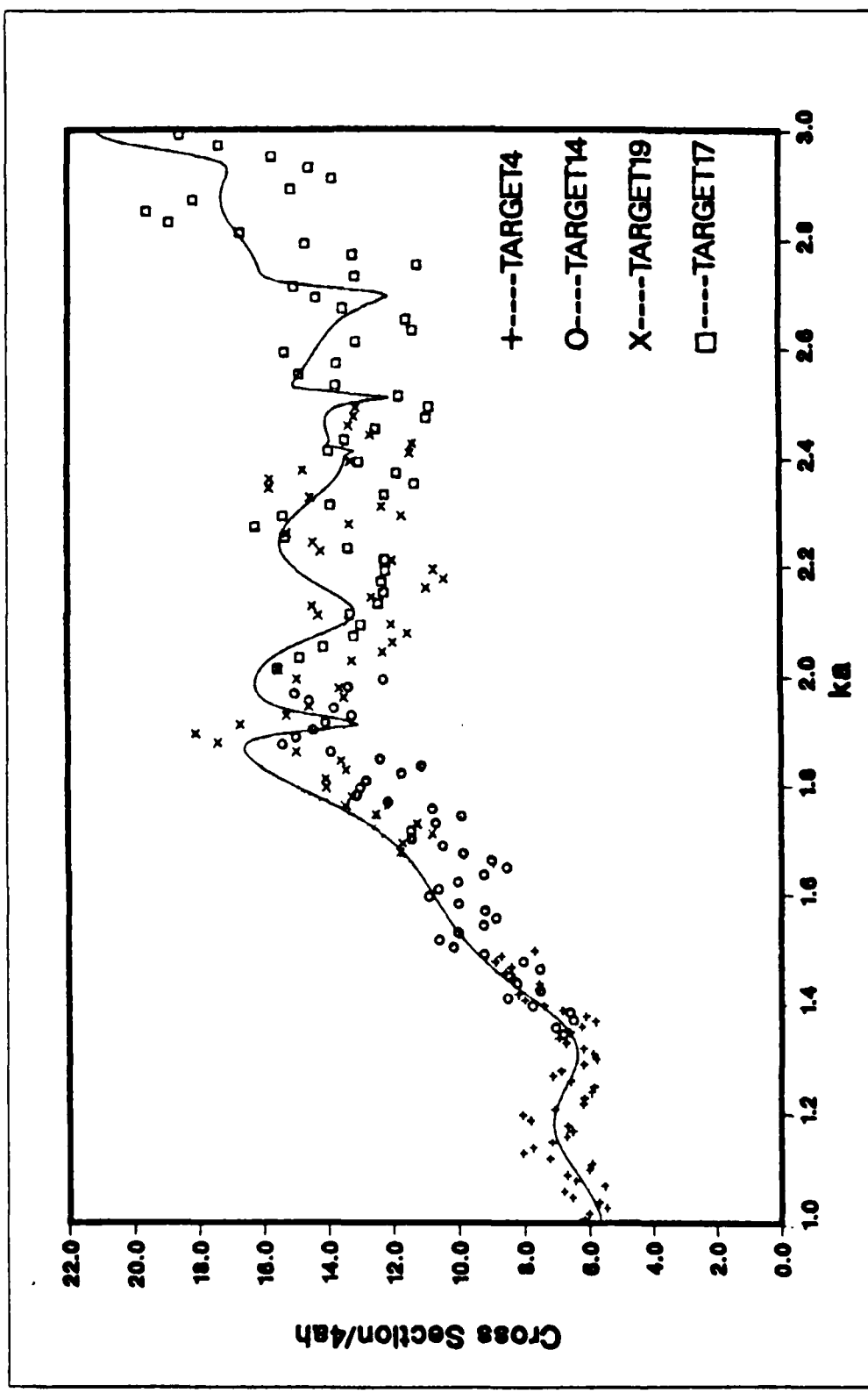


Figure 4.9 Comparison of Cross Section Data for  $h/a=6$ .  
Theoretical & Experimental Data

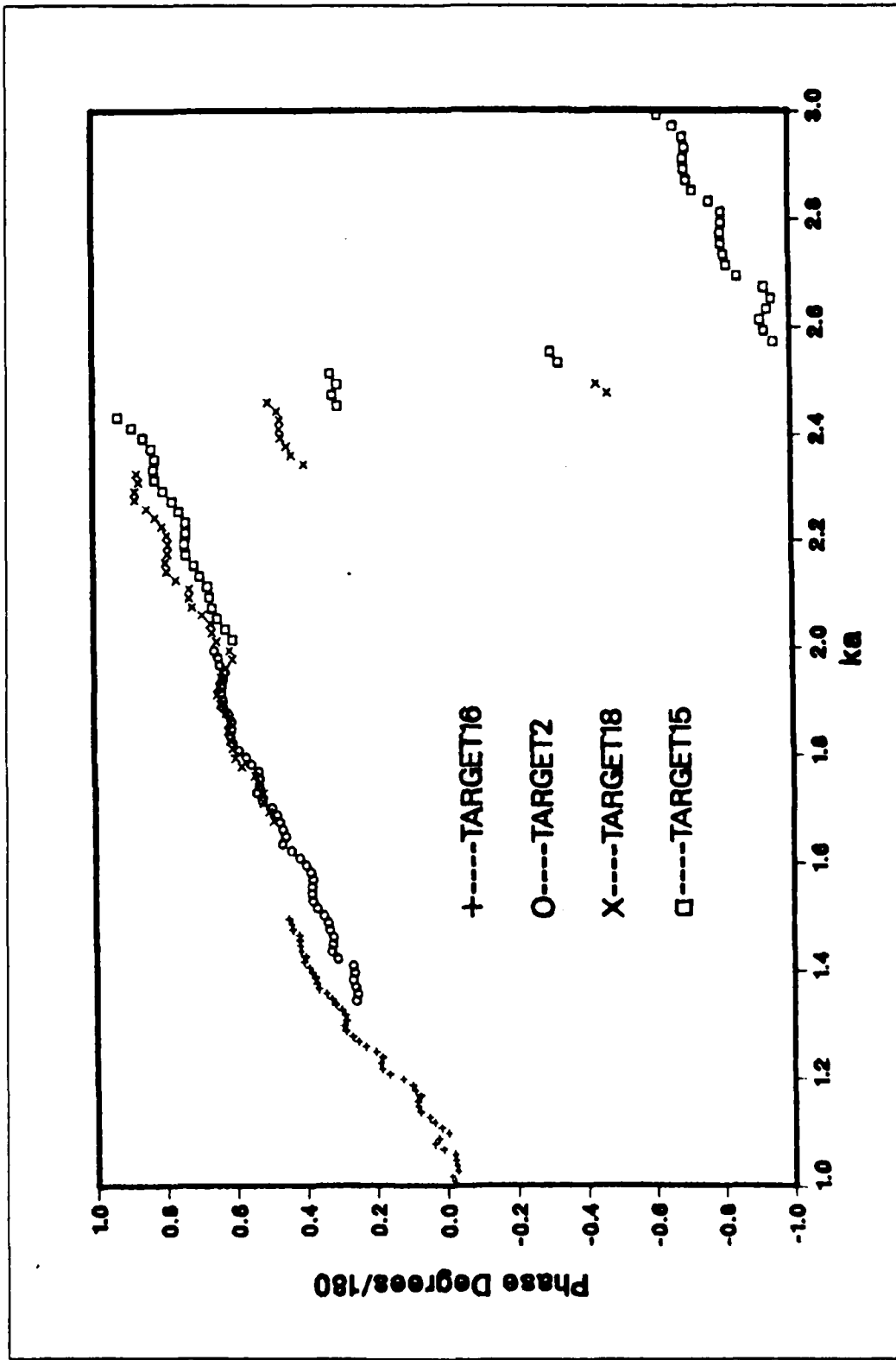


Figure 4.10 Measured Phase Shift vs. ka for  $h/a=4$

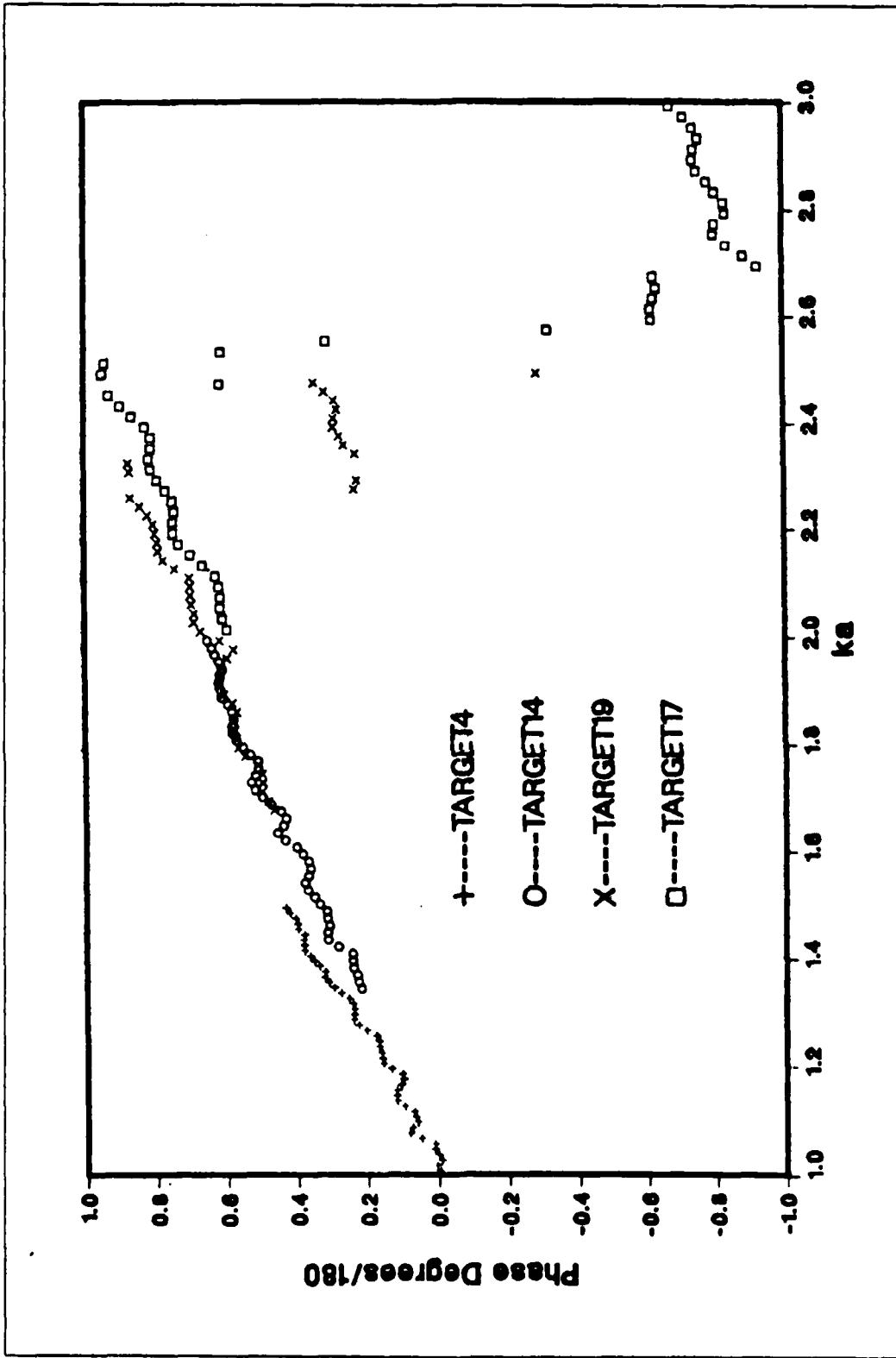


Figure 4.11 Measured Phase Shift vs. ka for  $h/a=6$

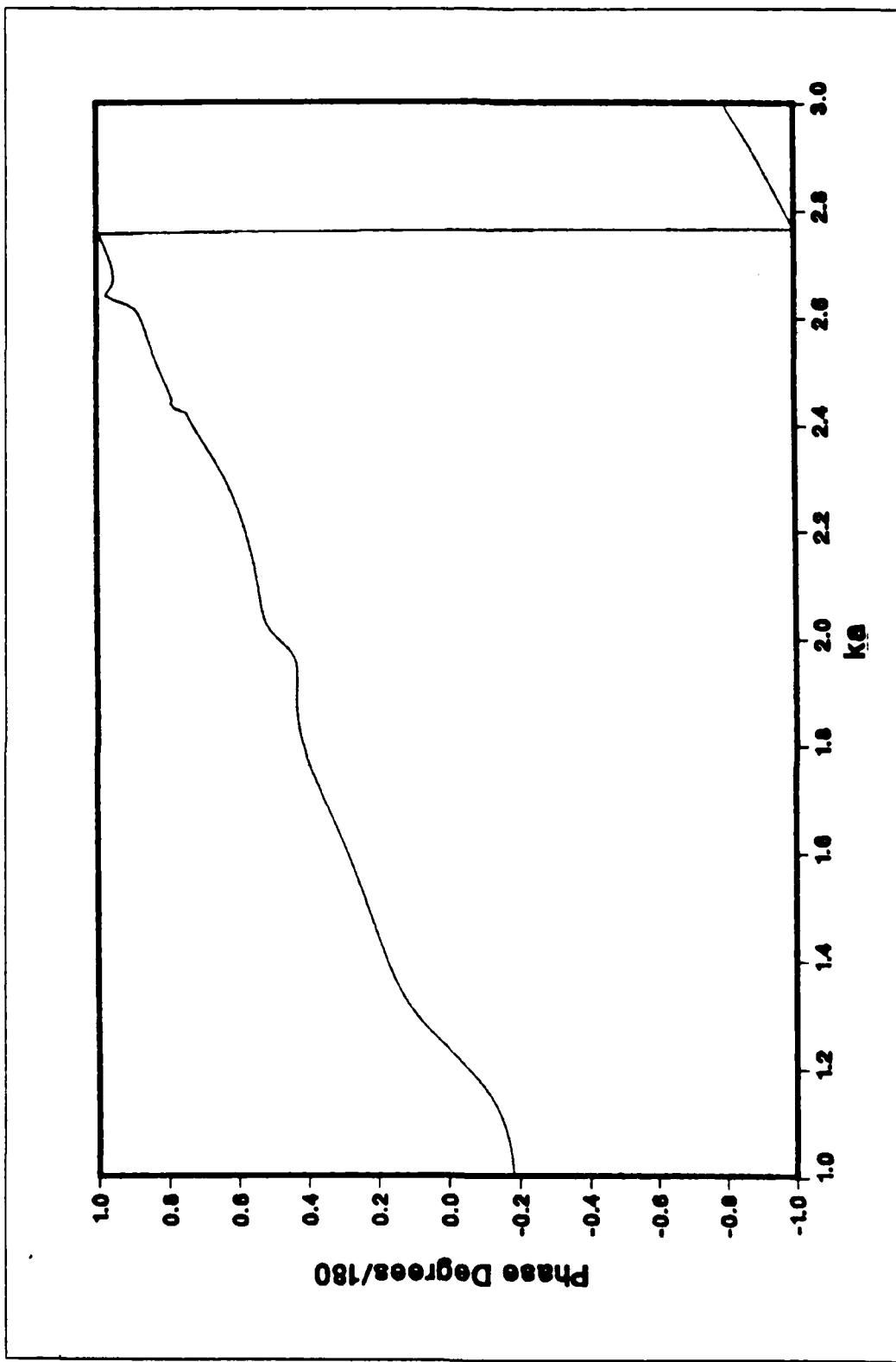


Figure 4.12 Theoretical Phase Shift for  $h/a=4$

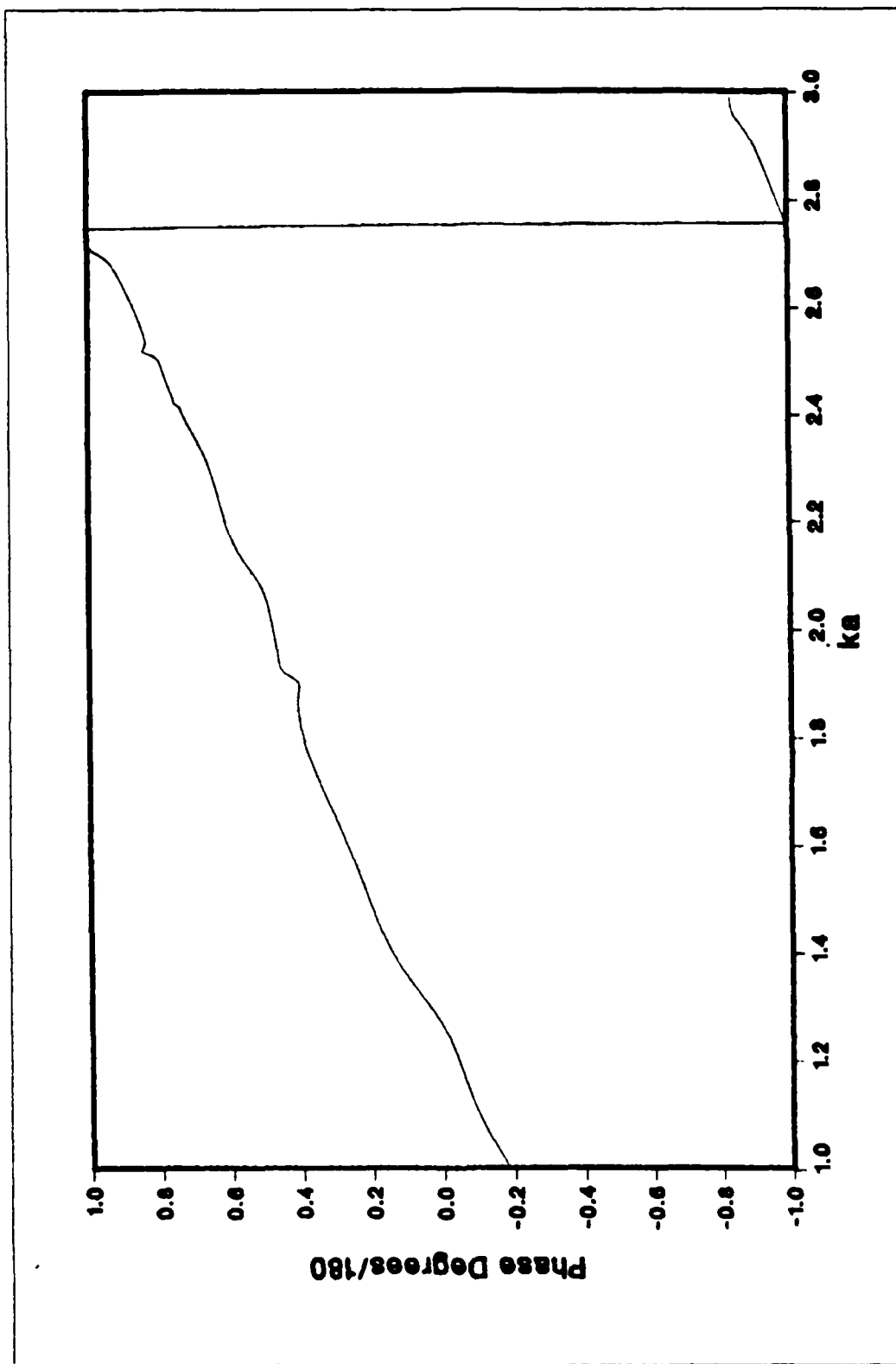


Figure 4.13 Theoretical Phase Shift for  $h/a=6$

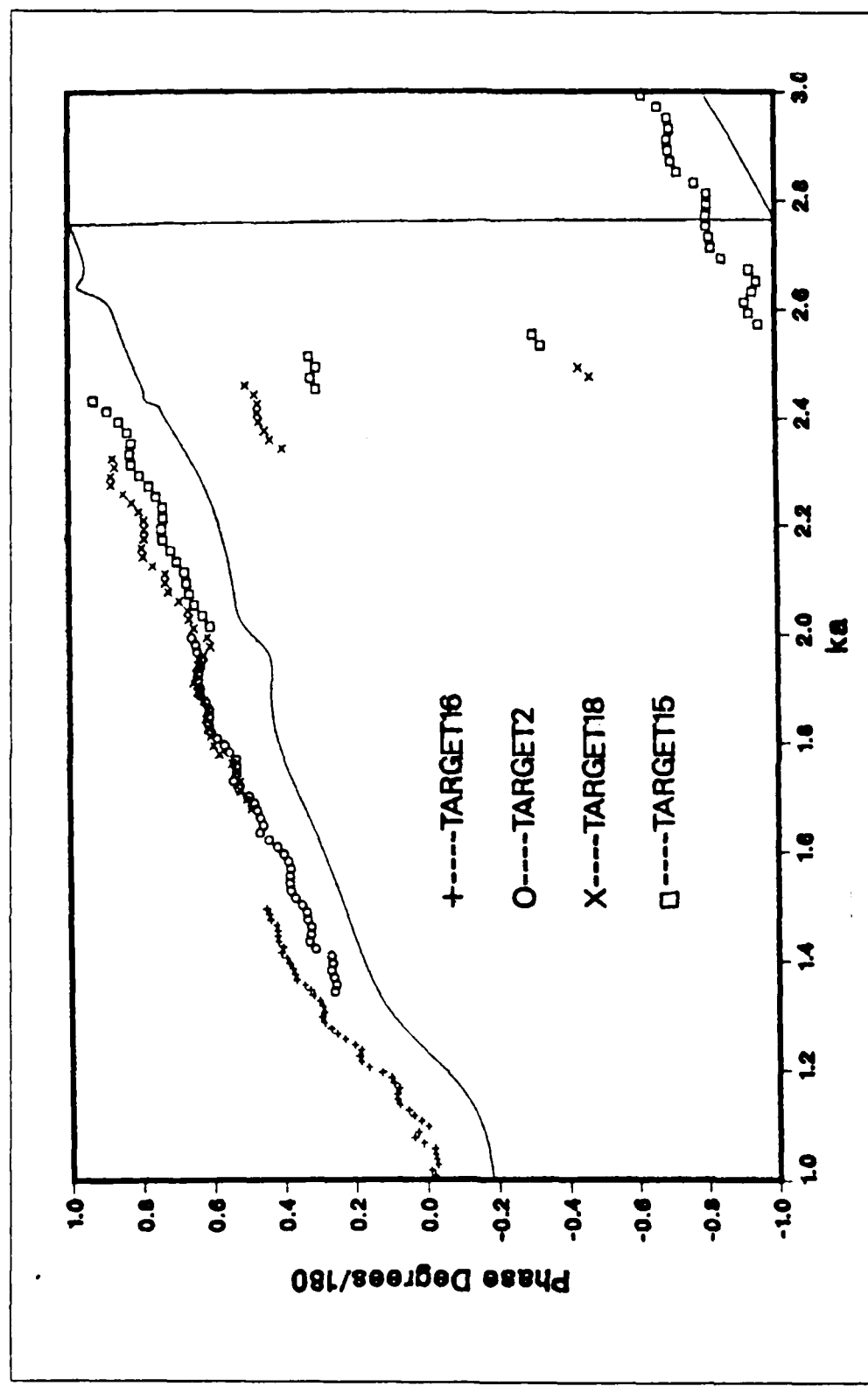


Figure 4.14 Comparison of Phase Shift Between Theoretical & Experimental Data for  $h/a=4$ .

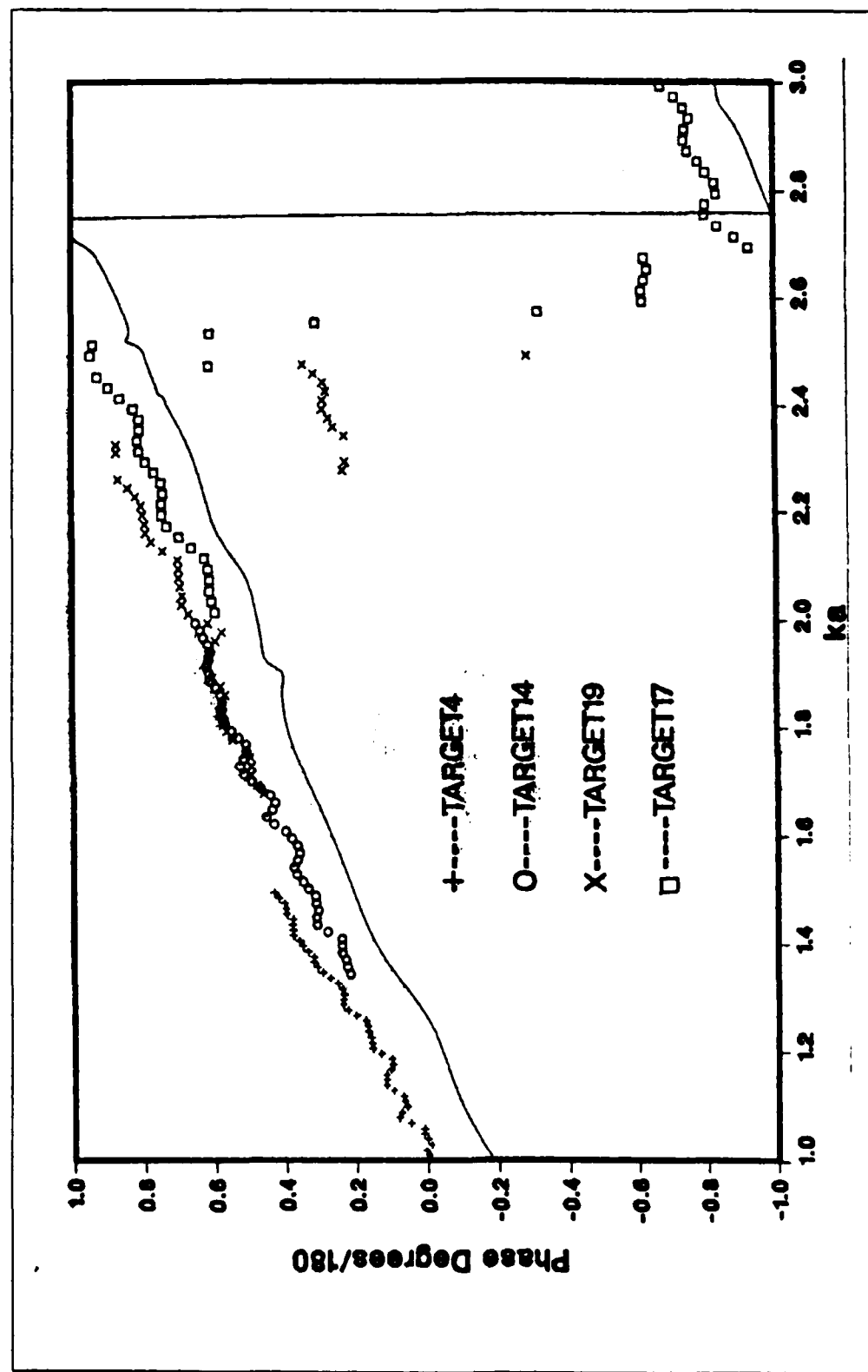


Figure 4.15 Comparison of Phase Shift Between Theoretical & Experimental Data for  $h/a=6$ .

## V. SUMMARY

The exact solution to the scattering by a tubular cylinder from the broadside was presented. From that solution one can see that at this aspect angle the scattered field depends only on the axial surface current flowing in the z direction. The exact solution was used to develop theoretical predictions to the broadside back scattering cross section and phase shift of a finite tubular cylinder. Measurements of cross section and phase shift have been done and the results were analyzed and compared to the theoretical data. The comparison shows that the results of the measurement and the theory are in very good agreement. Both theoretical and experimental data shows that the frequency range that has been chosen is good because the back scattering cross section is about fifteen times bigger than the cylinder dimensions, or equivalently, the cross section in the optical region. The increment in the cross section made the signal easier to be detected and analyzed.

These results as well as the problems that have been arised will be used for further work on this project in developing target identification schemes through the observation of the back scattered field from a target.

### A. KNOWN PROBLEM AREAS

When more complicated bodies than the tubular cylinder are used as targets, the only way to study thier back scattered field is by using the measured data. This is why the most important problem that has to be addressed is to understand the discrepancies between theory and experiment that have been discovered. As a first step, the effects of the support should be studied by using different supports.

Another problem that discovered is the error in the average procedure for phase shift near  $\pm 180$  degrees. That can be solve with a proper averaging procedure. Because of the system noise in the lower frequency range the measurements were done over the range of 10 to 15 Ghz and required the use of several scaled cylinders to expand the frequency range. This introduced errors due to the differences in the inner to outer diameters ratio. By achieving stability in the frequency response of the receiver, one cylinder can be used for a larger frequency range and thus all the parameters will remain constant for all the frequencies.

#### B. WHERE FUTURE WORK IS NEEDED

To understand the effects of cylindrical waveguide modes on the back scattering of a tubular cylinder, the solid cylinder should be studied. The closed ends of the cylinder introduce current in the transverse directions but prevent the wave from propagating inside the cylinder. Adding fins to the cylinder to investigate their effects on the induced surface current on the cylinder should be carried out next. The effects of the dimensions of the fins and their position on the cylinder, on the scattered fields are the most interesting.

Tests on models of real targets are the last step in the evaluation of this scheme and different aspect angles should be studied. For real-life targets, the wavelength should be scaled as the ratio between the models and the targets. That means production of radars that will work at frequencies at a few hundreds of MHz. This system should include a computer that has the ability to store data about the parameters of different targets of interest and by comparison between measured data and stored data the target will be identified.

APPENDIX A  
ANTENNAS CHARACTERISTICS

Model Number	GTE AN/18I
Frequency range	4-18 GHz
Gain	6-12 dB
VSWR(maximum)	3.2:1
Isolation	<20dB below 5.5 GHz >20dB above 5.5 GHz

APPENDIX B  
ANECHOIC CHAMBER

The anechoic chamber is internally lined with absorber material; this material provides the necessary attenuation to the reflection from the walls. Under the absorber material there is an aluminium surface for isolation against external sources of noise such as atmospheric noise and man made noise sources.

Physical dimensions:

Longitudinal length	20 ft.
Lateral length	10 ft.
Height	10 ft.

The absorber material used in the walls of the chamber is EHP-8 Rantec microwave absorber; cut into a precise pyramidal configuration. Figure B.1 shows the mechanical specifications as well as the maximum reflections at normal incidence. For the material used in the floor, ceiling, lateral and front walls. The absorber material used for the back wall operates with more absorption at lower frequencies, and the height of the cones is also different. The specifications of the back wall absorber material are shown in Figure B.2 .

**MECHANICAL SPECIFICATIONS:**

Absorber Size (In.)	Absorber Height (In.)		Pyramid Base Size (In.)	Pyramids Per Absorber
	Overall	Base		
24 x 24	8-1/2	1-1/2	7	3 x 3
				64

**MAXIMUM REFLECTION AT NORMAL INCIDENCE:**

Ku Band	X Band	C Band	S Band	L Band	500 MHz	300 MHz	200 MHz	120 MHz
50 db	50 db	45 db	40 db	30 db				

Figure B.1 Specifications of the Absorber Material of the Front Wall.

**MECHANICAL SPECIFICATIONS:**

Absorber Size (In.)	Absorber Height (In.)			Pyramid Base Size (In.)	Pyramids Per Absorber
	Overall	Base	Pyramid		
24 x 24	18-1/4	2-1/4	16	6 x 6	16
<b>MAXIMUM REFLECTION AT NORMAL INCIDENCE:</b>					
Ku Band	X Band	C Band	S Band	L Band	120 MHz
50 db	50 db	50 db	45 db	40 db	30 db

**Figure B.2    Specifications of the Absorber Material  
of the Back Wall.**

APPENDIX C

SPHERE PROGRAM

```

10 ! "SPHERE.DRIVES"
20 !
30 ! COMPUTE BACK SCATTERRED
40 ! FAR-FIELD FROM A PERFECTLY
     CONDUCTING SPHERE.
50 !
60 ! THE INCIDENT FIELD IS A
70 ! LINEARLY POLARIZED PLANE W
     AVE WITH ZERO PHASE AT THE C
     ENTER OF THE SPHERE.
80 ! THE THEORETICAL VALUES TO
     BE COMPUTED ARE THE BACK-SC
     ATTERING CROSS-SECTION AND
90 ! THE PHASE OF THE FAR FIELD
     INTERPOLATED TO THE CENTER
     OF THE SPHERE.
100 !
110 ! THEORETICAL VALUES ARE
120 ! STORED IN FILES OF 800
130 ! RECORDS, ONE FOR EACH FREQ
     UENCY FROM 2.02 GHZ TO 18 GH
     Z AT 0.02 GHZ STEPS.
140 !
150 ! "THEOR1.DRIVE1" FOR THE
160 ! 1" DIAMETER SPHERE
170 ! "THEOR3.DRIVE1" FOR THE
180 ! 3.187" DIAMETER SPHERE
190 ! "THEOR4.DRIVE1" FOR THE
200 ! 4.75" DIAMETER SPHERE
210 ! "THEOR6.DRIVE1" FOR THE
220 ! 6" DIAMETER SPHERE
230 !
240 ! FILE H$ STORES THE
     COMPUTED RESULT
250 H$="THEOR6.DRIVE1"
260 !
270 R0=6*.0254/2 ! SPHERE
     RADIUS IN METERS
280 !
290 X0=2*PI ! PARAMETER
300 !
310 Q1=2 ! STARTING FREQ IN GHZ
320 Q2=18 ! FINAL FREQ IN GHZ
330 Q4=.02 ! FREQ STEP IN GHZ
340 ON ERROR GOTO 360
350 PURGE H$
360 OFF ERROR
370 CREATE H$,800,16 ! OPEN A NE
     W FILE WITH 800 RECORDS
380 ! OF 16 BYTES EACH. EVERY
390 ! RECORD STORES ONE MAGNITU
     DE AND ONE PHASE DATA.
400 !

```

```

410 R$SIGN# 1 TO H$
420 DIM B8(144),B9(144),D9(144),
D9(144) ! 144>L0=INT(2*K0*A0
+3)
430 F0=Q1
440 FOR I=1 TO 300
450 DISP "FREQ LOOP=",I
460 F0=F0+Q4
470 DISP "FREQ (GHZ)=",F0
480 K1=.3/F0 ! WAVELENGTH
490 K0=X9/K1 ! WAVE NUMBER
500 GOSUB 610
510 DISP "E =",E0
520 DISP "P =",P0
530 PRINT# 1,I ; E0,P0
540 NEXT I
550 R$IGN# 1 TO *
560 CLEAR
570 DISP "END OF COMPUTATION"
580 END
590 !
600 !
610 !
620 L0=INT(2*K0*A0+3)
630 IF L0<145 THEN 650
640 DISP "K0*A0 TOO LARGE FOR
CURRENT ARRAY DIM"
650 Z=K0*A0
660 GOSUB 890
670 E8=0
680 E9=0
690 FOR N=1 TO L0
700 L=L0-N+1
710 M8=D8(L)^2+D9(L)^2
720 M9=B8(L)^2+B9(L)^2
730 A7=(L+.5)/M8/M9
740 R8=A7*(B9(L)*D9(L)-B8(L)*D8(
L))
750 R9=A7*(B8(L)*D9(L)+B9(L)*D8(
L))
760 E8=R8-E8
770 E9=R9-E9
780 NEXT N
790 E8=-E8
800 E9=-E9
810 E0=E8^2+E9^2
820 P0=ATN2(E9,E8)
830 E0=E0/K0*2*K1 ! CROSS-SECTIO
N
840 P0=P0-X9*INT(P0/X9)
850 IF P0<PI THEN 870
860 P0=P0-X9
870 P0=-P0
880 RETURN
890 !
900 IF Z>L0-1 THEN 1210
910 Z2=Z^2/2

```

```

920 N2=2*Z2+L0+1
930 D1=2*N2+?
940 D2=D1*(2+N2+5)
950 D3=D2*(2+N2+7)
960 D4=73*(2*N2+9)
970 F1=-Z2/D1+Z2^2/(2*D2)-Z2^3/
(6*D3)
980 F2=Z*(1/D1-Z2/D2+Z2^2/(2*D3)-
-Z2^3/(6*D4))
990 M=2*Z2
1000 S1=F1
1010 F1=(2*M+1)*F1/Z-F2
1020 F2=S1
1030 IF ABS(F1)<1.E100 THEN 1070
1040 F1=F1*.1 E-100
1050 F2=F2*.1 E-100
1060 S1=S1*.1 E-100
1070 M=M-1
1080 IF M+1>L0 THEN 1000
1090 B8(L0)=F2
1100 B8(L0-1)=F1
1110 N0=L0-2
1120 FOR K=1 TO N0
1130 N=L0-K-1
1140 B8(N)=(2*N+3)*B8(N+1)/Z-B8(
N+2)
1150 NEXT K
1160 A1=(SIN(Z)/Z-COS(Z))/B8(1)
1170 FOR K=1 TO L0
1180 B8(K)=A1*B8(K)
1190 NEXT K
1200 GOTO 1260
1210 B8(1)=SIN(Z)/Z-COS(Z)
1220 B8(2)=(3/Z^2-1)*SIN(Z)-3*C0
S(Z)/Z
1230 FOR N=3 TO L0
1240 B8(N)=(2*N-1)*B8(N-1)/Z-B8(
N-2)
1250 NEXT N
1260 B9(1)=-SIN(Z)-COS(Z)/Z
1270 B9(2)=(1-3/Z^2)*COS(Z)-3*S1
H(Z)/Z
1280 FOR N=3 TO L0
1290 B9(N)=(2*N-1)*B9(N-1)/Z-B9(
N-2)
1300 NEXT N
1310 D8(1)=(1-1/Z^2)*SIN(Z)+COS(
Z)/Z
1320 D9(1)=(1/Z^2-1)*COS(Z)+SIN(
Z)/Z
1330 FOR N=2 TO L0
1340 D8(N)=B8(N-1)-N*B8(N)/Z
1350 D9(N)=B9(N-1)-N*B9(N)/Z
1360 NEXT N
1370 RETURN

```

APPENDIX D  
CALIB PROGRAM

```
10 ! "CALIE.DRIVE0"  
20 !  
30 ! CALIBRATION USING A SPHERE  
40 ! OVER LS-U9 GHZ AT F9 GHZ  
50 ! STEPS BASED ON THEORETICAL  
VALUES COMPUTED USING THE P  
ROGRAM "SPHERE.DRIVE0"  
60 ! THE RESULTED SYSTEM TRANS-  
FER FUNCTION IS STORED AS:  
70 ! "CALIB3.DRIVE1" (3.187")  
80 !  
90 ! R$ IS THE FILE STORING THE  
100 ! BACKGROUND DATA.  
110 ! C$ IS THE FILE STORING THE  
SYSTEM TRANSFER FUNCTION  
120 ! H$ IS THE FILE STORING  
THEORETICAL DATA OF THE SPHE-  
RE  
130 ! S$ DESCRIBES THE SPHERE  
140 !  
150 C$="CALIB3.DRIVE1"  
160 H$="THEOP3.DRIVE1"  
170 S$="3.187 INCH SPHERE"  
180 R$="BKGRND.DRIVE1"  
190 X9=2*PI ! A PARAMETER  
200 !  
210 OPTION BASE 1  
220 N0=3 ! NUMBER OF READINGS  
230 ! TAKEN AND AVERAGED FOR ONE  
240 ! FREQ.  
250 !  
260 F9=.1 ! FREQ. STEP IN GHZ  
270 !  
280 M1=51 ! M1=(U9-L9)/F9+2  
290 ! NUMBER OF FREQ. CHECKED.  
300 !  
310 L9=10.1 ! LOWER FREQ. IN GHZ  
320 U9=15 ! UPPER FREQ. IN GHZ  
330 !  
340 DIM A(51,2) ! BACKGROUND  
DATA  
350 DIM B(51,2) ! TARGET DATA  
360 DIM G3(51,2) ! THEORY  
370 ! CREATE C$,M1,16  
380 ! CREATE R$,M1,16  
390 ! STORE CALIBRATION AND BACK  
GROUND DATA IN A FILE OF M1  
RECORDS  
400 ! EACH RECORD CONTAINS ONE  
MAGNITUDE AND ONE PHASE  
410 ! DATA AT A FREQUENCY
```

```

420 !
430 ! READING THE THEORETICAL DA
    TA
440 !
450 ASSIGN# 1 TO H$
460 K0=(L9-2-F9*2)*50
470 FOR I=1 TO M1
480 K0=K0+50*F9
490 READ# 1,K0 : G3(I,1),G3(I,2)
500 NEXT I
510 ASSIGN# 1 TO *
520 GOSUB 2170 ! HEADER.
530 DISP "DO YOU WANT TO USE THE
        MOST RECENT BACKGROUND DATA
        ?      Y/N "
540 INPUT P$
550 IF P$="N" THEN 630
560 !
570 ! READING BACKGROUND DATA.
580 !
590 ASSIGN# 4 TO A$
600 READ# 4 , A(,)
610 ASSIGN# 4 TO *
620 GOTO 880
630 CLEAR
640 REMOTE 7 ! REMOTE ALL
        DEVICES
650 CLEAR 7 ! CLEAR ALL DEVICES
660 ! INITIALIZE SIG.GEN TO FIRS
        T FREQ.
670 OUTPUT 719 ;"P",L9,"Z1K0L3M0
        N601"
680 CLEAR
690 DISP "REMOVE TARGET FROM CHA
        MBER, PUSH 'CONT' WHEN READY"
700 LOCAL 7
710 BEEP @ BEEP
720 PAUSE
730 REMOTE 7
740 CLEAR
750 DISP "TAKING BACKGROUND DATA
        "
760 PRINT
770 ! PRINT "BACKGROUND DATA"
780 PRINT
790 OUTPUT 719 ;"P",L9,"Z1K0L3M0
        N601"
800 WAIT 200 ! WAIT FOR FREQ. TO
        STABILIZE
810 GOSUB 1320
820 !
830 ! STORING BACKGROUND DATA
840 !
850 ASSIGN# 3 TO A$
860 PRINT# 3 ; A(,)
870 ASSIGN# 3 TO *
880 CLEAR

```

```

890 LOCAL 7
900 DISP "PUT TARGET INTO CHAMBE
R, PUSH 'CONT' WHEN READY"
910 DISP "TARGET IS ",S$
920 BEEP @ BEEP
930 PAUSE
940 REMOTE 7
950 CLEAR
960 DISP "COMPUTING TARGET DATA"
970 PRINT
980 ! PRINT "TARGET DATA"
990 PRINT
1000 OUTPUT 719 , "P", L9, "Z1K0L3M
0N601"
1010 WAIT 200
1020 GOSUB 1910
1030 PRINT " "
1040 PRINT "TRANS. FUNCTION",S$
1050 PRINT " "
1060 !
1070 ! CALCULATE AND STORE TRANS
FER FUNCTION.
1080 !
1090 ASSIGN# 2 TO C$
1100 FOR M=1 TO M1
1110 N1=B(M,1)-A(M,1)
1120 N2=B(M,2)-A(M,2)
1130 X6=G3(M,1)/(N1^2+N2^2)
1140 X7=G3(M,2)-RTN2(N2,N1)
1150 X7=X7-X9*INT(X7/X9)
1160 IF X7>PI THEN X7=X7-X9
1170 PRINT# 2,M , X6,X7
1180 ! PRINT USING 970 ; M,X6,X7
1190 IMAGE DD,1X,"X6=",SD,DDDE,1
X,"X7=",SD,DDDE
1200 NEXT M
1210 ASSIGN# 2 TO *
1220 CLEAR
1230 DISP "CALIBRATION COMPLETED
, DATA STORED IN",C$
1240 BEEP @ BEEP @ BEEP
1250 LOCAL 7
1260 END
1270 !
1280 !
1290 !
1300 !
1310 !
1320 ! BACKGROUND DATA COLLECTIO
N SUBROUTINE
1330 !
1340 ! OUTPUT(L9-F9)TO U9 GHZ AT
F9 GHZ STEPS
1350 J=10*(L9-2*F9) ! FREQUENCY
STARS AT L9-F9 GHZ

```

```

1360 FOR K=1 TO M1 ! NUMBER OF
    FREQUENCY STEPS
1370 J=J+10*F9
1380 IMAGE 1A,3Z,14A
1390 OUTPUT 719 USING 1380 ; "P"
    ,J,"00Z1K0L3M0N601"
1400 ! TAKE DATA IN FROM 722&720

1410 GOSUB 1580
1420 !
1430 ! CALCULATE REAL&IMAGINARY
    FROM AMP.&PHASE
1440 !
1450 R1=A1*COS(P1)
1460 I1=A1*SIN(P1)
1470 A(K,1)=R1
1480 A(K,2)=I1
1490 ! PRINT USING 2040 ; A(K,1)
    ,A(K,2)
1500 NEXT K
1510 OUTPUT 719 ; "P",L9,"Z1K0L3M
    0N601"
1520 RETURN
1530 !
1540 !
1550 !
1560 !
1570 !
1580 ! SUBROUTINE TO ENTER AMPLI
    TITUDE AND PHASE DATA FROM DI
    GITAL VOLTMETERS
1590 !
1600 ! PREPARE DIGITAL VOLTMETER
    TO SEND AMPLITUDE DATA
1610 ! NO READINGS TAKEN AND AVE
    RAGED FOR ONE FREQ.
1620 !
1630 !
1640 V1=0 ! PARAMETERS FOR THE
1650 F1=0 ! AVERAGING PROCESS.
1660 FOR L=1 TO N0
1670 OUTPUT 720 ; "P0F1R1T1Z1FL0M
    0"
1680 WAIT 10
1690 ENTER 720 ; V
1700 WAIT 10
1710 OUTPUT 722 ; "F1R7T1M3A0H1"
1720 WAIT 10
1730 ENTER 722 ; F
1740 V1=V1+V
1750 F1=F1+F
1760 WAIT 10
1770 NEXT L
1780 V=V1/N0
1790 F=F1/N0
1800 A1=10^F ! TRANSFER TO MAG.
    FROM VOLTS.

```

```

1810 P1=100*IV ! TRANSFER TO DEG.
    FROM VOLTS.
1820 P1=DTR(P1)
1830 ! PRINT USING 1810 ; K,A1,P
    1
1840 IMAGE 00,2X,"R=",MD.000E,2X
    , "P=",SD.000E
1850 RETURN
1860 !
1870 !
1880 !
1890 !
1900 !
1910 ! TARGET DATA COLLECTION
    SUBROUTINE
1920 !
1930 ! OUTPUT(L9-F9)TO U9 GHZ AT
    F9 GHZ STEPS
1940 J=10*(L9-2*F9) ! FREQUENCY
    STARS AT L9-F9 GHZ

1950 FOR K=1 TO M1 ! NUMBER OF
    FREQUENCY STEPS
1960 J=J+10*F9
1970 IMAGE 1R,3Z,14A
1980 OUTPUT 719 USING 1970 ; "P"
    ,J,"00Z1K0L3M0N601"
1990 ! TAKE DATA IN FROM 722&720
    1820 GOSUB 1410
2000 GOSUB 1580
2010 ! CALCULATE REAL&IMAG. FROM
    AMP&PHASE
2020 R1=A1*COS(P1)
2030 I1=A1*SIN(P1)
2040 B(K,1)=R1
2050 B(K,2)=I1
2060 ! PRINT USING 2040 ; B(K,1)
    ,B(K,2)
2070 IMAGE 4X,"R=",SD.000E,2X,"I
    =",SD.000E
2080 NEXT K
2090 OUTPUT 719 ; "P",L9,"Z1K0L3M
    0N601"
2100 RETURN
2110 !
2120 !
2130 !
2140 !
2150 ! HEADER SUBROUTINE
2160 !
2170 PRINT " "
2180 PRINT " "
2190 CLEAR
2200 DISP "CALIBRATION STANDARD"
    ,S$
2210 PRINT "CALIBRATION STANDARD
    ",S$
```

```
2220 PRINT "*****  
2230 PRINT "*****  
2240 PRINT "  
2250 CLEAR  
2260 RETURN
```

APPENDIX E

TARGET PROGRAM

```

10 ! "TARGET.DRIVE0"
20 !
30 ! TARGET BACK-SCATTERING
40 ! USING C$ DATA & STORE
      RESULTS IN G$
50 ! FREQUENCIES:L9-U9 GHZ AT
      F9 GHZ STEPS
60 !
70 ! FILE C$ STORES THE SYSTEM
      TRANSFER FUNCTION
80 ! FILE G$ STORES TARGET DATA
      OBTAINED FROM THIS PROGRAM
90 ! FILE H$ STORES THEORETICAL
      VALUES FOR PLOTTING OVERLAY
100 ! FILE A$ STORES BACKGROUND
      DATA
110 C$="CALIB3.DRIVE1"
120 G$="SCR3.DRIVE1"
130 H$="THEOR3.DRIVE1"
140 R$="BKGRND.DRIVE1"
150 !
160 ! CREATE G$,52,24
170 ! STORE TARGET DATA IN FILE
180 ! OF M1+1 RECORDS. FIRST ONE
190 ! FOR THE AVERAGE PROCEDURE
200 ! AND THE REST CONTAINS THE
210 ! FREQUENCY MAGNITUDE AND
220 ! PHASE SHIFT.
230 !
240 ! CREATE A$,51,16
250 ! STORE CALIB. AND BACKGROUND
      DATA IN A FILE OF M1 RECORDS
260 ! EACH RECORD CONTAINS ONE M
      AG. AND PHASE AT A FREQ.
270 !
280 OPTION BASE 1
290 N0=2 ! NUMBER OF READINGS
300 ! TAKEN AND AVERAGED FOR ONE
      FREQUENCY.
310 !
320 DIM A(51,2) ! BACKGROUND DAT
      A
330 DIM B(51,2) ! TARGET DATA
340 DIM G4(51,2) ! CALIBRATION
350 DIM N(51,3) ! RESULTANT
360 DIM M9(51,3)
370 !
380 N1=51 !
390 ! N1=(U9-L9)/F9+2 NUMBER OF
400 ! FREQ. CHECKED.
410 F9=.1 ! FREQ. STEPS IN GHZ.

```

```

420 U9=15 ! UPPER FREQ. IN GHZ
430 L9=10.1 ! LOWER FREQ. IN GHZ
440 DIM T(800,2) ! STORES THEORE-
    TICAL DATA
450 X9=2*PI
460 !
470 ! READING TRANSFER FUNCTION
480 !
490 ASSIGN# 1 TO C$
500 READ# 1 ; G4(,)
510 ASSIGN# 1 TO *
520 ! MAT PRINT USING 330 ; G4
530 IMAGE 2X,30.40
540 !
550 REMOTE 7 ! REMOTE ALL
    DEVICES
560 CLEAR 7 ! CLEAR ALL DEVICES
570 OUTPUT 719 ; "P1Z1K0L3M0N601"
    ! INITIAL SETUP OF 719
580 CLEAR
590 DISP "DO YOU WANT TO USE THE
    MOST RECENT BACKGROUND DATA
    ?      Y/N"
600 INPUT P$
610 !
620 IF P$="N" THEN 700
630 !
640 ! READING BACKGROUND DATA
650 !
660 ASSIGN# 4 TO A$
670 READ# 4 ; A(,)
680 ASSIGN# 4 TO *
690 GOTO 860
700 DISP "REMOVE TARGET FROM
    CHAMBER, PUSH 'CONT' WHEN REA-
    DY"
710 LOCAL 7
720 BEEP @ BEEP
730 PAUSE
740 DISP "TAKING BACKGROUND DATA
    "
750 REMOTE 7
760 OUTPUT 719 ; "P",L9,"Z1K0L3M0
    N601" ! INITIAL SETUP OF 719
770 WAIT 100
780 GOSUB 2520
790 !
800 ! STORING BACKGROUND DATA.
810 !
820 ASSIGN# 5 TO A$
830 PRINT# 5 ; A(,)
840 ASSIGN# 5 TO *
850 CLEAR
860 DISP "PUT TARGET INTO CHAMBE-
    R, PUSH 'CONT' WHEN READY"
870 LOCAL 7
880 BEEP @ BEEP
890 PAUSE

```

```

900 REMOTE 7
910 OUTPUT 719 :"P",L9,"Z1K0L3M0
N601" ! INITIAL SETUP OF 719
920 WAIT 500
930 GOSUB 3370
940 CLEAR
950 DISP "COMPUTING TARGET DATA"
960 GOSUB 3090
970 !
980 ! COMPUTING TARGET DATA
990 ! WITHOUT BACKGROUND AND THE

1000 ! FREQ. FOR EACH RECORD.
1010 F0=L9-3*F9
1020 FOR M=1 TO N1
1030 F0=F0+F9
1040 N(M,1)=F0
1050 X7=B(M,1)-A(M,1)
1060 X8=B(M,2)-A(M,2)
1070 X6=(X7^2+X8^2)*G4(M,1)
1080 N(M,2)=X6
1090 X8=ATN2(X8,X7)+G4(M,2)
1100 X8=X8-X9*INT(X8/X9)
1110 IF X8>PI THEN X8=X8-PI
1120 N(M,3)=X8
1130 NEXT M
1140 DISP "PRINT DATA? Y/N"
1150 BEEP @ BEEP
1160 INPUT P$
1170 IF P$="N" THEN 1210
1180 PRINT "      FREQ      CRSEC
          PHASE"
1190 MAT PRINT USING 1200 : N
1200 IMAGE 2X,3D,40
1210 CLEAR
1220 LOCAL 7
1230 DISP "PLOT MAGNITUDE FOR
          THIS MEASURMENT? Y/N"
1240 INPUT P$
1250 IF P$="N" THEN 1290
1260 DISP "SELECT PEN. PUSH
          'CONT' WHEN READY"
1270 PAUSE
1280 GOSUB 3530
1290 CLEAR
1300 DISP "PLOT PHASE FOR THIS
          MEASURMENT ? Y/N"
1310 BEEP @ BEEP
1320 INPUT P$
1330 IF P$="N" THEN 1370
1340 DISP "SELECT PEN. PUSH
          'CONT' WHEN READY"
1350 PAUSE
1360 GOSUB 4570
1370 CLEAR

```

```

1380 DISP "DO YOU WANT TO MAKE
           AVERAGE WITH PREVIUSE
           DATA?"
1390 DISP "?Y/N"
1400 BEEP @ BEEP
1410 INPUT P$
1420 IF P$="Y" THEN 1710
1430 DISP "DO YOU WANT TO STORE
           DATA ? Y/N "
1440 INPUT P$
1450 IF P$="N" THEN 2240
1460 M0=1
1470 DISP "DO YOU WANT TO STORE
           DATA IN FILE"
1480 DISP G$
1490 DISP "? Y/N"
1500 INPUT P$
1510 IF P$="Y" THEN 1580
1520 DISP "ENTER NAME OF THE DAT
           A FILE TO BE USED FOR STORE
           GE"
1530 INPUT G$
1540 DISP "IS THIS AN OLD FILE
           TO BE UPDATED ? Y/N "
1550 INPUT P$
1560 IF P$="Y" THEN 1580
1570 CREATE G$,53,24
1580 DISP "ENTER LENGTH OF TARGE
           T"
1590 BEEP @ BEEP
1600 INPUT M1
1610 DISP "ENTER DIAMETER OF TAR
           GET"
1620 BEEP @ BEEP
1630 INPUT M2
1640 !
1650 ! STORE MEASURED DATA.
1660 !
1670 ASSIGN# 2 TO G$
1680 PRINT# 2 , M0,M1,M2,N(),)
1690 ASSIGN# 2 TO *
1700 GOTO 2240
1710 DISP "DOES THE DATA STORED
           IN FILE"
1720 DISP G$
1730 DISP "? Y/N"
1740 INPUT P$
1750 IF P$="Y" THEN 1830
1760 DISP "ENTER NAME OF DATA
           FILE TO BE USED FOR THE
           AVERAGE"
1770 !
1780 INPUT G$
1790 !
1800 ! READ OLD DATA
1810 ! AND MAKES WIGHTED AVERAGE
1820 ! WITH NEW DATA.

```

```

1830 ASSIGN# 6 TO G$
1840 READ# 6 : M0,M1,M2,M9(),)
1850 ASSIGN# 6 TO *
1860 FOR K=1 TO N1
1870 M9(K,2)=M9(K,2)*M0+N(K,2)
1880 M9(K,2)=M9(K,2)/(M0+1)
1890 M9(K,3)=M9(K,3)*M0+N(K,3)
1900 M9(K,3)=M9(K,3)/(M0+1)
1910 N(K,2)=M9(K,2)
1920 N(K,3)=M9(K,3)
1930 NEXT K
1940 M0=M0+1
1950 !
1960 ! STORE NEW AVERAGE.
1970 ASSIGN# 7 TO G$
1980 PRINT# 7 : M0,M1,M2,N(),)
1990 ASSIGN# 7 TO *
2000 PRINT "DATA IS AVERAGE OF",
      M0, "MEASURMENTS"
2010 DISP "PRINT DATA? Y/N"
2020 BEEP @ BEEP
2030 INPUT P$
2040 IF P$="N" THEN 2080
2050 PRINT "          FREQ      CRSEC
                  PHASE"
2060 MAT PRINT USING 1200 : N
2070 IMAGE 2X,3D,4D
2080 DISP "PLOT MAGNITUDE? Y/N"
2090 BEEP @ BEEP
2100 INPUT P$
2110 IF P$="N" THEN 2150
2120 DISP "SELECT PEN FOR MAGNIT
      UDE PLOT. PUSH 'CONT' WHEN
      READY."
2130 PAUSE
2140 GOSUB 3530
2150 CLEAR
2160 DISP "PLOT PHASE? Y/N"
2170 BEEP @ BEEP
2180 INPUT P$
2190 IF P$="N" THEN 2230
2200 DISP "SELECT PEN AND CHANGE
      PAPER FOR PHASE PLOT. PUS
      H 'CONT' WHEN READY."
2210 PAUSE
2220 GOSUB 4570
2230 CLEAR
2240 DISP "DO YOU WANT TO"
2250 DISP "OBTAIN DATA"
2260 DISP "FOR A NEW TARGET?"
2270 DISP ""
2280 DISP "ENTER Y/N"
2290 INPUT P$
2300 IF P$="N" THEN 2430
2310 DISP "DO YOU WANT TO USE
      THE SAME FILE"
2320 DISP G$

```

```

2330 DISP "TO STORE NEW DATA? Y/N"
2340 INPUT P$
2350 IF P$="Y" THEN 2420
2360 DISP "ENTER NEW FILE NAME TO STORE TARGET DATA"
2370 INPUT G$
2380 DISP "IS THIS AN OLD FILE TO BE UPDATED? Y/N"
2390 INPUT P$
2400 IF P$="Y" THEN 2420
2410 CREATE G$,52,24
2420 GOTO 550
2430 CLEAR
2440 DISP "END OF PROGRAM"
2450 BEEP @ BEEP @ BEEP
2460 END
2470 !
2480 !
2490 !
2500 !
2510 !
2520 ! BACKGROUND DATA COLLECTIO N SUBROUTINE
2530 ! OUTPUT(L9-F9)TO U9 GHZ
2540 J=10*(L9-2*F9) ! FREQUENCY STARTS AT L9-F9 GHZ TO BE INCREASED AT F9 GHZ STEPS
2550 FOR K=1 TO N1 ! NUMBER OF F
REQUENCY STEPS
2560 J=J+10*F9
2570 IMAGE 1A,3Z,14A
2580 OUTPUT 719 USING 2570 ; "P"
,J,"00Z1K0L3M0N601"
2590 ! 50 MSEC WAIT FOR FREQUENC Y TO STABILIZE
2600 WAIT 50
2610 ! TAKE DATA IN FROM 722 AND 720
2620 GOSUB 2780
2630 ! REAL AND IMAGINARY PARTS
2640 ! FROM AMP. AND PHASE.
2650 R1=A1*COS(P1)
2660 I1=A1*SIN(P1)
2670 A(K,1)=R1
2680 A(K,2)=I1
2690 ! PRINT "I1=",A(K,2)
2700 ! PRINT "R1=",A(K,1)
2710 NEXT K
2720 OUTPUT 719 ;"P",L9,"Z1K0L3M 0N601" ! INITIAL SETUP OF 7
19
2730 RETURN
2740 !
2750 !

```

```

2760 !
2770 !
2780 ! SUBROUTINE TO ENTER AMPLI
TUD E AND PHASE DATA FROM DI
GITAL VOLTMETER
2790 !
2800 ! PREPARE DIGITAL VOLTMETER
TO SEND AMPLITUDE DATA
2810 ! NO READINGS TAKEN AND AVE
RAGED FOR ONE FREQUENCY.
2820 V1=0 ! PARAMETERS FOR AVERA
GING PROCESS.
2830 W1=0
2840 FOR L=1 TO N0
2850 OUTPUT 720 ; "F1R1T1Z1FL0M0"
2860 WAIT 10
2870 ENTER 720 ; V0
2880 WAIT 10
2890 OUTPUT 722 ; "F1R7T1M3A0H1"
2900 WAIT 10
2910 ENTER 722 ; W0
2920 V1=V1+V0
2930 W1=W1+W0
2940 WAIT 10
2950 NEXT L
2960 V0=V1/N0
2970 W0=W1/N0
2980 ! TRANSFERS FROM VOLTS TO
AMPL.
2990 R1=10^W0
3000 ! TRANSFERS TO DEG. FROM V0
LTS.
3010 P1=100*V0
3020 ! PRINT "R1=",R1
3030 P1=DTR(P1)
3040 ! PRINT "P1=",P1
3050 RETURN
3060 !
3070 !
3080 !
3090 ! DATA COLLECTION SUBROUTIN
E
3100 ! OUTPUT(L9-F9)TO U9 GHZ AT
F9 GHZ STEPS
3110 J=10*(L9-2*F9) ! INITIAL FR
EQUENCY AT L9-F9 GHZ

3120 FOR K=1 TO N1 ! FREQUENCY S
TEPS
3130 J=J+10*F9 ! F9 GHZ INCREME
NTS
3140 IMAGE 1A,32,14A
3150 OUTPUT 719 USING 3140 ; "P"
,J,"00Z1K0L3M0N601"
3160 ! 50 MSEC WAIT FOR FREQUENC
Y TO STABILIZE
3170 WAIT 50

```

```

3180 ! TAKE DATA IN FROM 722&720
3190 GOSUB 2780
3200 !
3210 ! REAL&IMAG FROM AMP.&PHASE
3220 R1=A1*COS(P1)
3230 I1=A1*SIN(P1)
3240 B(K,1)=R1
3250 B(K,2)=I1
3260 ! PRINT "R1=",B(K,1)
3270 ! PRINT "I1=",B(K,2)
3280 NEXT K
3290 OUTPUT 719 , "P", L9, "Z1K0L3M
0N601" ! INITIAL SETUP OF 7
19
3300 RETURN
3310 !
3320 !
3330 !
3340 ! HEADER SUBROUTINE
3350 !
3360 D$="MONTH/DATE/YEAR"
3370 PRINT "
3380 PRINT "
3390 CLEAR
3400 DISP "ENTER TODAY'S DATE -
MONTH,DATE,YEAR"
3410 INPUT D$
3420 DISP "ENTER TGT DESCRIPTION
"
3430 INPUT T$
3440 PRINT D$
3450 PRINT "TARGET IS ",T$
3460 PRINT "*****"
3470 PRINT "*****"
3480 PRINT "
3490 CLEAR
3500 RETURN
3510 !
3520 !
3530 ! MAGNITUDE PLOTTING
3540 ! SUBROUTINE
3550 !
3560 PLOTTER IS 705
3570 LOCATE 32,122,20,85
3580 FRAME
3590 ! SEARCH FOR MAX. & MIN.
3600 ! S0=N(2,2)
3610 ! S1=S0
3620 ! FOR M=3 TO N1
3630 ! IF S0>N(M,2) THEN S0=N(M,
2)
3640 ! IF S1<N(M,2) THEN S1=N(M,
2)
3650 ! NEXT M
3660 DISP "ENTER LOWER VALUE FOR
MAGNITUDE PLOTTING"

```

```

3670 BEEP @ BEEP
3680 INPUT S0
3690 DISP "ENTER UPPER VALUE FOR
          MAGNITUDE PLOTTING"
3700 INPUT S1
3710 L1=INT(L9)
3720 U1=CEIL(U9)
3730 !
3740 ! CALCULATE SCALE STEPS
3750 ! FOR MAGNETUDE.
3760 S3=LGT(S1)
3770 S4=INT(S3)-1
3780 S5=S3-S4
3790 S5=INT(10^S5)+1
3800 S4=10^S4
3810 L0=INT(S0/S4)
3820 IF S5-L0<=14 THEN 3900
3830 IF S5-L0>=50 THEN 3870
3840 S5=.5*S5
3850 S4=S4*2
3860 GOTO 3810
3870 S5=.2*S5
3880 S4=5*S4
3890 GOTO 3810
3900 L0=S4*L0
3910 U0=S5*S4
3920 D0=U0-L0
3930 SCALE L1,U1,L0,U0
3940 FXD 0,4
3950 LAXES -1,S4,L1,L0
3960 MOVE L1,0
3970 FOR K=2 TO N1
3980 W9=N(K,1)
3990 R9=N(K,2)
4000 GOSUB .4470
4010 NEXT K
4020 M5=(U1+L1)/2
4030 MOVE M5,L0-.09*D0
4040 LORG 5 @ CSIZE 3,1,0
4050 ! LABEL "FREQUENCY (GHZ)"
4060 MOVE L1-1,.5*(L0+U0)
4070 LDIFR PI/2
4080 ! LABEL "CROSS SECTION (SQ.
          METERS)"
4090 MOVE M5,U0+.09*D0
4100 LDIFR 0
4110 CSIZE 3,1,0
4120 LABEL T$
4130 MOVE M5,U0+.03*D0
4140 LABEL D$
4150 PENUP
4160 DISP "OVERLAY THEORETICAL C
          URVE? Y/N"
4170 !
4180 INPUT P$
4190 IF P$="N" THEN 4450

```

```

4200 DISP "IS THE THEORETICAL
        DATA STORED IN THE FILE".H$
4210 DISP "? Y/N"
4220 INPUT P$
4230 IF P$="Y" THEN 4260
4240 DISP "ENTER NAME OF THE
        DATA FILE TO BE PLOTTED."
4250 INPUT H$
4260 BEEP @ BEEP
4270 DISP "CHANGE PEN IF DESIRED
        . PUSH 'CONT' WHEN READY."
4280 PAUSE
4290 ASSIGN# 3 TO H$
4300 J1=(L9-2)*50
4310 J2=(U9-2)*50
4320 FOR J=J1 TO J2
4330 READ# 3,J ; T(J,1),T(J,2)
4340 NEXT J
4350 ASSIGN# 3 TO *
4360 F0=L9
4370 R9=T(J1,1)
4380 MOVE F0,R9
4390 FOR I=J1+1 TO J2
4400 F0=F0+.02
4410 R9=T(I,1)
4420 DRAW F0,R9
4430 NEXT I
4440 PENUP
4450 RETURN
4460 !
4470 ! PLOT CROSS
4480 MOVE M9,R9
4490 CSIZE 2,.5,0
4500 LABEL "+"
4510 ! IMOVE .00025,.00025
4520 ! IDRAW -.0005,0
4530 RETURN
4540 !
4550 !
4560 !
4570 ! PHASE PLOTTING SUBROUTINE
4580 !
4590 PLOTTER IS 705
4600 LOCATE 32.122,20,85
4610 FRAME
4620 S4=.25
4630 U0=1
4640 L0=-1
4650 D0=U0-L0
4660 SCALE L1,U1,L0,U0
4670 FXD 0,3
4680 LAXES -1,S4,L1,L0
4690 MOVE L1,0
4700 FOR K=2 TO N1
4710 M9=N(K,1)
4720 R9=N(K,3)/PI
4730 GOSUB 5070

```

```

4740 NEXT K
4750 MOVE M5,L0-.03*00
4760 LORG 5 @ CSIZE 3,1,0
4770 ! LABEL "FREQUENCY (GHZ)"
4780 MOVE L1-1,.5*(L0+U0)
4790 LDIR PI/2
4800 LABEL "PHASE (PI)"
4810 MOVE M5,U0+.03*00
4820 LDIR 0
4830 CSIZE 3,1,0
4840 LABEL T$
4850 MOVE M5,U0+.03*00
4860 LABEL D$
4870 PENUP
4880 DISP "OVERLAY THEORETICAL C
URVE? Y/N"
4890 INPUT P$
4900 IF P$="N" THEN 5030
4910 BEEP @ BEEP
4920 DISP "CHANGE PEN IF DESIRED
PUSH 'CONT' WHEN READY."
4930 PAUSE
4940 F0=L9
4950 R9=T(J1,2)/PI
4960 MOVE F0,R9
4970 FOR I=J1+1 TO J2
4980 F0=F0+.02
4990 R9=T(I,2)/PI
5000 DRAW F0,R9
5010 NEXT I
5020 PENUP
5030 RETURN
5040 !
5050 !
5060 !
5070 ! PLOT DOT
5080 MOVE M9,R9
5090 CSIZE 2, 5,0
5100 LABEL "*"
5110 ! IMOVE .00025,.00025
5120 ! IDRAW -.0005,0
5130 RETURN

```

## LIST OF REFERENCES

1. Skolnik, I. Merill Radar Handbook, McGraw-Hill Book Company, pp. 27-2, New York 1970.
2. Ksienki, A. A., Lin, Y.T. and White, L.J. "Low Frequency Approach to Target Identification," IEEE Proceedings, Vol 63 pp. 1651-1660 Dec. 1975.
3. Senior, T.B.A., "A Survey of Analytical Techniques for Cross-Section Estimation," Proc. IEEE Special issue on Radar Reflectivity, pp. 822-832 Aug. 1965.
4. Stratton, J.A., Electromagnetic Theory, pp. 464, McGraw-Hills, New York, 1941.
5. Cruft Lab. Harvard University, Cambridge Mass. Tech Rep. 212, Theoretical Discussion of Circular Loops, by Storer, J.E., 1955.
6. Kennedy, P.A., "Loop Antenna Measurements," IRE Trans. on Antennas and Propagation, Vol AP-14, pp. 610-618, Oct. 1956.
7. Ross, R.A., "Scattering by a Finite Cylinder," Proc. IEE (London), Vol 144, pp. 864-868, 1967.
8. Lee, H.M., "Double Series Expansion of the Green's Function for a Perfectly Conducting Tubular Cylinder of Finite Length," Radio Science, Volume 18 Number 1, pp. 48-56, Jan.-Feb. 1983.
9. Stratton, J.A., "Diffraction Theory of Electromagnetic Waves," Phys. Rev., Vol 56, pp. 99-107, 1939.
10. Manuel, A. Mariategui, Development Calibration and Evaluation of a Free Field Scatering Rang, Master Thesis, Naval Postgraduate School, Monterey, California, pp. 21-25, Dec. 1983.
11. Mentzer, J.R., Scattering and Diffraction of Radio Waves, pp. 124, Pergamon Press, New York, 1955.
12. Lolic, Mario, Radar Target Identification Through Electromagnetic Scattering Studies, Master Thesis, Naval Postgraduate School, Monterey, California, pp. 81-105, Dec. 1984.

13. Prof. Lee, H.M., Privet Communication, Department of Electrical and Computer Engineering Naval Postgraduate School, Monterey California 93943.
14. Marcuvitz, N., Waveguide Handbook, pp. 66-72, Dover Publications Inc., New York, 1951.

## INITIAL DISTRIBUTION LIST

	No. Copies
1. Library, Code 0142 Naval Postgraduate School Monterey, California 93943	2
2. Defense Technical Information Center Cameron Station Alexandria, Virginia 22314	2
3. Department Chairman, Code 62 Department of Electrical and Computer Engineering Naval Postgraduate School Monterey, California 93943	2
4. Prof. Hung-Mou Lee, Code 62 Lh Department of Electrical and Computer Engineering Naval Postgraduate School Monterey, California 93943	2
5. Prof. J.M. Chang Code 62 cn Department of Electrical and Computer Engineering Naval Postgraduate School Monterey, California 93943	1
6. Lt. Boaz Haklay 11 Kiryat Moshe st. Jerusalem 96102 Israel	7

**END**

**FILMED**

**7-85**

**DTIC**